UNIVERSIDAD DE BUENOS AIRES
Facultad de Ciencias Exactas y Naturales
Departamento de Matemática

Métodos numéricos para problemas no locales de evolución

Tesis presentada para optar al título de Doctor de la Universidad de Buenos Aires en el área Ciencias Matemáticas

Lic. Francisco Vicente Mastroberti Bersetche

Director de tesis: Dr. Gabriel Acosta Rodríguez
Consejero de estudios: Dr. Gabriel Acosta Rodríguez
Lugar de trabajo: Departamento de matemática, FCEyN, UBA

Fecha de defensa: 6 de marzo, 2019

Métodos numéricos para problemas no locales de evolución

El objetivo de este trabajo es estudiar aproximaciones numéricas para problemas de evolución de la forma

$$ {}^{C}\partial_t^{\alpha} u + (-\Delta)^s u = f \text{ in } \Omega \times (0,T), $$

donde $(-\Delta)^s$ representa el operador Laplaciano fraccionario en su forma integral y ${}^{C}\partial_t^{\alpha} u(x,t)$ denota la derivada de Caputo.

Para ser más precisos,

$$ (-\Delta)^s u(x) = C(n,s) \text{ p.v. } \int_{\mathbb{R}^n} \frac{u(x)-u(y)}{|x-y|^{n+2s}}\, dy, $$

y

$$ {}^{C}\partial_t^{\alpha} u(x,t) = \begin{cases} \frac{1}{\Gamma(k-\alpha)} \int_0^t \frac{1}{(t-r)^{\alpha-k+1}} \frac{\partial^k u}{\partial r^k}(x,r)\, dr & \text{if } k-1 < \alpha < k,\ k \in \mathbb{N}, \\ \frac{\partial^k u}{\partial t^k} u(x,t) & \text{if } \alpha = k \in \mathbb{N}. \end{cases} $$

Estudiamos existencia, unicidad y regularidad de las soluciones en el contexto lineal (es decir, $f = f(x,t)$). Los casos tratados incluyen contrapartes fraccionarias de los modelos de difusión estándar y de ondas. Elementos finitos lineales se utilizan para la variable espacial y técnicas de cuadratura de convolución son usadas para tratar el operador fraccionario en la variable temporal. Estimaciones del error, uniformes en los parámetros de discretización para valores de t lejos de cero, son proporcionadas.

Estos resultados son extendidos al caso semilineal con $f(u) = u - u^3$, siendo este el término no lineal que aparece en las ecuaciones clásicas de Allen-Cahn, utilizadas para modelar la separación de fases para aleaciones binarias. Adicionalmente, el comportamiento asintótico de las soluciones para $s \to 0$ es estudiado en este contexto particular.

Detalles de implementación, particularmente para el método de elementos finitos, en el cual se ven involucradas matrices de rigidez fraccionarias no esparsas y cuadraturas numéricas para núcleos singulares, son cuidadosamente expuestos.

Palabras clave: Laplaciano fraccionario, Derivada de Caputo, Método de Elementos Finitos.

Numerical methods for non-local evolution problems

The aim of this work is to study numerical approximations for evolution problems of the form

$$ {}^C\partial_t^\alpha u + (-\Delta)^s u = f \text{ in } \Omega \times (0,T), $$

where $(-\Delta)^s$ stands for the fractional Laplacian operator in its integral form and ${}^C\partial_t^\alpha u(x,t)$ represents the Caputo derivative.

To be more precise,

$$ (-\Delta)^s u(x) = C(n,s) \text{ p.v. } \int_{\mathbb{R}^n} \frac{u(x)-u(y)}{|x-y|^{n+2s}}\, dy, $$

and

$$ {}^C\partial_t^\alpha u(x,t) = \begin{cases} \frac{1}{\Gamma(k-\alpha)} \int_0^t \frac{1}{(t-r)^{\alpha-k+1}} \frac{\partial^k u}{\partial r^k}(x,r)\, dr & \text{if } k-1 < \alpha < k,\ k \in \mathbb{N}, \\ \frac{\partial^k u}{\partial t^k} u(x,t) & \text{if } \alpha = k \in \mathbb{N}. \end{cases} $$

We deal with existence, uniqueness and regularity of solutions in the linear context (i.e. $f = f(x,t)$). The cases under study include fractional counterparts of the standard diffusion and wave models. Linear finite elements are used for the spatial variable and convolution quadrature techniques for handling the time fractional operator. Error bounds, uniform in the discretization parameters for values of t away from zero, are given.

These results are extended to the semi-linear case with $f(u) = u - u^3$ appearing in the classical Allen-Cahn equations modeling phase separation for binary alloys. Additionally, the asymptotic behaviour of the solutions for $s \to 0$ is studied in this particular context.

Implementation details, particularly for the finite element method involving full fractional stiffness matrices and numerical quadratures for singular kernels, are carefully documented.

Key words: Fractional Laplacian, Caputo derivative, Finite Element Method.

Contents

Introduction

The Finite Element Method (FEM) is one of the preferred numerical tools in scientific and engineering communities. It counts with a solid and long established theoretical foundation, mainly in the linear case of second order *elliptic* partial differential equations. These kind of operators, with the Laplacian as a canonical example, are involved in modeling *local* diffusive processes. On the other hand, nonlocal or *anomalous* diffusion models have increasingly impacted upon a number of important areas in science. Indeed, non-local formulations can be found in physical and social contexts, modeling as diverse phenomena as human locomotion in relation to crime diffusion [25], electrodiffusion of ions within nerve cells [52] or machine learning [73].

The Fractional Laplacian (FL) is among the most prominent examples of a non-local operator. For $0 < s < 1$, it is defined as

$$(-\Delta)^s u(x) = C(n,s) \text{ p.v.} \int_{\mathbb{R}^n} \frac{u(x) - u(y)}{|x-y|^{n+2s}}\, dy, \tag{0.0.1}$$

where

$$C(n,s) = \frac{2^{2s} s \Gamma(s + \frac{n}{2})}{\pi^{n/2} \Gamma(1-s)}$$

is a normalization constant. The FL, given by (0.0.1), is one of the simplest pseudo-differential operators and can also be regarded as the infinitesimal generator of a $2s$-stable Lévy process [17].

Given a function f defined in a bounded domain Ω, the homogeneous Dirichlet problem associated to the FL reads: find u such that

$$\begin{cases} (-\Delta)^s u = f & \text{in } \Omega, \\ u = 0 & \text{in } \Omega^c. \end{cases} \tag{0.0.2}$$

In contrast to elliptic PDEs, numerical developments for problems involving these non-local operator, even in simplified contexts, are seldom found in the literature. The reason for that is related to two major challenging tasks usually involved in its numerical treatment: the handling of highly singular kernels and the need to cope with an unbounded region of integration. This is precisely the case of (0.0.2), for which just

a few numerical methods have been proposed. Effectively implemented *in one space dimension*, we mention, for instance: a finite difference scheme by Huang and Oberman [43], a FE approach developed by D'Elia and Gunzburger [29] that relies on a volume-constrained version of the non-local operator and a simple one-dimensional spectral approach [7]. We refer the reader to [3] for a more detailed account of these schemes and a discussion on other fractional diffusion operators on bounded domains and their discretizations.

Numerical computations for (0.0.2) in higher dimensions have become available only recently [3]. In that paper a complete n-dimensional finite element analysis for the FL has been carried out, including regularity of solutions of (0.0.2) in standard and weighted fractional spaces. Moreover, the convergence for piecewise linear elements is proved with optimal order for both uniform and graded meshes.

In that work there are presented error bounds in the energy norm and numerical experiments (in 2D), demonstrating an accuracy of the order of $h^{1/2}\log h$ and $h\log h$ for solutions obtained by means of uniform and graded meshes, respectively.

On the other hand, since the introduction of Continuous Time Random Walks (CTRW) by Montroll and Weiss [67], anomalous diffusion phenomena has been an active area of research among the scientific community. The CTRW assign a joint space-time distribution to individual particle motions: when the tails of these distributions are heavy enough, non-Fickian dispersion results for all time and space scales. A heavy-tailed jump (waiting time) distribution implies the absence of a characteristic space (time) scale.

The equivalence between these heavy-tailed motions and transport equations that use fractional-order derivatives has been shown by several authors; see, for example [40]. Space nonlocality is a direct consequence of the existence of arbitrarily large jumps in space, whereas time nonlocality is due to the history dependence introduced in the dynamics by the presence of anomalously large waiting times.

The evidence of anomalous diffusion phenomena has been thoroughly reported in physical and social environments, such as plasma turbulence [27, 28], hidrology [15, 16, 70], finance [62], human travel [23] and predator search [77] patterns. Models of transport dynamics in complex systems taking into account this non-Fickian behavior have been proposed accordingly. Also, evolution processes intermediate between diffusion and wave propagation have shown to govern the propagation of stress waves in viscoelastic materials [34, 61].

Integer-order differentiation operators are local, because the derivative of a function at a given point depends only on the values of the function in a neighborhood of it. In contrast, fractional-order derivatives are nonlocal, integro-differential operators. A left-sided fractional-order derivative in time may be employed to represent memory effects, while a nonlocal differentiaton operator in space accounts for long-range dispersion

processes, as we have mentioned before.

We now describe the problems we are going to consider. Let $\Omega \subset \mathbb{R}^n$ be a domain with smooth enough boundary, $\alpha \in (0,2]$, $s \in (0,1)$ and a forcing term $f\colon \Omega \times (0,T) \to \mathbb{R}$. We aim to solve the fractional differential equation

$$ {}^C\partial_t^\alpha u + (-\Delta)^s u = f \text{ in } \Omega \times (0,T). \tag{0.0.3}$$

Here, ${}^C\partial_t^\alpha$ denotes the Caputo derivative, given by

$${}^C\partial_t^\alpha u(x,t) = \begin{cases} \frac{1}{\Gamma(k-\alpha)} \int_0^t \frac{1}{(t-r)^{\alpha-k+1}} \frac{\partial^k u}{\partial r^k}(x,r)\, dr & \text{if } k-1 < \alpha < k,\ k \in \mathbb{N}, \\ \frac{\partial^k u}{\partial t^k} u(x,t) & \text{if } \alpha = k \in \mathbb{N}. \end{cases}$$

When $\alpha \in (0,1]$, equation (0.0.3) with a non-linear source term $f(u)$ will be also considered.

Closely related to the Caputo derivative, the Riemann-Liouville fractional derivative is needed in the sequel. Let us recall here its definition,

$$\partial_t^\alpha u(x,t) = \begin{cases} \frac{1}{\Gamma(k-\alpha)} \frac{\partial^k}{\partial t^k} \int_0^t \frac{1}{(t-r)^{\alpha-k+1}} u(x,r)\, dr & \text{if } k-1 < \alpha < k,\ k \in \mathbb{N}, \\ \frac{\partial^k u}{\partial t^k} u(x,t) & \text{if } \alpha = k \in \mathbb{N}. \end{cases}$$

For $0 < \alpha \leq 1$, equation (0.0.3) is usually called a *fractional diffusion* equation. On the other hand, for $1 < \alpha \leq 2$ it is sometimes called a *fractional diffusion-wave* equation. Analyzing scaling and similarity properties of the Green function $G_{\alpha,s}$ associated to the operator ${}^C\partial_t^\alpha + (-\Delta)^s$, in [60] it is shown that

$$G_{\alpha,s}(x,t) = t^{\frac{-\alpha}{2s}} \Phi_{\alpha,s}\left(\frac{x}{t^{\frac{\alpha}{2s}}}\right),$$

for a certain one-variable function $\Phi_{\alpha,s}$. Notice that in case $\alpha = s$, although the CTRW associated to equation (0.0.3) has the same scaling properties as Brownian motion, the lack of finite moments makes the diffusion process anomalous. On the other hand, the term *fractional wave* equation has been utilized to refer to the problem with $1 < \alpha = 2s < 2$, since for this choice of the parameters some features of the standard wave equation are preserved [58].

In order to obtain a well-posed problem, we impose the initial and boundary value conditions

$$\begin{cases} u = 0 & \text{in } \Omega^c \times (0,T), \\ u(\cdot,0) = v & \text{in } \Omega, \end{cases} \tag{0.0.4}$$

and the additional condition for $1 < \alpha \leq 2$

$$\partial_t u(\cdot,0) = b \text{ in } \Omega, \tag{0.0.5}$$

with data $v, b \in L^2(\Omega)$.

It is noteworthy that the fractional Laplace operator defined by (0.0.2) does not coincide with the operator considered, for example, in [18, 69, 79]. Indeed, the spatial operator considered in those works is a power of the Laplacian in the spectral sense.

Our work does not include the case $s = 1$, which corresponds to a local-in-space process, as it is already covered by other authors' work. For the range $0 < \alpha \leq 1$, reference [44] develops a semidiscrete Galerkin method and studies the error both for smooth and non-smooth data. Naturally, the local-in-space case is also covered by the previously mentioned works [18, 69, 79] regarding spectral fractional powers of the Laplacian. For the full range of time derivatives we are considering in this work, [65] deals with an alternative formulation of (0.0.3) and a method based on the Laplace transform is developed, while in [68] an approach via discontinuous Galerkin discretization in time is introduced.

Contributions

Chapters 2, 4 and 5 summarize results from

- [5] Acosta G., Bersetche F., Borthagaray J.P. *Finite element approximations for fractional evolution problems*, Submitted, `https://arxiv.org/abs/1705.09815`
- [4] Acosta G., Bersetche F., *Numerical approximations for a fully fractional Allen-Cahn equation*, Preprint, `https://arxiv.org/abs/1903.08964`

Chapter 3 collects results from

- [6] Acosta G., Bersetche F., Borthagaray J.P. *A short FE implementation for a 2d homogeneous Dirichlet problem of a Fractional Laplacian.* Computers and Mathematics with Applications, 74(4), 784-816.

Introducción

El método de elementos finitos (MEF) es una de las herramientas numéricas preferidas en ciencia e ingeniería. Cuenta con un sólido fundamento teórico de larga data, principalmente en el caso lineal para ecuaciones en derivadas partiales *elípticas* de segundo orden. Este tipo de operadores, con el laplaciano como ejemplo canónico, están involucrados en el modelado de procesos difusivos *locales*. Por otro lado, los modelos de difusión no locales o *anómalos* han impactado cada vez más en una serie de importantes áreas en la ciencia. De hecho, formulaciones no locales se pueden encontrar en contextos físicos y sociales, modelando fenómenos tan diversos como la locomoción humana en relación con la difusión del delito [25], electrodifusión de iones dentro de las células nerviosas [52] o el aprendizaje automático [73].

El laplaciano fraccionario (LF) se encuentra entre los ejemplos más destacados de un operador no local. Para $0 < s < 1$, se define como

$$(-\Delta)^s u(x) = C(n,s) \text{ p.v.} \int_{\mathbb{R}^n} \frac{u(x) - u(y)}{|x-y|^{n+2s}}\, dy,$$

donde

$$C(n,s) = \frac{2^{2s} s \Gamma(s + \frac{n}{2})}{\pi^{n/2} \Gamma(1-s)}$$

es una constante de normalización. El LF, dado por (0.0.1), es uno de los operadores pseudo-diferenciales más simples y también pueden ser considerado como el generador infinitesimal de un proceso de Lévy $2s$ -stable [17].

Dada una función f definida en un dominio acotado Ω, el problema de Dirichlet homogéneo asociado al LF se establece como: hallar u tal que

$$\begin{cases} (-\Delta)^s u = f & \text{in } \Omega, \\ u = 0 & \text{in } \Omega^c. \end{cases}$$

A diferencia de las EDP elípticas, los desarrollos numéricos para problemas que involucran operadores no locales, incluso en contextos simplificados, rara vez se encuentra en la literatura. La razón de esto está relacionada con dos grandes desafíos, usualmente relacionados con su tratamiento numérico: el manejo de núcleos altamente singulares y

la necesidad de tratar con una región de integración no acotada. Este es precisamente el caso de (0.0.2), para lo cual solo unos pocos métodos numéricos han sido propuestos. Implementaciones *en una dimensión espacial*, podemos mencionar por ejemplo: un esquema de diferencias finitas de Huang y Oberman [43], un enfoque de EF desarrollado por D'Elia y Gunzburger [29] basado en una versión de volumen acotado del operador no local y un enfoque espectral unidimensional simple [7]. Referimos al lector a [3] para una explicación más detallada de estos esquemas y una discusión sobre otros operadores de difusión fraccionaria en dominios acotado y sus discretizaciones.

Técnicas numéricas para (0.0.2) en dimensiones más altas han sido desarrolladas recientemente [3]. En ese articulo un análisis completo de elementos finitos n-dimensionales para el FL ha sido llevado a cabo, incluyendo el estudio de la regularidad de soluciones de (0.0.2) en espacios fraccionarios estándar y con pesos. Por otra parte, es probada la convergencia para elementos finitos lineales con un orden óptimo para mallas uniformes y graduadas.

En ese trabajo también se presentan estimaciones del error en norma energía y experimentos numéricos (en 2D) que demuestran una precisión del orden de $h^{1/2}\log h$ y $h\log h$ para soluciones obtenidas mediante mallas uniformes y graduadas, respectivamente.

Por otro lado, desde la introducción de paseos aleatorios de tiempo continuo (PATC) por Montroll y Weiss [67], los fenómenos de difusión anómalos han sido un área activa de investigación entre la comunidad científica. El PATC asigna una distribución conjunta espacio-tiempo a movimientos individuales partículas: cuando las colas de estas distribuciones son lo suficientemente pesadas, dispersión no Fickiana se aparece para todas las escalas de tiempo y espacio. Una distribución con salto de cola pesada (tiempo de espera) implica la ausencia de una escala característica de espacio o tiempo.

Varios autores han demostrado la equivalencia entre estos movimientos de cola pesada y las ecuaciones de transporte que involucran derivadas de orden fraccionario; ver, por ejemplo [40]. La no localidad espacial es una consecuencia directa de la existencia de saltos arbitrariamente grandes en el espacio, mientras que la no localidad temporal se debe a la dependencia de la historia introducida en la dinámica por la presencia de tiempos de espera anormalmente grandes.

La evidencia de fenómenos de difusión anómalos ha sido exhaustivamente documentada en entornos físicos y sociales, como turbulencia del plasma [27, 28], hidrología [15, 16, 70], finanzas [62] y desplazamiento humano [23] y patrones de búsqueda de depredadores [77]. En conseciencia modelos de dinámica de transporte en sistemas complejos que tienen en cuenta este comportamiento no fickiano han sido propuestos. Además, se ha demostrado que los procesos de evolución intermedios entre la difusión y la propagación de la onda gobiernan la propagación de las ondas de tensión en los materiales viscoelásticos [34, 61].

Los operadores de diferenciales de orden entero son locales, ya que la derivada de una función en un punto dado depende solo de los valores de la función en un entorno de la misma. En contraste, las derivadas de orden fraccionario son operadores integro-diferenciales no locales. Se puede emplear una derivada de orden fraccionario del lado izquierdo en el tiempo para representar los efectos memoria, mientras que un operador de diferencia no local en el espacio da cuenta de los procesos de dispersión de largo alcance, como hemos mencionado antes.

Describimos ahora los problemas que vamos a considerar. Sea $\Omega \subset \mathbb{R}^n$ un dominio con un borde suficientemente suave, $\alpha \in (0, 2]$, $s \in (0, 1)$ y un término forzante $f \colon \Omega \times (0, T) \to \mathbb{R}$. Nuestro objetivo es resolver la ecuación diferencial fraccionaria:

$$ {}^C\partial_t^\alpha u + (-\Delta)^s u = f \text{ in } \Omega \times (0, T). $$

Aquí, ${}^C\partial_t^\alpha$ denota la derivada de Caputo, dada por

$$ {}^C\partial_t^\alpha u(x,t) = \begin{cases} \frac{1}{\Gamma(k-\alpha)} \int_0^t \frac{1}{(t-r)^{\alpha-k+1}} \frac{\partial^k u}{\partial r^k}(x,r)\, dr & \text{si } k-1 < \alpha < k,\ k \in \mathbb{N}, \\ \frac{\partial^k u}{\partial t^k} u(x,t) & \text{si } \alpha = k \in \mathbb{N}. \end{cases} $$

Para el caso $\alpha \in (0, 1]$, se estudiará también la ecuación (0.0.3) con un término no lineal $f(u)$.

Relacionada estrechamente con la derivada de Caputo, la derivada fraccionaria de Riemann-Liouville será utilizada a lo largo de este trabajo. Recordamos aquí su definición,

$$ \partial_t^\alpha u(x,t) = \begin{cases} \frac{1}{\Gamma(k-\alpha)} \frac{\partial^k}{\partial t^k} \int_0^t \frac{1}{(t-r)^{\alpha-k+1}} u(x,r)\, dr & \text{if } k-1 < \alpha < k,\ k \in \mathbb{N}, \\ \frac{\partial^k u}{\partial t^k} u(x,t) & \text{if } \alpha = k \in \mathbb{N}. \end{cases} $$

Para $0 < \alpha \leq 1$, la ecuación (0.0.3) es referida como ecuación de *difusión fraccionaria*. Por otro lado, para $1 < \alpha \leq 2$ suele ser llamada ecuación de *difusión-ondas fraccionaria*. Analizando las propiedades de escala y similaridad de la función Green $G_{\alpha,s}$ asociada a la operador
${}^C\partial_t^\alpha + (-\Delta)^s$, en [60] se muestra que

$$ G_{\alpha,s}(x,t) = t^{\frac{-\alpha}{2s}} \Phi_{\alpha,s}\left(\frac{x}{t^{\frac{\alpha}{2s}}} \right), $$

para una determinada función de una variable $\Phi_{\alpha,s}$. Notar que en el caso $\alpha = s$, aunque el PATC asociado a la ecuación (0.0.3) tiene Las mismas propiedades de escala que el movimiento browniano, la falta de momentos finitos hacen que el proceso de difusión sea anómalo. Por otro lado, el término ecuación de *ondas fraccionaria* ha sido utilizado para referirse al problema con $1 < \alpha = 2s < 2$, ya que para esta elección de los parámetros se conservan algunas características de la ecuación de ondas estándar [58].

Para obtener un problema bien planteado, imponemos las condiciones iniciales y de borde

$$\begin{cases} u = 0 & \text{en } \Omega^c \times (0,T), \\ u(\cdot,0) = v & \text{in } \Omega, \end{cases}$$

y la condición adicional para $1 < \alpha \leq 2$

$$\partial_t u(\cdot,0) = b \text{ en } \Omega,$$

con datos $v, b \in L^2(\Omega)$.

Cabe destacar que el operador de Laplace fraccionario definido por (0.0.2) no coincide con el operador considerado, por ejemplo, en [18, 69, 79]. De hecho, el operador espacial considerado en estos trabajos es una potencia del laplaciano en el sentido espectral.

Nuestro trabajo no incluye el caso $s = 1$, que corresponde a un proceso local en el espacio, ya que ha sido cubierto por el trabajo de otros autores. Para el rango $0 < \alpha \leq 1$, [44] desarrolla un método de Galerkin semidiscreto y estudia el error para datos iniciales suaves y datos poco regulares. Naturalmente, el caso local en el espacio también está cubierto por los trabajos mencionados anteriormente [18, 69, 79] utilizando potencias fraccionarias espectrales del laplaciano clásico. Para el rango completo de derivadas temporales que estamos considerando en este trabajo, en [65] se brinda una formulación alternativa de (0.0.3) y se desarrolla un método basado en la transformada de Laplace, mientras que en [68] se introduce un enfoque a través del uso de Galerkin discontinuo en la variable temporal.

Contribuciones

Los capítulos 2, 4 y 5 resumen resultados de

- [5] Acosta G., Bersetche F., Borthagaray J.P. *Finite element approximations for fractional evolution problems*, Enviado, `https://arxiv.org/abs/1705.09815`
- [4] Acosta G., Bersetche F., *Numerical approximations for a fully fractional Allen-Cahn equation*, Preprint, `https://arxiv.org/abs/1903.08964`

El Capítulo 3 recopila los resultados de

- [6] Acosta G., Bersetche F., Borthagaray J.P. *A short FE implementation for a 2d homogeneous Dirichlet problem of a Fractional Laplacian.* Computers and Mathematics with Applications, 74(4), 784-816.

Chapter 1

Preliminaries

In this section we set the basic notation and present some preliminary and necessary concepts for the analysis of the fractional elliptic and fractional evolution problems under consideration. We recall elliptic regularity results for the fractional Laplacian and some important properties of the Mittag-Leffler function.

1.1 Fractional Sobolev spaces

Given an open set $\Omega \subset \mathbb{R}^n$ and $s \in (0,1)$, define the fractional Sobolev space $H^s(\Omega)$ as

$$H^s(\Omega) = \left\{ v \in L^2(\Omega) \colon |v|_{H^s(\Omega)} < \infty \right\},$$

where $|\cdot|_{H^s(\Omega)}$ is the Aronszajn-Slobodeckij seminorm

$$|v|^2_{H^s(\Omega)} = \iint_{\Omega^2} \frac{|v(x) - v(y)|^2}{|x-y|^{n+2s}}\, dx\, dy.$$

associated to the bilinear form $\langle \cdot, \cdot \rangle_{H^s(\Omega)}$ on $H^s(\Omega)$,

$$\langle u, v \rangle_{H^s(\Omega)} = \iint_{\Omega^2} \frac{(u(x) - u(y))(v(x) - v(y))}{|x-y|^{n+2s}}\, dx\, dy. \tag{1.1.1}$$

It is a well known fact that $H^s(\Omega)$ is a Hilbert space endowed with the norm $\|\cdot\|_{H^s(\Omega)} = \|\cdot\|_{L^2(\Omega)} + |\cdot|_{H^s(\Omega)}$.

Let us also define the space of functions supported in Ω,

$$\widetilde{H}^s(\Omega) = \left\{ v \in H^s(\mathbb{R}^n) \colon \text{ supp } v \subset \bar{\Omega} \right\}.$$

This space may be defined through interpolation,

$$\widetilde{H}^s(\Omega) = \left[L^2(\Omega), H^1_0(\Omega) \right]_s.$$

Moreover, depending on the value of s, different characterizations of this space are available. If $s < \frac{1}{2}$ then $\widetilde{H}^s(\Omega)$ coincides with $H^s(\Omega)$, and if $s > \frac{1}{2}$ it may be characterized as the closure of $C_0^\infty(\Omega)$ with respect to the $\|\cdot\|_{H^s(\Omega)}$ norm. In the latter case, it is also customary to denote it by $H_0^s(\Omega)$. The particular case of $s = \frac{1}{2}$ gives raise to the Lions-Magenes space $H_{00}^{\frac{1}{2}}(\Omega)$, which can be characterized by

$$H_{00}^{\frac{1}{2}}(\Omega) = \left\{ v \in H^{\frac{1}{2}}(\Omega) \colon \int_\Omega \frac{v(x)^2}{\operatorname{dist}(x, \partial\Omega)}\, dx < \infty \right\}.$$

Note that the inclusion $H_{00}^{\frac{1}{2}}(\Omega) \subset H_0^{\frac{1}{2}}(\Omega) = H^{\frac{1}{2}}(\Omega)$ is strict. We also need to introduce the dual space of $\widetilde{H}^s(\Omega)$, denoted with the standard negative exponent $H^{-s}(\Omega)$.

The following well known result implies that $\langle \cdot, \cdot \rangle_{H^s(\mathbb{R}^n)}$ (recall (1.1.1)) induces a norm on $\widetilde{H}^s(\Omega)$.

Proposition 1.1.1 (Poincaré inequality)**.** *There is a constant $c = c(\Omega, n, s)$ such that*

$$\|v\|_{L^2(\Omega)} \leq c|v|_{H^s(\mathbb{R}^n)} \quad \forall v \in \widetilde{H}^s(\Omega).$$

Additionally, Sobolev spaces of order greater than 1 are defined in the following way: given $k \in \mathbb{N}$, then

$$H^{k+s}(\Omega) = \left\{ v \in H^k(\Omega) \colon |D^\alpha v| \in H^s(\Omega)\, \forall \alpha \text{ with } |\alpha| = k \right\},$$

furnished with the norm

$$\|v\|_{H^{k+s}(\Omega)} = \|v\|_{H^k(\Omega)} + \sum_{|\alpha|=k} |D^\alpha v|_{H^s(\Omega)}.$$

Also, we can define negative order Sobolev spaces by duality, using $L^2(\Omega)$ as pivot space. Of interest in the problems we are considering is the space

$$H^{-s}(\Omega) = \left(\widetilde{H}^s(\Omega)\right)'.$$

1.2 Elliptic regularity

We recall regularity results for the homogeneous problem

$$\begin{cases} (-\Delta)^s u &= g \text{ in } \Omega, \\ u &= 0 \text{ in } \Omega^c. \end{cases} \tag{1.2.1}$$

Even though the fractional Laplacian is an operator of order $2s$ in $\mathbb{R}^n$, in the sense that $(-\Delta)^s \colon H^\ell(\mathbb{R}^n) \to H^{\ell-2s}(\mathbb{R}^n)$ is bounded and invertible, the theory is much more delicate for problems posed on bounded domains.

Grubb [38] provides regularity estimates for solutions of (1.2.1) in the setting of Hörmander $\mu-$spaces. We express these results in terms of standard Sobolev spaces, and refer to [38] for further details.

Proposition 1.2.1. *Let $\Omega \subset \mathbb{R}^n$ be a bounded domain with smooth boundary, $g \in H^r(\Omega)$ for some $r \geq -s$ and consider $u \in \widetilde{H}^s(\Omega)$, the solution of the Dirichlet problem* (1.2.1). *Then, there exists a constant $C(n,s)$ such that*

$$|u|_{H^{s+\gamma}(\mathbb{R}^n)} \leq C\|g\|_{H^r(\Omega)}.$$

Here, $\gamma = \min\{s+r, 1/2-\varepsilon\}$, with $\varepsilon > 0$ arbitrary small.

Remark 1.2.2. Observe that, in general, it is not true that solutions of (1.2.1) have $2s$ more derivatives than the right-hand side function g. No matter how regular g is, the solution of (1.2.1) is not expected to be more regular than $H^{s+\gamma}(\mathbb{R}^n)$. In spite of this, the singular behavior of solutions can be localized at the boundary and described appropriately in weighted spaces [3, 7].

Remark 1.2.3. In view of Proposition 1.2.1, assuming $(-\Delta)^s v \in L^2(\Omega)$ is weaker than assuming that $v \in H^{2s}(\mathbb{R}^n)$. This kind of weaker conditions on the initial/boundary data are frequently employed as hypothesis throughout this work.

Additionally, the following two theorems summarize classical global and interior regularity for solutions of (1.2.1) in Hölder spaces, and we refer to [33] for further details.

Theorem 1.2.4. *Let $\Omega \subset \mathbb{R}^n$ be any bounded $C^{1,1}$ domain, $s \in (0,1)$, and u be the solution of* (1.2.1). *If $g \in L^\infty(\Omega)$; then $u \in C^s(\mathbb{R}^n)$. Moreover,*

$$\|u\|_{C^s(\mathbb{R}^n)} \leq C\|g\|_{L^\infty(\Omega)},$$

where the constant C depends only on Ω and s.

Theorem 1.2.5. *Let Ω be a bounded domain of $\mathbb{R}^n$, and let u be a solution for* (1.2.1). *If $\delta(x) = dist(x, \partial\Omega)$, for each $\rho > 0$ define $\Omega_\rho := \{x \in \Omega : \delta(x) > \rho\}$. Then, if $\beta + 2s$ is not an integer, for every $0 < \rho' < \rho$ we have*

$$\|u\|_{C^{\beta+2s}(\Omega_\rho)} \leq C\|g\|_{C^\beta(\Omega_{\rho'})}, \tag{1.2.2}$$

with $C = C(n, s, \Omega, \beta, \rho, \rho')$.

1.3 Mittag-Leffler function

Let $\alpha > 0$ and $\mu \in \mathbb{R}$, then the Mittag-Leffler function $E_{\alpha,\mu} \colon \mathbb{C} \to \mathbb{C}$ is defined as

$$E_{\alpha,\mu}(z) = \sum_{k=0}^{\infty} \frac{z^k}{\Gamma(\alpha k + \mu)}.$$

This is a complex function that depends on two parameters; in particular, it generalizes the exponentials, in view of the identity $E_{1,1}(z) = e^z$ for all $z \in \mathbb{C}$. The following properties of this family of functions are useful to derive the regularity estimates we present below.

Lemma 1.3.1 (cf. [51, Pag 46]). *If $\alpha, \lambda > 0$, then*

$$ {}^{C}\partial_t^{\alpha} E_{\alpha,1}(-\lambda t^{\alpha}) = -\lambda E_{\alpha,1}(-\lambda t^{\alpha}). \tag{1.3.1}$$

Moreover, the following identities hold for $m \geq 1$:

$$\partial_t^m E_{\alpha,1}(-\lambda t^{\alpha}) = -\lambda t^{\alpha-m} E_{\alpha,\alpha+1-m}(-\lambda t^{\alpha}).$$

Lemma 1.3.2 (cf. [51, Eq. 1.8.28]). *Let $0 < \alpha < 2$ and $\mu \in \mathbb{R}$ be arbitrary, and $\frac{\alpha\pi}{2} < \mu < \min(\pi, \alpha\pi)$. Then for $\mu \leq |\arg(z)| \leq \pi$,*

$$E_{\alpha,\beta}(z) = -\sum_{k=1}^{N} \frac{1}{\Gamma(\beta - \alpha k)} \frac{1}{z^k} + O\big(\frac{1}{z^{N+1}}\big),$$

with $|z| \to \infty$. Particularly, for $\mu \leq |\arg(z)| \leq \pi$ we have

$$|E_{\alpha,\mu}(z)| \in \begin{cases} O\Big(\dfrac{1}{1+|z|^2}\Big), & \mu - \alpha \in \mathbb{Z}^- \cup \{0\}, \\ O\Big(\dfrac{1}{1+|z|}\Big), & \textit{otherwise.} \end{cases} \tag{1.3.2}$$

Now we show a result about the behavior of the Mittag-Leffler function under Laplace transform (see [26, Prop. 2.43] or [63, Eq. (2.2.26)]). Given a locally integrable function $f : [0, +\infty) \to \mathbb{R}$ we define its Laplace transform as

$$\mathcal{L}(f)[z] := \int_0^{\infty} f(t) e^{-zt}\, dt.$$

With this definition, we have the following lemma

Lemma 1.3.3. *Let α, $\mu > 0$, we have*

$$\mathcal{L}(t^{\mu-\alpha} E_{\alpha,\mu}(-\lambda t^{\alpha}))[z] = z^{\mu-\alpha}(z^{\alpha} + \lambda)^{-1}, \tag{1.3.3}$$

for $\Re(z) > 0$, and $\lambda > 0$.

Finally, we end this section by giving a property about the positivity of $E_{\alpha,\alpha}$ with a negative argument.

Lemma 1.3.4 (cf. [74, Lemma 3.3]). *Let $\alpha \in (0, 1)$, we have*

$$E_{\alpha,\alpha}(-\eta) \geq 0, \quad \textit{for } \eta \geq 0.$$

Resumen del Capítulo

En este capítulo se recopilan resultados y conceptos necesarios para el desarrollo tanto de la teoría de elementos finitos, como de los resultados de existencia y regularidad para los problemas en consideración.

En la Sección 1.1 se presentan conceptos básicos en relación a los espacios de Sobolev fraccionarios. La Sección 1.2 está dedicada al repaso de resultados clásicos de regularidad para el problema de Poisson fraccionario, mientras que la Sección 1.3 recopila resultados y propiedades de utilidad para las funciones de Mittag-Leffler.

Chapter 2

Fractional evolution problems

In this chapter, formulations for the evolution problems under consideration are established, as well as existence and regularity results. Since the regularity theory for these problems is still an ongoing area, we have imposed some requirements on the problem data in order to avoid some technical details (see Remark 2.1.5). In spite of the fact that these requirements may be too restrictive in some cases, examples used for the computation of the numerical convergence rate in Section 4.3 meet these conditions. In any case, this chapter should be understood as a complementary content to the ideas displayed in chapters 4 and 5.

Let $\{(\phi_k, \lambda_k)\}_{k=1}^{\infty}$ denote the solutions of the fractional eigenvalue problem

$$\begin{cases} (-\Delta)^s u = \lambda\, u & \text{in } \Omega, \\ \qquad u = 0 & \text{in } \Omega^c. \end{cases} \tag{2.0.1}$$

It is well-known that the fractional Laplacian has a sequence of eigenvalues

$$0 < \lambda_1 < \lambda_2 \leq \ldots, \quad \lambda_k \to \infty \text{ as } k \to \infty,$$

and that the eigenfunctions' set $\{\phi_k\}_{k=1}^{\infty}$ may be taken to constitute an orthonormal basis of $L^2(\Omega)$.

Remark 2.0.1. Unlike the classical Laplacian, eigenfunctions of the fractional Laplacian are in general non-smooth [39, 72]. Indeed, considering a smooth function d that behaves like $\operatorname{dist}(x, \partial\Omega)$ near to $\partial\Omega$, all eigenfunctions ϕ_k belong to the space $d^s C^{2s(-\varepsilon)}(\Omega)$ (the ε is active only if $s = 1/2$) and $\frac{\phi_k}{d^s}$ does not vanish near $\partial\Omega$. The best Sobolev regularity guaranteed for solutions of (2.0.1) is $\phi_k \in H^{s+1/2-\varepsilon}(\mathbb{R}^n)$ for $\varepsilon > 0$ (see [20]).

The reduced Sobolev regularity of eigenfunctions precludes the possibility of solutions to equation (0.0.3) being smooth, even for $\alpha = 1$. This is in stark contrast with the case of the classical Laplacian. However, solutions of diffusion equations with memory –local in space but fractional in time– are known to be less regular than their classical

counterparts [64]. The effect of fractional differentiation in time is that high-frequency modes are less strongly damped than in classical diffusion, and the time derivatives of the solution are unbounded as $t \to 0$.

In order to represent the solutions in terms of the eigenfunctions, considering $t \in (0, T]$, we define now two useful operators, $E^\alpha(t), F^\alpha(t) : L^2(\Omega) \to L^2(\Omega)$,

$$E^\alpha(t)(v) := \sum_k E_{\alpha,1}(-\lambda_k t^\alpha)\phi_k(\phi_k, v)_{L^2(\Omega)}, \tag{2.0.2}$$

$$F^\alpha(t)(v) := \sum_k t^{\alpha-1} E_{\alpha,\alpha}(-\lambda_k t^\alpha)\phi_k(\phi_k, v)_{L^2(\Omega)}. \tag{2.0.3}$$

For technical purposes we define the norm

$$\|w\|_{\theta,s} := \Big(\sum_k \lambda_k^\theta (w, \phi_k)^2_{L^2(\Omega)}\Big)^{\frac{1}{2}}. \tag{2.0.4}$$

It can be easily verified that $\|w\|_{0,s} = \|w\|_{L^2(\Omega)}$, $\|w\|_{1,s} = |w|_{H^s(\mathbb{R}^n)}$, and $\|w\|_{2,s} = \|(-\Delta)^s w\|_{L^2(\Omega)}$. Additionally, we denote $\dot{H}^\theta(\Omega) \subset H^{-s}(\Omega)$, $\theta \geq -1$, the space induced by the norm (2.0.4).

The following two lemmas are helpful estimates involving the operators (2.0.2) and (2.0.3), which will be used later both in regularity results and in error estimates for numerical approximations.

Lemma 2.0.2. *Consider $t > 0$, then we have*

$$\|E^\alpha(t)v\|_{p,s} \leq Ct^{-\alpha(p-q)/2}\|v\|_{q,s}, \quad \text{if } 0 \leq p - q \leq 2, \tag{2.0.5}$$

$$\|F^\alpha(t)v\|_{p,s} \leq Ct^{-1+\alpha(1+(q-p)/2)}\|v\|_{q,s}, \quad \text{if } 0 \leq p - q \leq 4, \tag{2.0.6}$$

Proof. From the definition of F^α and Lemma 1.3.2 we have

$$\begin{aligned}
\|F^\alpha(t)v\|^2_{p,s} &= \sum_k \lambda_k^p |t^{\alpha-1}E_{\alpha,\alpha}(-\lambda_k)|^2 (v, \phi_k)^2 \\
&= Ct^{-2+(2+q-p)\alpha} \sum_k (\lambda_k t^\alpha)^{p-q} |E_{\alpha,\alpha}(-\lambda_k t^\alpha)|^2 \lambda_k^q (v, \phi_k)^2 \\
&\leq Ct^{-2+(2+q-p)\alpha} \sum_k \frac{(\lambda_k t^\alpha)^{p-q}}{(1 + (\lambda_k t^\alpha)^2)^2} \lambda_k^q (v, \phi_k)^2 \\
&\leq Ct^{-2+(2+q-p)\alpha} \sum_k \lambda_k^q (v, \phi_k)^2 \leq Ct^{-2+(2+q-p)\alpha}\|v\|^2_{q,s},
\end{aligned}$$

where we have used that $\sup_{t>0} \frac{(\lambda_k t^\alpha)^{p-q}}{(1+(\lambda_k t^\alpha)^2)^2} \leq C$ for $0 \leq p-q \leq 4$, and then (2.0.6) follows. Finally, (2.0.5) can be derived with similar arguments. □

Another useful result is the following estimation on the time derivatives of the operator E^α.

Lemma 2.0.3. *If $v \in \dot{H}^q$, $q \in [0,2]$, then for $m \geq 1$*

$$\|\partial_t^m E^\alpha(t)v\|_{L^2(\Omega)} \leq Ct^{q\alpha/2-m}\|v\|_{\dot{H}^q}.$$

Proof. From (1.3.1), we have $\frac{d^m}{dt^m}E_{\alpha,1}(-\lambda t^\alpha) = -\lambda t^{\alpha-m}E_{\alpha,\alpha+1-m}(-\lambda t^\alpha)$. Then, by (1.3.2), we deduce

$$\begin{aligned}
\|\partial_t^m E^\alpha(t)v\|^2_{L^2(\Omega)} &= \|\sum_{k=1}^{\infty} \frac{d^m}{dt^m}E_{\alpha,1}(-\lambda_k t^\alpha)(v,\phi_k)_{L^2(\Omega)}\phi_k\|^2_{L^2(\Omega)} \\
&= \sum_{k=1}^{\infty}(\lambda_k t^\alpha)^{2-q}t^{q\alpha-2m}E_{\alpha,\alpha-m+1}(-\lambda_k t^\alpha)^2(v,\phi_k)^2_{L^2(\Omega)}\lambda_k^q \\
&\leq ct^{q\alpha-2m}\sup_{k\geq 1}\frac{(\lambda_k t^\alpha)^{2-q}}{(1+\lambda_k t^\alpha)^2}\sum_{k=1}^{\infty}(v,\phi_k)^2_{L^2(\Omega)}\lambda_k^q \leq ct^{q\alpha-2m}\|v\|^2_{\dot{H}^q},
\end{aligned}$$

and the lemma follows. □

Additionally, we define the operator $A : \widetilde{H}^s(\Omega) \subset H^{-s}(\Omega) \to H^{-s}(\Omega)$ as the one that satisfies

$$(Au,\varphi)_{L^2(\Omega)} = \langle u,\varphi\rangle_{H^s(\mathbb{R}^n)} \quad \forall \varphi \in \widetilde{H}^s(\Omega). \tag{2.0.7}$$

From the previous definition, we observe that $(Av,v)_{L^2(\Omega)} = \langle v,v\rangle_{H^s(\mathbb{R}^n)} \geq 0$, for all $v \in \widetilde{H}^s(\Omega)$. And also, from the fact that $R(A) = H^{-s}(\Omega)$, and A^{-1} is a compact operator, it is possible to show that $R(I+A) = H^{-s}(\Omega)$, or in other words,

$$\forall w \in H^{-s}(\Omega), \quad \exists u \text{ such that } u + Au = w.$$

From this, and [22, Proposition 7.1], we can assert that

$$\|(I+\lambda A)^{-1}\|_{L^2(\Omega)} \leq 1, \quad \forall \lambda > 0. \tag{2.0.8}$$

Now we finish this section by giving an auxiliary result regarding the differentiation under the integral sign, when the integral is computed in the Bochner sense.

Lemma 2.0.4. *Let $f \in C([0,T], L^2(\Omega))$, with f differentiable in $(0,T)$ in such a way that $\|f'(t)\|_{L^2(\Omega)} \leq Ct^{-\gamma}$ with $\gamma \in (0,1)$ for all $t \in (0,T)$. Then we have*

$$\partial_t\Big(\int_0^t f(t-s)\,ds\Big) = f(0) + \int_0^t \partial_t f(t-s)\,ds \quad \forall t \in (0,T). \tag{2.0.9}$$

Proof. We have

$$\int_0^{t+h} f(t+h-s)\,ds - \int_0^t f(t-s)\,ds \tag{2.0.10}$$

$$= \int_0^t f(t+h-s) - f(t-s)\,ds + \int_t^{t+h} f(t+h-s)\,ds.$$

From the mean value inequality in Banach spaces (see [66, Appendix B] for instance) we can estimate

$$\|f(t+h-s) - f(t-s)\|_{L^2(\Omega)} \le h\|f'(r-s)\|_{L^2(\Omega)}$$

$$\le Ch(r-s)^{-\gamma} \le Ch(t-s)^{-\gamma}, \quad \forall s \in [0,t).$$

This, along with the fact that f' exists in $(0,T)$, allows us to use the Domitated Convergence Theorem (see [66, Appendix B]) and get

$$\lim_{h\to 0} \int_0^t \frac{f(t+h-s) - f(t-s)}{h}\,ds = \int_0^t f'(t-s)\,ds. \tag{2.0.11}$$

On the other hand, from the fact that $f(t)$ is a continuous function in $t = 0$, we have

$$\frac{1}{h}\int_t^{t+h} f(t+h-s)\,ds = \frac{1}{h}\int_h^0 -f(r)\,dr = \frac{1}{h}\int_0^h f(r)\,dr \xrightarrow[h\to 0]{} f(0), \tag{2.0.12}$$

where the convergence is in $L^2(\Omega)$ sense.

Finally, combining (2.0.10), (2.0.11) and (2.0.12), we obtain (2.0.9). □

2.1 Fractional diffusion equation

Considering problem (0.0.3) with $\alpha \in (0,1)$, we say that u is a *weak solution* of (0.0.3) if $u \in W^{1,1}((0,T), L^2(\Omega)) \cap C((0,T], \widetilde{H}^s(\Omega))$ and satisfies the equation (in $L^2(\Omega)$)

$${}^C\partial_t^\alpha u + Au = f, \tag{2.1.1}$$

almost everywhere in $(0,T)$, and $u(0) = v$. Here A is the operator defined in (2.0.7), and $v \in L^2(\Omega)$. Note we are forcing u to have a weak derivative in $L^1([0,T], L^2(\Omega))$, this condition, in particular, ensures the existence of ${}^C\partial_t^\alpha u$.

2.1.1 Solution representation

Now we formally derive a representation for solutions of (0.0.3) with $\alpha \in (0,1)$, and then we introduce the concept of *mild solution*.

Notice that we can write solutions of (0.0.3) by means of separation of variables,

$$u(x,t) = \sum_{k=1}^{\infty} u_k(t)\,\phi_k(x). \tag{2.1.2}$$

Then, for every $k \geq 1$ it must hold that

$$\begin{cases} {}^{C}\partial_t^{\alpha} u_k + \lambda_k u_k = f_k, \\ u_k(0) = v_k, \end{cases} \tag{2.1.3}$$

where $f_k = (f, \phi_k)_{L^2(\Omega)}$, and $v_k = (v, \phi_k)_{L^2(\Omega)}$. Existence and uniqueness of solutions to (2.1.3) follow from standard theory for fractional-order differential equations [31, Theorem 7.2]. Moreover, solutions of (2.1.3) may be represented as the superposition of the respective solution of the problem with initial data equal to zero and the solution of the problem with vanishing right-hand side. Namely, defining

$$F_k(t)w = \int_0^t (t-r)^{\alpha-1} E_{\alpha,\alpha}(-\lambda_k (t-r)^{\alpha})\, w(r)\, dr,$$

the solution of (2.1.3) may be written as

$$u_k(t) = F_k(t) f_k + v_k E_{\alpha,1}(-\lambda_k t^{\alpha}) \tag{2.1.4}$$

This fact can be derived from the following result.

Lemma 2.1.1. *Considering $F_k(t)$ defined as before, we have*

$${}^{C}\partial_t^{\alpha} F_k(t)w = -\lambda_k F_k(t)w + f_k(t). \tag{2.1.5}$$

Proof. First, using the relation ([31, Theorem 3.1])

$${}^{C}\partial_t^{\alpha} w = \partial_t^{\alpha}(w - w(0)), \tag{2.1.6}$$

along with the properties of the Laplace transform involving the fractional integral and the usual derivative, it is possible to write

$$\mathcal{L}(\partial_t^{\alpha} w)[z] = z^{\alpha}\mathcal{L}(F_k w)[z] - z^{\alpha-1} F_k(0)w.$$

Note that, since we are deriving a solution representation in a *formal* fashion, we are ignoring regularity conditions on w. However, (2.1.1) requires some smoothness on w (see Remark 2.1.5, below).

Applying the Laplace transform at both sides of (2.1.5) we obtain

$$z^\alpha \mathcal{L}(F_k w)[z] - z^{\alpha-1} F_k(0) w = -\lambda_k \mathcal{L}(F_k w)[z] + \mathcal{L}(f_k)[z], \tag{2.1.7}$$

and observing that $F_k(0)w = 0$ we have

$$\mathcal{L}(F_k w)[z] = (z^\alpha + \lambda_k)^{-1} \mathcal{L}(f_k)[z].$$

Applying $\mathcal{L}^{-1}$ at both sides we get

$$F_k(t)w = \mathcal{L}^{-1}((z^\alpha + \lambda_k)^{-1}) * f_k(t) = \int_0^t (t-r)^{\alpha-1} E_{\alpha,\alpha}(-\lambda_k (t-r)^\alpha)\, w(r)\, dr,$$

where in the last step we have used Lemma 1.3.3. Then (2.1.5) follows. □

Note that for the particular value of $\alpha = 1$ expression (2.1.4) yields the well-known formula

$$u_k(t) = \int_0^t e^{-\lambda_k (t-r)} f_k(r)\, dr \ + v_k e^{-\lambda_k t},$$

usually derived by the method of variation of parameters.

Summing the solutions for every eigenmode, we obtain the representation

$$u(t) = E^\alpha(t)v + \int_0^t F^\alpha(t-s) f(s)\, ds =: M(v,f)(t), \tag{2.1.8}$$

with E^α and F^α the operators defined in (2.0.2) and (2.0.3) respectively. We say that $u(t) = M(v,f)(t)$ is a *mild solution* of (0.0.3). Next result tells us that, under suitable regularity conditions on the initial data, $M(v,f)$ is a weak solution.

Theorem 2.1.2. *Let Ω be a bounded, smooth domain, $s \in (0,1)$ and $\alpha \in (0,1]$ and $u(t) = M(v,f)$ a mild solution of (0.0.3). Assume that $f \in C([0,T], L^2(\Omega))$, differentiable in $(0,T)$, and $\|f'(t)\|_{L^2(\Omega)} \le C t^{\gamma-1}$ with $C > 0$ and $\gamma \in (0,1)$. Finally, assume that $v \in \dot{H}^q(\Omega)$ for some $q > 0$. Then u is a weak solution of (0.0.3).*

Proof. Suppose first $f \equiv 0$. Then $u = E^\alpha(t)v$. For this case we have

$$|E^\alpha(t)v|^2_{H^s(\mathbb{R}^n)} = \sum_k \lambda_k E^2_{\alpha,1}(-\lambda_k t^\alpha)(v, \phi_k)^2_{L^2(\Omega)}.$$

From the uniform convergence of the series with $t > 0$ we can assert that $u \in C((0,T], \widetilde{H}^s(\Omega))$. On the other hand, from Lemma 2.0.3 we know that $\partial_t E^\alpha(t)v \in C((0,T], L^2(\Omega))$, and

$$\|\partial_t E^\alpha(t)v\|_{L^2(\Omega)} \le t^{q\alpha/2-1} \|v\|_{q,s}.$$

Then we can conclude that $u \in W^{1,1}((0,T),L^2(\Omega))$.

Assume now that $v \equiv 0$. In this case we have $u(t) = \int_0^t F^\alpha(t-s)f(s)\,ds$. Arguing as before, it can be seen that $u \in C((0,T],\widetilde{H}^s(\Omega))$. Now, using Lemma 2.0.4 , we obtain

$$\partial_t u(t) = F^\alpha(t)f(0) + \int_0^t F^\alpha(s)f'(t-s)\,ds,$$

from here we can conclude that $\partial_t u \in C((0,T],L^2(\Omega))$. Moreover, in view of Lemma 2.0.2, we can estimate

$$\|\partial_t u(t)\|_{L^2(\Omega)} \leq Ct^{\alpha-1}\|f(0)\|_{L^2(\Omega)} + C\int_0^t s^{\alpha-1}(t-s)^{\gamma-1}\,ds$$

$$= Ct^{\alpha-1}\|f(0)\|_{L^2(\Omega)} + Ct^{\alpha+\gamma-1}\int_0^1 r^{\alpha-1}(1-r)^{\gamma-1}\,dr = Ct^{\alpha-1}\|f(0)\|_{L^2(\Omega)} + Ct^{\alpha+\gamma-1}B(\alpha,\gamma),$$

where in the third step we have made the change of variable $r = s/t$, and $B(\alpha,\gamma)$ denotes the beta function. Finally, the last estimation implies $u \in W^{1,1}((0,T),L^2(\Omega))$ and the statement of the theorem follows. □

2.1.2 Regularity of solutions

In this section we state some regularity results for solutions of the problems under consideration. We split the estimates according to whether the initial values or the forcing term are null. We also recall also that throughout this chapter we are assuming that Ω is a domain with smooth boundary, so that Proposition 1.2.1 holds. According to that proposition, we fix the notation $\gamma := \min\{s, 1/2-\varepsilon\}$, with $\varepsilon > 0$ arbitrarily small.

Theorem 2.1.3. *Let $0 < \alpha < 1$ and suppose that $f \equiv 0$. Let u, given by (2.1.2), be the mild solution of (0.0.3) with initial and boundary conditions according to (0.0.4).*

a. If $v \in L^2(\Omega)$, then $u \in C([0,T];L^2(\Omega)) \cap C((0,T];\widetilde{H}^s(\Omega)\cap H^{s+\gamma}(\Omega))$ and ${}^C\partial_t^\alpha u \in C((0,T];L^2(\Omega))$. Moreover, there exists a constant $C > 0$ such that

$$\|u\|_{C([0,T];L^2(\Omega))} \leq C\|v\|_{L^2(\Omega)}, \tag{2.1.9}$$

$$\|u(\cdot,t)\|_{H^{s+\gamma}(\Omega)} + \|{}^C\partial_t^\alpha u(\cdot,t)\|_{L^2(\Omega)} \leq Ct^{-\alpha}\|v\|_{L^2(\Omega)}. \tag{2.1.10}$$

b. Assume that $v \in \widetilde{H}^s(\Omega)$. Then, $u \in L^2(0,T;\widetilde{H}^s(\Omega)\cap H^{s+\gamma}(\Omega))$, ${}^C\partial_t^\alpha u \in L^2(\Omega\times(0,T))$, and the following estimate holds:

$$\|u\|_{L^2(0,T;H^{s+\gamma}(\Omega))} + \|{}^C\partial_t^\alpha u\|_{L^2(\Omega\times(0,T))} \leq C\|v\|_{H^s(\mathbb{R}^n)}. \tag{2.1.11}$$

c. *Furthermore, if* $v \in \widetilde{H}^s(\Omega)$ *is such that* $(-\Delta)^s v \in L^2(\Omega)$*, then* $u \in C([0,T];\widetilde{H}^s(\Omega)\cap H^{s+\gamma}(\Omega))$, ${}^C\partial_t^\alpha u \in C([0,T];L^2(\Omega))$ *and the bound*

$$\|u\|_{C([0,T];H^{s+\gamma}(\Omega))} + \|{}^C\partial_t^\alpha u\|_{C([0,T];L^2(\Omega))} \leq C\|(-\Delta)^s v\|_{L^2(\Omega)} \tag{2.1.12}$$

is satisfied for some $C > 0$ *independent of* v.

Proof. Using (2.0.5) we can estimate

$$\|u(\cdot,t)\|_{L^2(\Omega)} = \|E^\alpha(t)v\|_{L^2(\Omega)} \leq C\|v\|_{L^2(\Omega)},$$

from which we can conclude (2.1.9). Next, recalling that $\|u\|_{H^{s+\gamma}(\Omega))} \leq \|(-\Delta)^s u\|_{L^2(\Omega)}$ (from Proposition 1.2.1) and using (2.0.5) with $p = 2, q = 0$, we have

$$\|u(\cdot,t)\|_{H^{s+\gamma}(\Omega))} \leq \|(-\Delta)^s u(\cdot,t)\|_{L^2(\Omega)} \leq \|(-\Delta)^s E^\alpha(t)v\|_{L^2(\Omega)} \leq t^{-\alpha}\|v\|_{L^2(\Omega)}.$$

Since u is a solution for (0.0.3) with $f \equiv 0$, we have ${}^C\partial_t^\alpha u = -(-\Delta)^s u$, and using again (2.0.5) we obtain (2.1.10).

For the second item, proceeding analogously as in the previous step, and using (2.0.5) with $p = 2, q = 1$, we have

$$\|u\|_{H^{s+\gamma}(\Omega)} + \|{}^C\partial_t^\alpha u\|_{L^2(\Omega)} \leq Ct^{-\alpha/2}\|v\|_{H^s(\mathbb{R}^n)}.$$

Noticing that $0 < \alpha < 1$, (2.1.11) follows. Finally, (2.1.12) can be derived by means of similar arguments. □

Regularity estimates for the *fractional diffusion* problem with a non-homogeneous right-hand side function f are also attainable.

Theorem 2.1.4. *Let* $0 < \alpha \leq 1$ *and consider* u*, given by* (2.1.2)*, the mild solution of* (0.0.3) *with homogeneous initial and boundary conditions. If* $f \in L^\infty(0,T;L^2(\Omega))$*, then* $u \in L^2(0,T;\widetilde{H}^s(\Omega)\cap H^{s+\gamma}(\Omega))$, ${}^C\partial_t^\alpha u \in L^2(\Omega\times(0,T))$ *and*

$$\|u\|_{L^2(0,T;H^{s+\gamma}(\Omega))} + \|{}^C\partial_t^\alpha u\|_{L^2(\Omega\times(0,T))} \leq C\|f\|_{L^\infty(0,T;L^2(\Omega))}. \tag{2.1.13}$$

Proof. First we observe that, as a consequence of Lemma 1.3.4 and Lemma 1.3.1, we have

$$\int_0^\eta |t^{\alpha-1}E_{\alpha,\alpha}(-\lambda_k t^\alpha)|\,dt = \int_0^\eta t^{\alpha-1}E_{\alpha,\alpha}(-\lambda_k t^\alpha)\,dt = \tag{2.1.14}$$

$$-\frac{1}{\lambda_k}\int_0^\eta \partial_t E_{\alpha,1}(-\lambda_k t^\alpha)\,dt = \frac{1}{\lambda_k}\big(1 - E_{\alpha,1}(-\lambda_k\eta^\alpha)\big), \quad \eta > 0.$$

On the other hand, by means of Lemma 2.1.1, it can be shown that

$$
\begin{aligned}
&{}^{C}\partial_t^{\alpha} \int_0^t f_k(s)(t-s)^{\alpha-1} E_{\alpha,\alpha}\big(-\lambda_k(t-s)^{\alpha}\big)\, ds \qquad (2.1.15)\\
&= -\lambda_k \int_0^t f_k(s)(t-s)^{\alpha-1} E_{\alpha,\alpha}\big(-\lambda_k(t-s)^{\alpha}\big)\, ds + f_k(t).
\end{aligned}
$$

At this point, we can estimate

$$
\begin{aligned}
&\left\| {}^{C}\partial_t^{\alpha} \int_0^t f_k(s)(t-s)^{\alpha-1} E_{\alpha,\alpha}\big(-\lambda_k(t-s)^{\alpha}\big)\, ds \right\|^2_{L^2([0,T])}\\
&\leq C\|f_k\|^2_{L^2([0,T])} + C\left\| \lambda_k \int_0^t f_k(s)(t-s)^{\alpha-1} E_{\alpha,\alpha}\big(-\lambda_k(t-s)^{\alpha}\big)\, ds \right\|^2_{L^2([0,T])}\\
&\leq C\|f_k\|^2_{L^2([0,T])} + C\|f_k\|^2_{L^2([0,T])} \left(\int_0^T |\lambda_k s^{\alpha-1} E_{\alpha,\alpha}(-\lambda_k s^{\alpha})|\, ds \right)\\
&\leq C\|f_k\|^2_{L^2([0,T])},
\end{aligned}
$$

where we have used (2.1.15) in the first inequality, Young's inequality for the convolution in the second step, and (2.1.14) in the last inequality. Now, the previous estimate implies

$$
\|{}^{C}\partial_t^{\alpha} u\|^2_{L^2(\Omega\times(0,T))} \leq C \sum_k \|f_k\|^2_{L^2([0,T])} = C \sum_k \int_0^T |f_k(s)|^2\, ds = C\|f\|^2_{L^2(\Omega\times(0,T))}.
$$

Finally, observing that

$$
\|u(t)\|_{H^{s+\gamma}(\Omega)} \leq C\|(-\Delta)^s u(t)\|_{L^2(\Omega)} \leq \|{}^{C}\partial_t^{\alpha} u(t)\|_{L^2(\Omega)} + \|f(t)\|_{L^2(\Omega)},
$$

and integrating between 0 and T on both sides of the inequality, we obtain (2.1.13). □

Remark 2.1.5. It is worth mentioning that regularity conditions on v and f in theorems 2.1.3 and 2.1.4 may not guarantee that $M(v, f)$ is a weak solution. This implies that a special attention must be paid in some aspects of the classical theory. Specifically, since we could have $u \notin W^{1,1}((0,T), L^2(\Omega))$, ${}^{C}\partial_t^{\alpha} u$ may not be well defined. Furthermore, relation (4.1.12) (also used in [45]) may not be hold. The regularity conditions in Theorems 2.1.3 and 2.1.4 also allow $f \notin W^{1,1}((0,T), L^2(\Omega))$. In that case, equalities (2.1.15) ([74, eq. 3.8]) and (2.1.7) may not be hold.

In order to avoid these technicalities, throughout this work we are going to assume v and f verify the hypotheses of Theorem 2.1.2. Nonetheless, we think that the restrictions on f can be relaxed, Lemma 2.0.3 suggests that if $v \in L^2(\Omega)$ and

$v \notin \dot{H}^q(\Omega)$ for any $q > 0$, then we could have $\partial_t E^\alpha(t)v \notin L^1((0,T), L^2(\Omega))$. In fact, it is possible to show an explicit example of a function $v \in L^2(\Omega)$ in such a way that $\partial_t E^\alpha(t)v \notin L^1((0,T), L^2(\Omega))$. Indeed, consider $s = 1$ for the sake of simplicity, and set $a_k := 1/\sqrt{k}\log(k)$. We can define

$$v_0 := \sum_{k\geq 2} a_k \phi_k. \tag{2.1.16}$$

Taking $t \in (0,T]$ and using the uniform convergence of the series it can be seen that $\partial_t E^\alpha(t)v_0 \in C^1((0,T], L^2(\Omega))$. Our goal is to prove that $\partial_t E^\alpha(t)v_0 \notin L^1((0,T), L^2(\Omega))$. To this end, we can estimate

$$\begin{aligned} \|\partial_t E^\alpha(t)v_0\|^2_{L^2(\Omega)} &= \sum_{k\geq 2} \lambda_k^2 t^{2\alpha-2} E^2_{\alpha,\alpha}(-\lambda_k t^\alpha) a_k^2 \geq Ct^{-2} \sum_{k\geq 2} (\lambda_k t^\alpha)^2 E^2_{\alpha,\alpha}(-\lambda_k t^\alpha) a_k^2 \\ &\geq Ct^{-2} \sum_{k\geq 2} \frac{(\lambda_k t^\alpha)^2}{1+(\lambda_k t^\alpha)^4} a_k^2, \end{aligned} \tag{2.1.17}$$

where we have used Lemma 1.3.2 in the last step. So we want to study the behavior of the last term when $t \to 0$. To this end, we define the auxiliary function

$$g(x) := \begin{cases} x^2, & \text{if } x \leq 1, \\ \dfrac{1}{x^2}, & \text{if } x > 1. \end{cases}$$

Observing that $\frac{x^2}{(1+x^4)g(x)} \in O(1)$, $\lambda_k \in O(k^2)$, and considering $t = (1/n^2)^{1-\alpha}$ we can estimate

$$\begin{aligned} \sum_{k\geq 2} \frac{(\lambda_k t^\alpha)^2}{1+(\lambda_k t^\alpha)^4} a_k^2 &\geq C \sum_{k\geq 2} g(\lambda_k t^\alpha) a_k^2 \geq C \sum_{k\geq 2} g((k/n)^2) a_k^2 \\ &\geq C \sum_{k\geq 2}^{n} (k/n)^4 a_k^2 = C \frac{1}{n^4} \sum_{k\geq 2}^{n} \frac{k^3}{\log^2(k)} \geq \frac{C}{\log^2(n)}, \end{aligned}$$

where in the third step we have used the fact that $(k/n)^2 \leq 1$ for all $k \leq n$ and the definition of g. The last bound can be obtained, for instance, by means of the Stolz-Césaro Theorem.

Combining the former inequality with (2.1.17) and recalling $t = (1/n)^{2-2\alpha}$, we deduce

$$\|\partial_t E^\alpha(t)v_0\|_{L^2(\Omega)} \geq Ct^{-1}\log^{-1}(t^{2\alpha-2}),$$

for small values of t, from we can conclude that $\partial_t E^\alpha(t)v_0 \notin L^1((0,T), L^2(\Omega))$.

Remark 2.1.6. There are many possible settings leading to right formulations of equations of the type considerer here. For instance, in [49] it is shown that the Caputo derivative is a linear and bounded operator on a time-fractional Sobolev-Bochner space. The author considers a variational formulation based exclusively on Sobolev regularity and proves that if the initial condition belongs to $H^{1-1/\alpha+\varepsilon}(\Omega)$ for some $\varepsilon > 0$ and $\alpha > 1/2$, then the time-fractional problem is well posed with $u \in H^{\alpha}((0,T), H_0^1(\Omega))$. Another approach is given in [37] Gorenflo, Luchko and Yamamoto, where the authors define a weak solution as the limit of the solutions with smooth source term, with u belonging to $H^{\alpha}((0,T), L^2(\Omega)) \cap L^2(0,T; H^2(\Omega) \cap H_0^1(\Omega))$. A special mention deserves the theory developed by Gal and Warma [35], where a general semilinear problem (including the problem treated in this work) is defined by the Caputo derivative directly through the Riemann-Liouville differential operator. In this way, they obtain global existence and regularity results under mild assumptions of data.

In any case, the aforementioned alternative formulations do not guarantee the condition $u \in W^{1,1}((0,T), L^2(\Omega))$ that is pivotal in our treatment of the numerical error for the semilinear problem. Since this condition can be obtained under rather weak regularity assumptions on the initial datum (i.e. $v \in \dot{H}^q(\Omega)$ for some $q > 0$), we consider that our formulation, although not completely general, is appropriate in the context of this work.

2.2 A semilinear fractional evolution problem

Now our goal is to study a semi-linear version of problem (0.0.3). That is: find u such that

$$\begin{cases} {}^C\partial_t^{\alpha} u + \varepsilon^2(-\Delta)^s u &= f(u) \text{ in } \Omega \times (0,T], \\ u(0) &= v \text{ in } \Omega, \\ u &= 0 \text{ in } \Omega^c \times [0,T], \end{cases} \tag{2.2.1}$$

where, as before, Ω is a bounded domain in $\mathbb{R}^n$ with a sufficiently smooth boundary, $v \in L^2(\Omega)$, and $0 < \alpha \leq 1$. All the analysis will be made for a very restricted non-linear term. That is, we are going to consider $f : \mathbb{R} \to \mathbb{R}$, such that

$$f \in C^2(\mathbb{R}), f(0) = 0, \text{ and} \tag{2.2.2}$$

$$|f|, |f'|, |f''| < B \text{ for some } B > 0. \tag{2.2.3}$$

The idea is, once we have established the theory for this problem, to extend our results to other kind of non-linear terms, by taking advantage of certain L^{∞} bounds. For example, in Chapter 5, we present the analysis for the fractional Allen-Cahn equation, where $f(u) = u - u^3$, that obviously does not comply with (2.2.3). There we show how

to handle this case by proving that, for a suitable truncation of f verifing conditions (2.2.2) (2.2.3), the solution remains bounded between 1 and -1. L^∞ bounds for u are first proved for the semidiscrete in time scheme and then extended to the continuous solution by means of density arguments.

2.2.1 Weak formulation and solution representation

We call u a weak solution of problem (2.2.1) if $u \in W^{1,1}((0,T), L^2(\Omega)) \cap C((0,T], \widetilde{H}^s(\Omega))$ and

$$\begin{cases} ({}^C\partial_t^\alpha u, \varphi) + \varepsilon^2 \langle u, \varphi \rangle_{H^s(\mathbb{R}^n)} &= (f(u), \varphi) \quad \forall \varphi \in \widetilde{H}^s(\Omega), \\ u(0) &= v \text{ in } \Omega, \end{cases} \tag{2.2.4}$$

for almost all $t \in (0,T)$.

Using the operator A defined in (2.0.7), the formulation (2.2.4) can be understood as find $u \in W^{1,1}((0,T), L^2(\Omega)) \cap C((0,T], \widetilde{H}^s(\Omega))$ such that

$${}^C\partial_t^\alpha u + \varepsilon^2 A u = f(u), \tag{2.2.5}$$

for almost all $t \in (0,T)$ with $u(0) = v$ in Ω.

For every $v \in L^2(\Omega)$, the solution of (2.2.5) should satisfy the integral equation

$$u(t) = E^\alpha(\varepsilon^2 t)v + \int_0^t F^\alpha(\varepsilon^2(t-s)) f(u(s))\, ds. \tag{2.2.6}$$

If u is a solution of equation (2.2.6), we say that u is a mild solution of problem (2.2.1), and we use the notation $u(t) =: M(v, f)$.

2.2.2 Existence and Uniqueness

For the sake of simplicity we are going to consider $\varepsilon^2 = 1$ along this section.

To obtain an existence and uniqueness result for the integral equation (2.2.6), we base our framework in the one displayed by Larsson in [53] and Mendes de Carvalho in [26]. With the aim of giving a local existence result, first we define the space

$$\mathbb{V}_\tau^q := \{w \in C([0,\tau], L^2(\Omega)) \cap C^1((0,\tau], L^2(\Omega)) \text{ such that } \|w\|_{\mathbb{V}_\tau^q} < \infty\}$$

where the norm $\|w\|_{\mathbb{V}_\tau^q}$ is defined as

$$\|w\|_{\mathbb{V}_\tau^q} := \sup_{t\in[0,\tau]} \|w(t)\|_{L^2(\Omega)} + \sup_{t\in[0,\tau]} t^{(1-q)\alpha/2} |w(t)|_s + \sup_{t\in[0,\tau]} t^{1-q\alpha/2} \|\partial_t w(t)\|_{L^2(\Omega)},$$

with $q \in (0,1]$. By means of standard arguments it can be proved that $\mathbb{V}_\tau^q$ is a Banach space.

Now we give a local existence result.

Theorem 2.2.1. *Suppose we have an initial datum $\|v\|_{q,s} \leq R_0$ for some $R_0 > 0$ with $q \in (0,1]$. Then, there exists $\tau > 0$ small enough, such that equation (2.2.6) has a unique solution $u \in \mathbb{V}_\tau^q$.*

Proof. First, we define the operator $\mathcal{S}(u)$

$$\mathcal{S}(u)(t) := E^\alpha(t)v + \int_0^t F^\alpha(t-s)f(u(s))\,ds, \tag{2.2.7}$$

and $B_R = \{w \in \mathbb{V}_\tau^q \text{ such that } \|w\|_{\mathbb{V}_\tau^q} \leq R, \text{ and } w(0) \equiv v\}$. It can be easily verified that $B_R \subset \mathbb{V}_\tau^q$ is a closed set. Our goal is to show that there are parameters $\tau > 0$ and $R > 0$, in such a way that we can apply Banach's fixed point Theorem. That is, we look for τ and R, such that $\mathcal{S}$ maps B_R into itself, and results in a contraction over B_R.

Indeed, observing first that $\mathcal{S}(u)(0) \equiv v$ for all $u \in \mathbb{V}_\tau^q$, then the condition $u(0) \equiv v$ is satisfied for every output of $\mathcal{S}$. Furthermore, by means of Lemma 2.0.4, it can be seen that $\mathcal{S}(u)(t) \in C([0,\tau], L^2(\Omega)) \cap C^1((0,\tau], L^2(\Omega))$. Suppose now $u \in B_R$, from (2.2.7), Lemma 2.0.2, and the definition of f, we have

$$t^{(1-q)\alpha/2}|\mathcal{S}(u)(t)|_{H^s(\mathbb{R}^n)} \leq$$

$$t^{(1-q)\alpha/2}|E^\alpha(t)v|_{H^s(\mathbb{R}^n)} + t^{(1-q)\alpha/2}\int_0^t |F^\alpha(t-s)f(u(s))|_{H^s(\mathbb{R}^n)}\,ds \leq$$

$$C\|v\|_{q,s} + Ct^{(1-q)\alpha/2}\int_0^t (t-s)^{\alpha/2-1}\|f(u(s))\|_{L^2(\Omega)}\,ds,$$

computing the integral, and using $t < \tau$, this estimation implies

$$t^{(1-q)\alpha/2}|\mathcal{S}(u)(t)|_{H^s(\mathbb{R}^n)} \leq CR_0 + C\tau^\alpha. \tag{2.2.8}$$

With the same idea we can obtain

$$\|\mathcal{S}(u)(t)\|_{L^2(\Omega)} \leq CR_0 + C\tau^\alpha \tag{2.2.9}$$

On the other hand, by means of Lemma 2.0.4, we have

$$\begin{aligned}\partial_t\Big(\int_0^t F^\alpha(t-s)f(u(s))\,ds\Big) &= \partial_t\Big(\int_0^t F^\alpha(s)f(u(t-s))\,ds\Big) \\ &= F^\alpha(t)f(v) + \int_0^t F^\alpha(s)f'(u(t-s))\partial_t u(t-s)\,ds,\end{aligned} \tag{2.2.10}$$

and we can estimate

$$t^{1-q\alpha/2}\|\partial_t \mathcal{S}(u)(t)\|_{L^2(\Omega)} \leq t^{1-q\alpha/2}\|\partial_t E^\alpha(t)v\|_{L^2(\Omega)} + t^{1-q\alpha/2}\|F^\alpha(t)f(v)\|_{L^2(\Omega)}$$

$$+t^{1-q\alpha/2}\int_0^t \|F^\alpha(s)f'(u(t-s))\partial_t u(t-s)\|_{L^2(\Omega)}\,ds$$

$$\leq CR_0 + CRt^{1-q\alpha/2}\int_0^t s^{\alpha-1}(t-s)^{q\alpha/2-1}\,ds$$

where we have applied Lemma 2.0.3, Lemma 2.0.2, the fact that $t^{1-q\alpha/2}\|\partial_t u(t)\|_{L^2(\Omega)} \leq \|u\|_{\mathbb{V}^q_\tau} \leq R$, and $t^{1-q\alpha/2}\|F^\alpha(t)f(v)\|_{L^2(\Omega)} \leq \tau^{(1-q/2)\alpha}\|v\|_{L^2(\Omega)}$. The integral in the second term can be estimated in terms of the beta function $B(\alpha, q\alpha/2)$. That is, making the change of variables $s/t = r$, we obtain

$$t^{1-q\alpha/2}\|\partial_t \mathcal{S}(u)(t)\|_{L^2(\Omega)} \leq CR_0 + CRt^\alpha\int_0^1 r^{\alpha-1}(1-r)^{q\alpha/2-1}\,dr \tag{2.2.11}$$

$$\leq CR_0 + CRB(\alpha, q\alpha/2)\tau^\alpha.$$

Combining (2.2.8), (2.2.9) and (2.2.11), we have

$$\|\mathcal{S}(u)\|_{\mathbb{V}^q_\tau} \leq CR_0 + CR\tau^\alpha,$$

where $C = C(\alpha)$. Then, fixing $R = 2CR_0$, we can choose $\tau > 0$ small enough to satisfy the inequality $\|\mathcal{S}(u)\|_{\mathbb{V}^q_\tau} < R$. Hence, for this τ, $\mathcal{S}$ maps B_R into itself.

Now we want to see that $\mathcal{S}$ is a contraction over B_R. Indeed, let u and $w \in B_R$, using $|f'| \leq B$ and Lemma 2.0.2, we have

$$t^{(1-q)\alpha/2}|\mathcal{S}(u)(t) - \mathcal{S}(w)(t)|_{H^s(\mathbb{R}^n)} \leq Ct^{(1-q)\alpha/2}\int_0^t (t-s)^{\alpha/2-1}\|f(u(s)) - f(w(s))\|_{L^2(\Omega)}\,ds \leq \tag{2.2.12}$$

$$\leq CBt^{(1-q)\alpha/2}\int_0^t (t-s)^{\alpha/2-1}\|u(s) - w(s)\|_{L^2(\Omega)}\,ds$$

$$\leq \|u-w\|_{\mathbb{V}^q_\tau} CBt^{(1-q)\alpha/2}\int_0^t (t-s)^{\alpha/2-1}\,ds$$

$$\leq Ct^{(2-q)\alpha}\|u-w\|_{\mathbb{V}^q_\tau} \leq C\tau^\alpha\|u-w\|_{\mathbb{V}^q_\tau}.$$

With similar arguments it can be seen that

$$\|\mathcal{S}(u)(t) - \mathcal{S}(w)(t)\|_{L^2(\Omega)} \leq C\tau^\alpha\|u-w\|_{\mathbb{V}^q_\tau}. \tag{2.2.13}$$

Recalling the equality (2.2.10), we have that

$$t^{1-q\alpha/2}\|\partial_t\big(\mathcal{S}(u)(t)-\mathcal{S}(w)(t)\big)\|_{L^2(\Omega)} \leq t^{1-q\alpha/2}\|F^\alpha(t)\big(u(0)-w(0)\big)\|_{L^2(\Omega)}$$

$$+t^{1-q\alpha/2}C\int_0^t s^{\alpha-1}\|f'(u(t-s))\partial_t u(t-s)-f'(w(t-s))\partial_t w(t-s)\|_{L^2(\Omega)}\,ds.$$

Using the identity

$$f'(u)\partial_t u - f'(w)\partial_t w = f'(u)(\partial_t u-\partial_t w)-(f'(u)-f'(w))\partial_t w,$$

and the fact that $u(0)\equiv w(0)\equiv v$, $t^{1-q\alpha/2}\|\partial_t w(t)\|_{L^2(\Omega)}\leq R$, $|f'|$, $|f''|\leq B$, we can write

$$t^{1-q\alpha/2}\|\partial_t\big(\mathcal{S}(u)(t)-\mathcal{S}(w)(t)\big)\|_{L^2(\Omega)} \leq t^{1-q\alpha/2}CB\int_0^t s^{\alpha-1}\|\partial_t\big(u(t-s)-w(t-s)\big)\|_{L^2(\Omega)}\,ds \tag{2.2.14}$$

$$+CBRt^{1-q\alpha/2}\int_0^t s^{\alpha-1}(t-s)^{\alpha/2-1}\|u(t-s)-w(t-s)\|_{L^2(\Omega)}\,ds$$

$$\leq C(1+R)\|u-w\|_{\mathbb{V}_\tau^q}t^{1-q\alpha/2}\int_0^t s^{\alpha-1}(t-s)^{q\alpha/2-1}\,ds$$

$$\leq CB(\alpha,q\alpha/2)\tau^\alpha\|u-w\|_{\mathbb{V}_\tau^q},$$

where the integrals in the last inequality have been estimated in terms of the beta function, as in (2.2.11), and $C=C(R)$.

Finally, combining (2.2.12), (2.2.13) and (2.2.14), we can conclude that

$$\|\mathcal{S}(u)(t)-\mathcal{S}(w)(t)\|_{\mathbb{V}_\tau^q}\leq C\tau^\alpha\|u-w\|_{\mathbb{V}_\tau^q},$$

with $C=C(\alpha,R)$, and it is clear that we can choose τ small enough, such that $\mathcal{S}$ results in a contraction over B_R. Hence, for that τ, there exists a unique solution for problem 2.2.1 in the interval $[0,\tau]$. □

Now, we need to derive an a priori estimate for the time derivative of the solution. To this end, we first state a useful and well known Gronwall type inequality.

Lemma 2.2.2. *Let the function $\varphi(t) \geq 0$ be continuous for $0 < t \leq T$. Then, if*

$$\varphi(t) \leq At^{-1+\alpha} + D + B\int_0^t (t-s)^{-1+\beta}\varphi(s)\,ds \quad 0 < t \leq T$$

for some constants A,D,B ≥ 0 and $\alpha, \beta > 0$, there exists a constant $C = C(B, T, \alpha, \beta)$ such that

$$\varphi(t) \leq C(At^{-1+\alpha} + D) \tag{2.2.15}$$

Proof. Iterating the first inequality $N-1$ times, using the identity

$$\int_0^t (t-s)^{-1+\alpha}s^{-1+\beta}\,ds = C(\alpha,\beta)t^{-1+\alpha+\beta} \quad \alpha, \beta > 0,$$

bounding t^β by T^β, and $\int_0^t (t-s)^{-1+\beta}ds$ by T^β/β, we obtain

$$\varphi(t) \leq C_1 At^{-1+\alpha} + C_2 D + C_3\int_0^t (t-s)^{-1+N\beta}\varphi(s), \quad 0 < t \leq T$$

where $C_1 = C_1(B, T, \alpha, \beta, N)$, $C_2 = C_2(B, T, \beta, N)$, and $C_3 = C_3(B, \beta, N)$. Now we choose the smallest N such that $-1 + N\beta \geq 0$, and estimate $(t-s)^{-1+N\beta}$ by $T^{-1+N\beta}$.

For the case $-1 + \alpha \geq 0$ we can conclude (2.2.15) by using a standard Gronwall type inequality. In other case, we can define $\psi(t) = t^{1-\alpha}\varphi(t)$ and obtain

$$\psi(t) \leq C_1 A + C_2 D t^{1-\alpha} + C_3 C\int_0^t s^{-1+\alpha}\psi(s)\,ds \quad 0 < t \leq T.$$

And again, using a standard Gronwall type inequality, we obtain

$$\psi(t) \leq C(A + Dt^{1-\alpha}),$$

from which we can derive (2.2.15). □

The following result gives us an estimation for $\|\partial_t u(t)\|_{L^2(\Omega)}$.

Lemma 2.2.3. *Let $u(t) = M(v, f)(t)$ with $v \in \dot{H}^q(\Omega)$ and $t \in [0, T]$, there exists a constant $C = C(\alpha, T)$ such that*

$$\|\partial_t u(t)\|_{L^2(\Omega)} \leq Ct^{\alpha/2-1} \tag{2.2.16}$$

Proof. For $h > 0$ we can write

$$u(t+h) - u(t) = \big(E^\alpha(t+h) - E^\alpha(t)\big)v + \int_0^{t+h} F^\alpha(t+h-s)f(u(s))\,ds \tag{2.2.17}$$

$$- \int_0^t F^\alpha(t-s) f(u(s))\, ds$$

$$= \big(E^\alpha(t+h) - E^\alpha(t)\big)v + \int_0^{t+h} F^\alpha(s) f(u(t+h-s))\, ds$$

$$- \int_0^t F^\alpha(s) f(u(t-s))\, ds$$

$$= \big(E^\alpha(t+h) - E^\alpha(t)\big)v + \int_t^{t+h} F^\alpha(s) f(u(t+h-s))\, ds$$

$$+ \int_0^t F^\alpha(s) \big(f(u(t+h-s)) - f(u(t-s))\big)\, ds$$

$$= \big(E^\alpha(t+h) - E^\alpha(t)\big)v + \int_t^{t+h} F^\alpha(s) f(u(t+h-s))\, ds$$

$$+ \int_0^t F^\alpha(t-s) \big(f(u(s+h)) - f(u(s))\big)\, ds.$$

Now, considering h small enough, and taking norms at both sides of the equality; using Lemma 2.0.3 in the first term on the left side; inequality (2.0.6), and $|f| < B$ in the second term and the same idea in the last one, we obtain

$$\|u(t+h)-u(t)\|_{L^2(\Omega)} \leq C\Big(ht^{q\alpha/2-1} + \int_t^{t+h} s^{\alpha-1}\, ds + \int_0^t (t-s)^{\alpha-1} \|u(s+h)-u(s)\|_{L^2(\Omega)}\, ds\Big)$$

$$\leq C(T)\Big(ht^{q\alpha/2-1} + \int_0^t (t-s)^{\alpha-1} \|u(s+h)-u(s)\|_{L^2(\Omega)}\, ds\Big). \tag{2.2.18}$$

Finally, applying Lemma 2.2.2 we derive (2.2.16). □

Combining the given results, we are now able to prove the global existence of the solution.

Theorem 2.2.4. *Under the hypotheses of Theorem 2.2.1, let u be the solution of* (2.2.7) *defined in $[0,\tau]$ and consider fixed numbers T and τ_0, such that $T > \tau > t_0$. Then, there exists a constant $C = C(T,\tau_0) > 0$ such that if $0 < \delta \leq C$, u can be extended to $[0,\tau+\delta]$ as a solution of* (2.2.7).

Proof. We are going to consider the space $\mathbb{V}^q_{\tau+\delta}$, for some $0 < \delta < 1$, and $B_R \subset \mathbb{V}^q_{\tau+\delta}$, defined as $B_R := \{w \in \mathbb{V}^q_{\tau+\delta}$ such that $w(t) \equiv u(t)\, \forall t \in [0,\tau]$, and $\|w\|_{\mathbb{V}^q_{\tau+\delta}} \leq R\}$, where u is the solution of (2.2.7) over $[0,\tau]$. Observe that, with this definition, B_R is a closed subset of $\mathbb{V}^q_{\tau+\delta}$. Our goal is, as in the proof of Theorem 2.2.1, to apply Banach's fixed point Theorem, showing that there exists $\delta > 0$ and R, such that $\mathcal{S}$ is a contraction over B_R, and maps B_R into itself.

Suppose $\tilde{u} \in B_R$, proceeding similarly as in (2.2.8), using the boundedness of f, we can obtain

$$t^{(1-q)\alpha/2}|\mathcal{S}(\tilde{u})|_{H^s(\mathbb{R}^n)} \leq CR_0 + C(\tau+\delta)^\alpha \leq C(R_0 + \tau^\alpha + \delta^\alpha) \tag{2.2.19}$$
$$\leq C(R_0, T) + \delta^\alpha.$$

With the same idea we can obtain

$$\|\mathcal{S}(\tilde{u})\|_{L^2(\Omega)} \leq C(R_0, T) + \delta^\alpha. \tag{2.2.20}$$

Also, applying the same arguments used to obtain (2.2.11), along with the fact that $\tilde{u}(s) = u(s)$ for all $s \in [0,\tau]$, and using $t > \tau$, we can estimate

$$t^{1-q\alpha/2}\|\partial_t \mathcal{S}(\tilde{u})\|_{L^2(\Omega)} = \tag{2.2.21}$$

$$t^{1-q\alpha/2}\|\partial_t E^\alpha(t)v + F^\alpha(t)f(v) + \int_0^t F^\alpha(s)f(\tilde{u}(t-s))\partial_t\tilde{u}(t-s)\,ds\|_{L^2(\Omega)} \leq$$

$$C(T)R_0 + t^{1-q\alpha/2}\| \int_0^t F^\alpha(t-s)f(\tilde{u}(s))\partial_t\tilde{u}(s)\,ds\|_{L^2(\Omega)} \leq$$

$$C(T)R_0 + t^{1-q\alpha/2}\| \int_0^\tau F^\alpha(t-s)f(u(s))\partial_t u(s)\,ds + \int_\tau^t F^\alpha(t-s)f(\tilde{u}(s))\partial_t\tilde{u}(s)\,ds\|_{L^2(\Omega)}$$

$$\leq C(T)R_0 + CBt^{1-q\alpha/2}\int_0^\tau (t-s)^{\alpha-1}s^{q\alpha/2-1}\,ds + CBRt^{1-q\alpha/2}\int_\tau^t (t-s)^{\alpha-1}s^{q\alpha/2-1}\,ds$$
$$= C(R_0,T) + (i) + (ii),$$

where in the last inequality we have used (2.2.16). Now, making the change of variables $s/t = r$, we can estimate

$$(i) \leq Ct^\alpha \int_0^{\tau/t} (1-r)^{\alpha-1}r^{q\alpha/2-1}\,dr \leq C(\tau+\delta)^\alpha \int_0^1 (1-r)^{\alpha-1}r^{q\alpha/2-1}\,dr \leq C\tau^\alpha + C\delta^\alpha,$$

$$\leq C(T) + C\delta^\alpha$$

and

$$(ii) \leq CRt^{\alpha} \int_{\tau/t}^{1} (1-r)^{\alpha-1} r^{q\alpha/2-1}\, dr \leq CRt^{\alpha}(\tau/t)^{q\alpha/2-1} \int_{\tau/t}^{1} (1-r)^{\alpha-1}\, dr$$

$$\leq CRt^{\alpha}(\tau/t)^{q\alpha/2-1}(1-\tau/t)^{\alpha} \leq CR(t-\tau)^{\alpha} \leq CR\delta^{\alpha},$$

where we have estimated $(\tau/t)^{q\alpha/2-1} < C(\tau_0)$ using the fact that $t \geq \tau > \tau_0 > 0$.

Applying this estimation to (2.2.21), we obtain

$$t^{1-q\alpha/2}\|\partial_t \mathcal{S}(\tilde{u})\|_{L^2(\Omega)} \leq C(R_0, T) + CR\delta^{\alpha}, \tag{2.2.22}$$

and combining (2.2.22) with (2.2.19) and (2.2.20), we obtain

$$\|\mathcal{S}(\tilde{u})\|_{\mathbb{V}^q_{\tau+\delta}} \leq C(R_0, T) + CR\delta^{\alpha}.$$

If we choose $R = 2C(R_0, T)$, taking $\delta^{\alpha} \leq 1/2C$ we have $\|\mathcal{S}(\tilde{u})\|_{\mathbb{V}^q_{\tau+\delta}} \leq R$.

Finally, we only need to show that $\mathcal{S}$ is a contraction on B_R. Consider $\tilde{u}$ and $w \in \mathbb{V}^q_{\tau+\delta}$, proceeding as in (2.2.12), and taking advantage of the fact that $\tilde{u}(s) = w(s) = u(s)$ for all $s \in [0, \tau]$, we can estimate

$$t^{(1-q)\alpha/2}|\mathcal{S}(\tilde{u})(t) - \mathcal{S}(w)(t)|_{H^s(\mathbb{R}^n)} \leq Ct^{(1-q)\alpha/2} \int_{\tau}^{t} (t-s)^{\alpha/2-1}\|f(\tilde{u}(s)) - f(w(s))\|_{L^2(\Omega)}\, ds \tag{2.2.23}$$

$$\leq CBt^{(1-q)\alpha/2} \int_{\tau}^{t} (t-s)^{\alpha/2-1}\|\tilde{u}(s) - w(s)\|_{L^2(\Omega)}\, ds$$

$$\leq CB\|\tilde{u} - w\|_{\mathbb{V}^q_{\tau+\delta}} t^{(2-q)\alpha/2} \int_{\tau/t}^{1} (1-r)^{\alpha/2-1}\, dr$$

$$\leq C\|\tilde{u} - w\|_{\mathbb{V}^q_{\tau+\delta}} t^{-q\alpha/2} t^{\alpha/2}(1-\tau/t)^{\alpha/2} \leq C\delta^{\alpha/2}\|\tilde{u} - w\|_{\mathbb{V}^q_{\tau+\delta}},$$

where in the last step we use the bound $t^{-q\alpha/2} \leq C(\tau_0)$, with $\tau > \tau_0 > 0$.

Also, arguing as in (2.2.14), we have

$$t^{1-q\alpha/2}\|\partial_t\big(\mathcal{S}(\tilde{u})(t) - \mathcal{S}(w)(t)\big)\|_{L^2(\Omega)} \leq \tag{2.2.24}$$

$$t^{1-q\alpha/2} CB \int_{\tau}^{t} s^{\alpha-1}\|\partial_t\big(\tilde{u}(s) - w(s)\big)\|_{L^2(\Omega)}\, ds$$

$$+CBRt^{1-q\alpha/2}\int_\tau^t (t-s)^{\alpha-1}s^{q\alpha/2-1}\|\tilde{u}(s)-w(s)\|_{L^2(\Omega)}\,ds$$

$$\leq C(R+1)\|\tilde{u}-w\|_{\mathbb{V}^q_{\tau+\delta}}t^{1-q\alpha/2}\int_\tau^t (t-s)^{\alpha-1}s^{q\alpha/2-1}\,ds$$

$$\leq C(R+1)\|\tilde{u}-w\|_{\mathbb{V}^q_{\tau+\delta}}t^{\alpha}\int_{\tau/t}^1 (1-r)^{\alpha-1}r^{q\alpha/2-1}\,dr$$

$$\leq C(R+1)\delta^\alpha\|\tilde{u}-w\|_{\mathbb{V}^q_{\tau+\delta}}.$$

Then, we can assert that

$$\|\mathcal{S}(\tilde{u})-\mathcal{S}(w)\|_{\mathbb{V}^q_{\tau+\delta}}\leq C\delta^\alpha(R+1)\|\tilde{u}-w\|_{\mathbb{V}^q_{\tau+\delta}},$$

and we can choose δ such that $\mathcal{S}$ results in a contraction. Since R depends on T and R_0, the statement of the theorem follows. □

Notice, in previous theorem, that δ does not depend on τ. As a consequence, we have proved that equation 2.2.6 has a unique solution in $\mathbb{V}^q_T$. Moreover, in view of the regularity of functions belonging to the space $\mathbb{V}^q_T$, we can assert that a mild solution is also a weak solution.

2.3 Fractional diffusion-wave equation

The aim of this section is to reproduce the classical results for problem (0.0.3) with $\alpha\in(1,2]$. As in section 2.1, we first define the concept of weak solution of problem (0.0.3). Indeed, we say that u is a weak solution for (0.0.3) with $\alpha\in(1,2]$ if $u\in W^{2,1}((0,T),L^2(\Omega))\cap C((0,T],\widetilde{H}^s(\Omega))$ and satisfies the equation (in $L^2(\Omega)$)

$$^C\partial_t^\alpha u+Au=f, \tag{2.3.1}$$

for almost all $t\in(0,T)$, with $u(0)=v$ and $\partial_t u(0)=b$. Here v and $b\in L^2(\Omega)$. Note that since $u\in W^{2,1}((0,T),L^2(\Omega))$ then $^C\partial_t^\alpha u$ is well defined.

2.3.1 Solution representation

Arguing as in the fractional diffusion case in Section 2.1, we write solutions of (0.0.3) by means of separation of variables as in (2.1.2), so for every $k\geq 1$, it must hold that

$$\begin{cases} {}^C\partial_t^\alpha u_k+\lambda_k u_k=f_k,\\ u_k(0)=v_k,\\ u_k'(0)=b_k. \end{cases} \tag{2.3.2}$$

where, as before, $f_k = (f, \phi_k)$, $v_k = (v, \phi_k)$, and $b_k = (b, \phi_k)$. Again, solutions of (2.3.2) may be represented as the superposition of the respective solution of the problem with initial data equal to zero and the solution of the problem with vanishing forcing term. Using the same notation as in Section 2.1 the solution of (2.3.2) may be written as

$$u_k(t) = F_k(t) f_k + v_k E_{\alpha,1}(-\lambda_k t^\alpha) + b_k t E_{\alpha,2}(-\lambda_k t^\alpha). \tag{2.3.3}$$

For the particular value of $\alpha = 2$, in virtue of the identities $E_{2,1}(z) = \cosh(\sqrt{z})$ and $E_{2,2}(z) = \frac{\sinh(\sqrt{z})}{\sqrt{z}}$, expression (2.3.3) becomes

$$u_k(t) = \frac{1}{\sqrt{\lambda_k}} \int_0^t \sin(\sqrt{\lambda_k}(t-r)) f_k(r)\, dr \ + v_k \cos(\sqrt{\lambda_k} t) + b_k \frac{\sin(\sqrt{\lambda_k} t)}{\sqrt{\lambda_k}}.$$

Finally, summing the solutions for every eigenmode, and defining

$$\tilde{E}^\alpha(t) w := \sum_k t E_{\alpha,2}(-\lambda_k t^\alpha) \phi_k (\phi_k, w)_{L^2(\Omega)}, \tag{2.3.4}$$

we can write the solution as follow:

$$u(t) = E^\alpha(t) v + \tilde{E}^\alpha(t) b + \int_0^t F^\alpha(t-s) f(s)\, ds =: M(v, b, f)(t), \tag{2.3.5}$$

and as before, we say that $u(t) = M(v, b, f)(t)$ is a mild solution.

Next result (analogous of Theorem 2.1.2) tells us that under suitable regularity conditions, a mild solution is a weak solution.

Theorem 2.3.1. *Let Ω be a bounded, smooth domain, $s \in (0,1)$ and $\alpha \in (1,2]$ and $u(t) = M(v,b,f)$ a mild solution of (0.0.3). Assume that $f \in C([0,T], L^2(\Omega))$, differentiable in $(0,T)$, and $\|f'(t)\|_{L^2(\Omega)} \leq C t^{\gamma-1}$ with $C > 0$ and $\gamma \in (0,1)$, $v \in \dot{H}^q(\Omega)$ for some $q > 2/\alpha$ and $b \in \dot{H}^r(\Omega)$ for some $r > 0$. Then u is a weak solution of (0.0.3).*

Proof. Suppose first $f \equiv 0$. Then $u = E^\alpha(t) v + \tilde{E}^\alpha(t) b$. Arguing as in Theorem 2.1.2 it is possible to check $u \in C((0,T], \widetilde{H}^s(\Omega))$.

Now, using the same ideas for the proof of Lemma 2.0.3, we can obtain the following bound ([45, Theorem A.2])

$$\|\partial_t^m u\|_{L^2(\Omega)} \leq C t^{q\alpha/2 - m} \|v\|_{q,s} + C t^{q\alpha/2 - m + 1} \|b\|_{r,s}, \tag{2.3.6}$$

for any integer $m \geq 1$. From this, we can conclude that if $v \in \dot{H}^q(\Omega)$ for some $q > 2/\alpha$ and $b \in \dot{H}^r(\Omega)$ for some $r > 0$ then $u \in W^{2,1}((0,T), L^2(\Omega))$.

Suppose now $v \equiv b \equiv 0$. In this case we have $u(t) = \int_0^t F^\alpha(t-s) f(s)\, ds$. Again, as in Theorem 2.1.2 it can be seen that $u \in C((0,T], \widetilde{H}^s(\Omega))$. From Lemma 1.3.1 we know that

$$\partial_t^m E_{\alpha,1}(-\lambda t^\alpha) = -\lambda t^{\alpha-m} E_{\alpha,\alpha+1-m}(-\lambda t^\alpha).$$

Since $\alpha > 1$, the function $t^{\alpha-1}E_{\alpha,\alpha}(-\lambda t^\alpha)$ complies the hypothesis of Lemma 2.0.4 and using this result we can compute

$$\partial_t u(t) = \int_0^t \partial_t F^\alpha(t-s) f(s)\, ds,$$

from which we can conclude that $\partial_t u \in C((0,T], L^2(\Omega))$. In view of Lemma 2.0.2 we have the estimation

$$\|\partial_t u(t)\|_{L^2(\Omega)} \leq C \int_0^t (s-t)^{\alpha-2} \|f(s)\|_{L^2(\Omega)}\, ds \leq C t^{\alpha-1} \|f\|_{L^\infty((0,T),L^2(\Omega))}$$

and we can assert $\partial_t u(t) \in L^1((0,T), L^2(\Omega))$.

Now, using the the properties of f and again Lemma 2.0.4, we can compute

$$\partial_t^2 u(t) = \partial_t F^\alpha(t) f(0) + \int_0^t \partial_t F^\alpha(s) f'(t-s)\, ds.$$

Hence $\partial_t u \in C((0,T], L^2(\Omega))$ and we can estimate

$$\|\partial_t^2 u(t)\|_{L^2(\Omega)} \leq C t^{\alpha-2} \|f(0)\|_{L^2(\Omega)} + C \int_0^t s^{\alpha-2}(t-s)^{\gamma-1}\, ds$$

$$= C t^{\alpha-2} \|f(0)\|_{L^2(\Omega)} + C t^{\alpha+\gamma-2} \int_0^1 r^{\alpha-2}(1-r)^{\gamma-1}\, dr = C t^{\alpha-2} \|f(0)\|_{L^2(\Omega)} + C t^{\alpha+\gamma-2} B(\alpha-1,\gamma),$$

where in the third step we have made the change of variable $r = s/t$, and $B(\alpha-1,\gamma)$ denotes the beta function. As before, the former previous implies $u \in W^{2,1}((0,T), L^2(\Omega))$ and the statement of the theorem follows. □

2.3.2 Regularity of solutions

Estimates for the *fractional diffusion-wave* can be reached as in the *fractional diffusion* case by means of Lemmas 2.0.2 and 2.0.3, and similar arguments. The following theorem summarizes the regularity results for *fractional diffusion-wave* with a vanishing forcing term.

Theorem 2.3.2. *Let $1 < \alpha \leq 2$ and suppose that $f \equiv 0$. Let u be the solution of* (0.0.3)*, given by* (2.1.2)*, with initial/boundary conditions* (0.0.4) *and* (0.0.5)*.*

a. Assume that $v \in L^2(\Omega)$ and $b \in L^2(\Omega)$. Then, $u \in C([0,T]; L^2(\Omega)) \cap C((0,T]; \widetilde{H}^s(\Omega) \cap H^{s+\gamma}(\Omega))$ and ${}^C\partial_t^\alpha u \in C((0,T]; L^2(\Omega))$. Moreover, there exists a constant $C > 0$ such that

$$\|u\|_{C([0,T];L^2(\Omega))} \leq C \left(\|v\|_{L^2(\Omega)} + \|b\|_{L^2(\Omega)} \right),$$
$$\|u(\cdot,t)\|_{H^{s+\gamma}(\Omega)} + \|{}^C\partial_t^\alpha u(\cdot,t)\|_{L^2(\Omega)} \leq C \left(t^{-\alpha} \|v\|_{L^2(\Omega)} + t^{1-\alpha} \|b\|_{L^2(\Omega)} \right).$$

b. If $v \in \widetilde{H}^s(\Omega)$ and $b \in L^2(\Omega)$, then $\partial_t u \in C([0,T]; H^{-s}(\Omega))$, and

$$\|\partial_t u\|_{C([0,T];H^{-s}(\Omega))} \leq C(\|v\|_{H^s(\mathbb{R}^n)} + \|b\|_{L^2(\Omega)}).$$

c. Moreover, if $v \in \widetilde{H}^s(\Omega)$ is such that $(-\Delta)^s v \in L^2(\Omega)$ and $b \in \widetilde{H}^s(\Omega)$, then $u \in C([0,T]; \widetilde{H}^s(\Omega) \cap H^{s+\gamma}(\Omega)) \cap C^1([0,T]; L^2(\Omega))$, ${}^C\partial_t^\alpha u \in C([0,T]; L^2(\Omega))$, and the following estimates hold:

$$\|u\|_{C([0,T];H^{s+\gamma}(\Omega))} + \|{}^C\partial_t^\alpha u\|_{C([0,T];L^2(\Omega))} \leq C\left(\|(-\Delta)^s v\|_{L^2(\Omega)} + \|b\|_{H^s(\mathbb{R}^n)}\right),$$
$$\|u\|_{C^1([0,T];L^2(\Omega))} \leq C\left(\|(-\Delta)^s v\|_{L^2(\Omega)} + \|b\|_{L^2(\Omega)}\right).$$

Finally, estimates for problems with non-null forcing term have the following form.

Theorem 2.3.3. *Let $1 < \alpha \leq 2$, $v \equiv 0$ and $b \equiv 0$. Consider u, given by (2.1.2), be the solution of (0.0.3) with homogeneous initial and boundary conditions. If $f \in C([0,T]; L^2(\Omega))$ is such that $(-\Delta)^s f \in L^2(\Omega \times (0,T))$, then $u \in C([0,T]; \widetilde{H}^s(\Omega) \cap H^{s+\gamma}(\Omega))$, ${}^C\partial_t^\alpha u \in C([0,T]; L^2(\Omega))$ and*

$$\|u\|_{C([0,T];H^{s+\gamma}(\Omega))} + \|{}^C\partial_t^\alpha u\|_{C([0,T];L^2(\Omega))} \leq$$
$$\leq C\left(\|(-\Delta)^s f\|_{L^2(\Omega\times(0,T))} + \|f\|_{C([0,T];L^2(\Omega))}\right).$$

Remark 2.3.4. As in the case $0 < \alpha < 1$, regularity conditions in theorems 2.3.2 and 2.3.3 do not guarantee that $u(t) = M(v,b,f)$ is actually a weak solution, and this results in certain problems, similar to those mentioned in remark 2.1.5. As before, in order to avoid these technicalities we are going to consider through this work v, b and f as in hypothesis of Theorem 2.3.1. These conditions are more restrictive than those required for the diffusion case, and we speculate that can be relaxed.

Also, as we have mentioned in Remark 2.1.6, an alternative solution theory can be developed starting from a weaker definition of the Caputo derivative, where some of these technical details may be solved without strong regularity requirements.

Resumen del Capítulo

En este capítulo se establecen las formulaciones de los problemas de evolución a tratar, así como también resultados de existencia y regularidad para los mismos. Asimismo, se discuten hipótesis razonables de regularidad en las condiciones iniciales bajo las cuales los problemas resultan bien planteados (ver 2.1.5 y 2.1.6).

En la Sección 2.1 se tratan los aspectos antes mencionados para el problema de difusión fraccionaria. La Sección 2.2 está dedicada a una versión semi lineal del problema anterior, mientras que en la Sección 2.3 se estudia el problema de difusión-ondas.

Chapter 3

Implementation details for the elliptic problem

The aim of this chapter is to provide an exhaustive description of a FEM implementation addressed to approximate solutions for problem (1.2.1). To this end, we have tried to emulate as much as possible the spirit of [12], where a *MATLAB*® implementation for *linear* finite elements and *local* elliptic operators is presented in a concise way. Notwithstanding that and in spite of our efforts, some intrinsic technicalities make our code inevitably slightly longer and more complex than that. Just to clarify this point, we take a glimpse in advance at the nonlocal stiffness matrix K. It involves expressions of the type

$$\int_{\mathbb{R}^2}\int_{\mathbb{R}^2} \frac{(\varphi_i(x)-\varphi_i(y))(\varphi_j(x)-\varphi_j(y))}{|x-y|^{2+2s}}\,dxdy, \tag{3.0.1}$$

where φ_i, φ_j are arbitrary nodal basis functions associated to a triangulation $\mathcal{T}$. Two difficulties become apparent in the calculation of (3.0.1). First, at the element level, computing (3.0.1) leads to terms like

$$\int_{T}\int_{\tilde{T}} \frac{(\varphi_i(x)-\varphi_i(y))(\varphi_j(x)-\varphi_j(y))}{|x-y|^{2+2s}}\,dxdy, \tag{3.0.2}$$

for arbitrary pairs $T, \tilde{T} \in \mathcal{T}$. If T and $\tilde{T}$ are not neighboring then the integrand in (3.0.2) is a regular function and can be integrated numerically in a standard fashion. On the other hand, if $T \cap \tilde{T} \neq \emptyset$ an accurate algorithm to compute (3.0.2) is not easy to devise. Fortunately, (3.0.2) bears some resemblances to typical integrals appearing in the Boundary Element Method [75] and we extensively exploit this fact. Indeed, a basic and well known technique in the BEM community is to rely on Duffy-type transforms. This approach leads us to the decomposition of such integrals into two parts: a highly singular but explicitly integrable part and a smooth, numerically treatable part. We use this method to show how (3.0.2) can be handled with an arbitrary degree of precision (this is carefully treated in Appendices A.1.1, A.1.2, A.1.3, A.1.4).

Yet another difficulty is hidden in the calculation of K. Although Ω is a bounded domain and the number of potential unknowns is always finite, (3.0.1) involves a computation in $\mathbb{R}^2 \times \mathbb{R}^2$. In particular, in the homogeneous setting, we need to accurately compute the function

$$\int_{\Omega^c} \frac{1}{|x-y|^{2+2s}}\, dy, \tag{3.0.3}$$

for any $x \in \Omega$. That, of course, can be hard to achieve for a domain with a complex boundary. Nonetheless, introducing an extended secondary mesh, as it is explained in Section 3.2, it is possible to reduce such problem to a simple case in which $\partial\Omega$ is a circle. We show that in this circumstance a computation of (3.0.3) can be both fast and accurately delivered (see also Appendix A.1.5). Remarkably, this simple idea applies in arbitrary space dimensions.

Regarding the code itself, our main concern has been to keep a compromise between readability and efficiency. First versions of our code were plainly readable but too slow to be satisfactory. In the code presented here many computations have been vectorized and a substantial speed up gained, sometimes at the price of losing (hopefully not too much) readability.

This chapter is organized as follows. In Section 3.1, we set an appropriate weak formulation for problem (0.0.2). Section 3.2 deals with basic aspects of the FE setting. The data structure is carefully discussed in Section 3.3 and the main loop of the code is described in Section 3.4. Section 3.5, in turn, shows a numerical example for which a nontrivial (i.e. with a non constant source term f) solution is explicitly known. Moreover, the e.o.c. in $L^2(\Omega)$ is presented for some values of s. These numerical results are in very good agreement with those expected by using standard duality arguments together with the theory given in [3]. Appendix A.1 may be found rather technical for people not coming from the Boundary Element community and deals with the quadrature rules used in each singular case. Appendices A.2 and A.3 describe respectively auxiliary functions and data used along the program. Finally, the full code, including the line numbers, is exhibited in Appendix A.4.

3.1 Weak formulation

Weak solutions of (0.0.2) are straightforwardly defined multiplying by a test function and integrating by parts. Indeed, the weak formulation of (0.0.2) reads: find $u \in \widetilde{H}^s(\Omega)$ such that

$$\frac{C(n,s)}{2}\langle u, v\rangle_{H^s(\mathbb{R}^n)} = \int_\Omega fv, \quad v \in \widetilde{H}^s(\Omega). \tag{3.1.1}$$

Notice that the inner product

$$\langle u, v\rangle_{H^s(\mathbb{R}^n)} = \iint_{\mathbb{R}^n\times\mathbb{R}^n} \frac{(u(x)-u(y))(v(x)-v(y))}{|x-y|^{n+2s}}\, dx\, dy. \tag{3.1.2}$$

involves integrals in $\mathbb{R}^n$.

Throughout this chapter, we assume $f \in H^r(\Omega)$ for some $r \geq -s$. Existence and uniqueness of solutions in $\tilde{H}^s(\Omega)$ and well-posedness of problem (3.1.1) are immediate consequences of the Lax-Milgram lemma.

3.2 FE setting

Consider an admissible triangulation $\mathcal{T}$ of Ω consisting of $N_{\mathcal{T}}$ elements. For the discrete space $\mathbb{V}_h^q$, we take standard *continuous* piecewise linear elements over $\mathcal{T}$. With the usual notation, we introduce the nodal basis $\{\varphi_1, \ldots, \varphi_N\} \subset \mathbb{V}_h^q$ corresponding to the internal nodes $\{x_1, \ldots, x_N\}$, that is $\varphi_i(x_j) = \delta_i^j$. Given an element $T \in \mathcal{T}$, we denote by h_T and ρ_T its diameter and inner radius, respectively. As customary, we write $h = \max_{T\in\mathcal{T}} h_T$. The family of triangulations considered is assumed to be shape-regular, namely, there exists $\sigma > 0$ independent of $\mathcal{T}$ such that

$$h_T \leq \sigma \rho_T \text{ for all } T \in \mathcal{T}.$$

In this context, the discrete analogous of (3.1.1) reads: find $u_h \in \mathbb{V}_h^q$ such that

$$\frac{C(n,s)}{2}\langle u_h, v_h\rangle_{H^s(\mathbb{R}^n)} = \int_\Omega f v_h, \quad v_h \in \mathbb{V}_h^q, \tag{3.2.1}$$

providing a *conforming*[1] FEM for any $0 < s < 1$.

Writing the discrete solution as $u_h = \sum_j u_j \varphi_j$, problem (3.2.1) is equivalent to solving the linear system

$$KU = F, \tag{3.2.2}$$

where the coefficient matrix $K = (K_{ij}) \in \mathbb{R}^{N\times N}$ and the right-hand side $F = (f_j) \in \mathbb{R}^N$ are defined by

$$K_{ij} = \frac{C(n,s)}{2}\langle \varphi_i, \varphi_j\rangle_{H^s(\mathbb{R}^n)}, \quad f_j = \int_\Omega f\varphi_j,$$

and the unknown is $U = (u_j) \in \mathbb{R}^N$.

The *fractional* stiffness matrix K is symmetric and positive definite, so that (3.2.2) has a unique solution. Notice that the integrals in the inner product involved in computation of K_{ij} should be carried over $\mathbb{R}^n$. For this reason we find it useful to consider a ball B containing Ω and such that the distance from $\bar{\Omega}$ to B^c is an arbitrary positive number. As it is explained in Appendix A.1.5, this is needed in order to avoid difficulties caused by lack of symmetry when dealing with the integral over Ω^c when Ω is not a ball. Together with B, we introduce an auxiliary triangulation $\mathcal{T}_A$ on $B \setminus \Omega$ such that the complete triangulation $\tilde{\mathcal{T}}$ over B (that is $\tilde{\mathcal{T}} = \mathcal{T} \cup \mathcal{T}_A$) is admissible (see Figure 3.1).

[1]Notice that even P_0 elements are conforming for $0 < s < 1/2$. We restrict ourselves to continuous P_1 in order to give an unified conforming approach for any $0 < s < 1$.

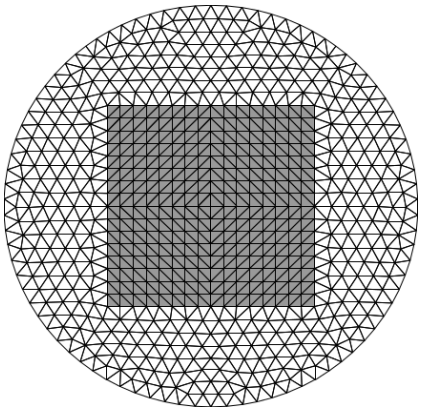

Figure 3.1: A square domain Ω (gray) and an auxiliary ball containing it. Regular triangulations $\mathcal{T}$ and $\mathcal{T}_A$ for Ω and $B \setminus \Omega$ are shown. The final symmetry of the admissible triangulation $\tilde{\mathcal{T}} = \mathcal{T} \cup \mathcal{T}_A$, exhibited in the example, is not relevant.

Let us call $N_{\tilde{\mathcal{T}}}$ the number of elements on the triangulation of B. Then, defining for $1 \leq \ell, m \leq N_{\tilde{\mathcal{T}}}$ and $1 \leq \ell \leq N_{\tilde{\mathcal{T}}}$

$$\begin{aligned} I_{\ell,m}^{i,j} &= \int_{T_\ell} \int_{T_m} \frac{(\varphi_i(x) - \varphi_i(y))(\varphi_j(x) - \varphi_j(y))}{|x-y|^{2+2s}} \, dxdy, \\ J_\ell^{i,j} &= \int_{T_\ell} \int_{B^c} \frac{\varphi_i(x)\varphi_j(x)}{|x-y|^{2+2s}} \, dydx, \end{aligned} \tag{3.2.3}$$

we may write

$$K_{ij} = \frac{C(n,s)}{2} \sum_{\ell=1}^{N_{\tilde{\mathcal{T}}}} \left(\sum_{m=1}^{N_{\tilde{\mathcal{T}}}} I_{\ell,m}^{i,j} + 2J_\ell^{i,j} \right).$$

As mentioned above, the computation of each integral $I_{\ell,m}^{i,j}$ and $J_\ell^{i,j}$ is challenging for different reasons: the former involves a singular integrand if $\overline{T_\ell} \cap \overline{T_m} \neq \emptyset$ (Appendices A.1.2, A.1.3, A.1.4 are devoted to handle it) while the latter needs to be calculated on an unbounded domain. In this case notice that

$$J_\ell^{i,j} = \int_{T_\ell} \varphi_i(x)\varphi_j(x)\psi(x) \, dx,$$

with $\psi(x) := \int_{B^c} \frac{1}{|x-y|^{2+2s}} \, dy$. Therefore all we need is an accurate computation of $\psi(x)$ for each quadrature point used in $T_\ell \subset \bar{\Omega}$ (notice that $\psi(x)$ is a smooth function up to the boundary of Ω since $|x-y| > dist(\bar{\Omega}, B^c) > 0$).

Taking this into account, we observe that it is possible to take advantage of the fact that $\psi(x)$ is a radial function that can be either quickly computed on the fly or

even precomputed with an arbitrary degree of precision (see Appendix A.1.5 for a full treatment of $\psi(x)$).

For the reader's convenience, we finish this section with Table 3.1, containing some handy notations.

Table 3.1: Main Variables

Notation	Meaning
$\mathcal{T}, \mathcal{T}_A, \tilde{\mathcal{T}}$	Meshes: of Ω, $B \setminus \Omega$ and B resp.
$\mathcal{N}$	Nodes of $\mathcal{T}$
$\mathcal{E}$	Edges of $\mathcal{T}$
$\mathcal{B}$	Boundary edges of $\mathcal{T}$
$N_{\mathcal{T}}$	$\#\mathcal{T}$
$N_{\mathcal{N}}$	$\#\mathcal{N}$
$N_{\mathcal{B}}$	$\#\mathcal{B}$

3.3 Data structure and auxiliary variables

We assume that the mesh $\mathcal{T}$ has been generated in advance[2]. The information related to $\mathcal{T}$ should be encoded in some specific variables `p`, `t`, `bdrynodes`, `nt_aux nf R`, as follows:

- `p` is a $2 \times N_{\mathcal{N}}$ array, such that `p(:,n)` are the coordinates of the `n`-th node.
- `t` is a $N_{\tilde{\mathcal{T}}} \times 3$ index array, and `t(l,:)` are the indices of the vertices of T_l. Triangles belonging to $\mathcal{T}_A$ must be listed at the end.
- `nt_aux` $= \#\mathcal{T}_A$.
- `bdrynodes` is an index column vector listing the nodes lying on $\partial\Omega$.
- `nf` is an index column vector contiaining the free nodes (those in Ω).
- `R` the radius of B.

These data have to be available in the *MATLAB*® workspace before the execution of the main code.

Next, we begin by creating some variables that refer to problem (0.0.2):

[2]For the sake of convenience an stored example mesh -as well as a suitable mesh generator- is provided together with the source code.

```
s = 0.5;
f = @(x,y) 1;
cns = s*2^(-1+2*s)*gamma(1+s)/(pi*gamma(1-s));
load('data.mat');
```

Here, `s` is the order of the fractional Laplacian involved, `f` is a function handle containing the volume force (which as an example we have set to be $f \equiv 1$), and `cns` is equal to the constant $C(n,s)$ previously defined.

In order to compute the stiffness matrix we need to estimate the bilinear form $\langle \cdot, \cdot \rangle_{H^s(\mathbb{R}^n)}$ evaluated at the nodal basis through an appropriate quadrature rule.

To perform an efficient vectorized computation, we require some pre-calculated data, given in the file `data.mat`. This file contains information about nodes and weights for the quadratures performed throughout the code. The content of `data.mat` is listed in Table 3.2 and further details can be found in Appendix A.3.

As mentioned before, some auxiliary elements are added to the original mesh in order to have a triangulation on a ball B containing Ω (see Figure 3.1). The nodes in this auxiliary domain $B \setminus \Omega$ are regarded as Dirichlet nodes.

Next, we define some mesh parameters and set to zero the factors involved in equation (3.2.2). The following lines do not need extra explanation beyond the in-line comments:

```
nn = size(p,2); % number of nodes
nt = size(t,1) % number of elements
uh = zeros(nn,1); % discrete solution
K  = zeros(nn,nn); % stiffness matrix
b  = zeros(nn,1); % right hand side
```

Then, the measures of all the elements in the mesh are calculated:

```
area = zeros(nt,1);
for i=1:nt
    aux = p( : , t(i,:) );
    area(i) = 0.5.*abs(...
         det([ aux(:,1) - aux(:,3)  aux(:,2) - aux(:,3)]) );
end
```

So, `area` is a vector of length $N_{\tilde{\mathcal{T}}}$ satisfying `area(l)` $= |T_{\mathtt{l}}|$, `l` $\in \{1, ..., N_{\tilde{\mathcal{T}}}\}$.

The quadratures we employ to compute the integrals $I^{i,j}_{\ell,m}$ (defined in (3.2.3)) depend on whether the elements T_ℓ and T_m coincide or their intersection is an edge, a vertex or empty. Therefore, it is important to distinguish theses cases in an efficient way. We construct a data structure called `patches` as follows, using a linear number of operations:

```
deg = zeros(nn,1);
for i=1:nt
    deg( t(i,:) ) = deg( t(i,:) ) + 1;
end
patches = cell(nn , 1);
for i=1:nn
    patches{i} = zeros( 1 , deg(i) );
end
for i=1:nt
    patches{ t(i,1) }(end - deg( t(i,1) ) + 1) = i;
    patches{ t(i,2) }(end - deg( t(i,2) ) + 1) = i;
    patches{ t(i,3) }(end - deg( t(i,3) ) + 1) = i;
    deg( t(i,:) ) = deg( t(i,:) ) - 1;
end
```

The output of this code block is a $N_{\tilde{N}} \times 1$ cell, called `patches`, such that `patches{n}` is a vector containing the indices of all the elements in the neighborhood of the node `n`.

3.4 Main loop

One of the main challenges to build up a FE implementation to problem (0.0.2) is to assemble the stiffness matrix in an efficient mode. Independently of whether the supports of two given basis functions φ_i and φ_j are disjoint, the interaction $\langle \varphi_i, \varphi_j \rangle_{H^s(\mathbb{R}^n)}$ is not null. This yields a paramount difference between FE implementations for the classical and the fractional Laplace operators; in the former the stiffness matrix is sparse, while in the latter it is full. Therefore, unless some care is taken [3],

the amount of memory required and the number of operations needed to assembly the stiffness matrix increases quadratically with the number of nodes. Due to this, the code we present takes advantage of vectorized operations as much as possible.

Moreover, as the computation of the entries of the stiffness matrix requires calculating integrals on *pairs* of elements, it is required to perform a double loop. It is simple to check the identity $I^{i,j}_{\ell,m} = I^{i,j}_{m,\ell}$ for all i, j, ℓ, m, and therefore it is enough to carry the computations only for the pairs of elements T_ℓ and T_m with $\ell \leq m$.

In the following lines we preallocate memory and create the auxiliary index array `aux_ind` (to be used in code line 58).

```
vl = zeros(6,2);
vm = zeros(6*nt,2);
norms = zeros(36,nt);
ML = zeros(6,6,nt);
```

[3] In [50, 8] some clever ways to reduce the complexity of the assembling process are analyzed.

```
empty = zeros(nt,1);
aux_ind = reshape( repmat( 1:3:3*nt , 6 , 1 ) , [] , 1 );
empty_vtx = zeros(2,3*nt);
BBm = zeros(2,2*nt);
```

The main loop goes through all the elements T_ℓ of the mesh of Ω, namely, $1 \leq \ell \leq N_{\mathcal{T}}$. Observe that auxiliary elements are excluded from it. Fixed ℓ, the first task is to classify all the mesh elements T_m ($1 \leq m \leq N_{\tilde{\mathcal{T}}}$, $m \neq \ell$) according to whether $\overline{T_\ell} \cap \overline{T_m}$ is empty, a vertex or an edge. This is accomplished employing a linear number of operations by using the `patches` data structure as follows:

```
edge =  [ patches{t(l,1)} patches{t(l,2)} patches{t(l,3)} ];
[nonempty M N] = unique( edge , 'first' );
edge(M) = [];
vertex = setdiff(  nonempty , edge  );
ll = nt - l + 1 - sum( nonempty>=l );
edge( edge<=l ) = [];
vertex( vertex<=l ) = [];
empty( 1:ll ) = setdiff_( l:nt , nonempty );
empty_vtx(: , 1:3*ll) = p( : , t( empty(1:ll) , : )' );
```

At this point, `ll` is the number of elements –including the auxiliary ones– whose intersection with T_ℓ is empty and have not been visited yet (namely, those with index `m>l`). By considering only the elements with index greater than ℓ, we are taking advantage of the symmetry of the stiffness matrix. The arrays `empty`, `vertex` and `edge` contain the indices of all those elements whose intersection with T_ℓ is empty, a vertex or an edge respectively, and have not been computed yet. In `empty_vtx` we store the coordinates of the vertices of the triangles indexed in `empty`.

Then, the code proceeds to assemble the right hand side vector in equation (3.2.2)

```
nodl = t(l,:);
xl = p(1 , nodl); yl = p(2 , nodl);
Bl = [xl(2)-xl(1) yl(2)-yl(1); xl(3)-xl(2) yl(3)-yl(2)]';
b(nodl) = b(nodl) + fquad(area(l),xl,yl,f);
```

Here, `nodl` stores the indices of the vertices of T_ℓ; `xl` and `yl` are the x and y coordinates of these vertices, respectively. The element T_ℓ is the image of a reference element $\hat{T}$ via an affine transformation,

$$(\hat{x}, \hat{y}) \mapsto \texttt{Bl}(\hat{x}, \hat{y}) + (\texttt{xl(1)}, \texttt{yl(1)}).$$

Recall that `b` stores the numerical approximation to the right hand side vector from equation (3.2.2), namely, `b(j)` $\approx \int_\Omega f\varphi_j$. The routine `fquad` uses a standard quadrature rule, interpolating f on the edge midpoints of T_l (see Appendix A.2).

Remark 3.4.1. Let $1 \leq \ell, m \leq \mathcal{N}_{\tilde{T}}$. When computing $I^{i,j}_{\ell,m}$ or $J^{i,j}_{\ell}$, the basis function indices i and j do not refer to a global numbering but to a local one. This means, for example, that if $\overline{T_\ell} \cap \overline{T_m} = \emptyset$, then $1 \leq i, j \leq 6$. See Remark A.1.1 for details on this convention.

3.4.1 Identical elements

The first interaction to be computed by the code corresponds to the case $m = \ell$ in (3.2.3). The values calculated are assembled in the stiffness matrix `K`.

```
K(nodl, nodl) = K(nodl, nodl) +...
triangle_quad(Bl,s,tpsi1,tpsi2,tpsi3,area(l),p_I) +...
comp_quad(Bl,xl(1),yl(1),s,cphi,alpha*R,area(l),p_I,w_I,p_T_12);
```

The function `triangle_quad` estimates $I^{i,j}_{\ell,\ell}$, while `comp_quad` computes numerically the value of $J^{i,j}_{\ell}$. These functions use pre-built data from the file `data.mat`: the first one employs the variables `tpsi1`, `tpsi2` and `tpsi3`, and the second one `cphi`, `p_I`, `w_I` and `p_T_12`. Implementation details can be found in appendixes A.1.4 and A.1.5, respectively. The output of both `triangle_quad` and `comp_quad` are 3 by 3 matrices, such that:

$$\texttt{triangle\_quad}_{ij} \approx I^{i,j}_{\ell,\ell}, \quad \texttt{comp\_quad}_{ij} \approx 2J^{i,j}_{\ell}.$$

3.4.2 Non-touching elements

The next step is to compute the interactions between T_ℓ and all the elements T_m whose closure is disjoint $\overline{T_\ell}$ (so that their indices are stored in the variable `empty`). In order to do this, we calculate and store quadrature points for all the triangles involved in the operation as follows:

```
BBm(:,1:2*ll) = reshape( [ empty_vtx( : , 2:3:3*ll ) -...
  empty_vtx( : , 1:3:3*ll ) , ...
  empty_vtx( : , 3:3:3*ll ) -...
  empty_vtx( : , 2:3:3*ll ) ] , [] , 2)' ;
vl = p_T_6*(Bl') + [ ones(6,1).*xl(1) ones(6,1).*yl(1) ];
vm(1:6*ll,:) = reshape( permute( reshape( p_T_6*BBm(:,1:2*ll), ...
 [6 1 2 ll] ) , [1 4 3 2] ) , [ 6*ll 2 ] ) +...
 empty_vtx(: , aux_ind(1:6*ll) )';
```

The matrix `BBm` has size $2 \times 2 * \texttt{nt}$, and it contains `nt` submatrices of dimension 2×2. The m-th submatrix corresponds to the affine transformation that maps $\hat{T}$ into T_m. The vectors `vl` and `vm` contain the coordinates of all quadrature points in T_ℓ and T_m for $m \in$ `empty`, respectively.

Here, the matrix `BBm` satisfies

$$\texttt{BBm(:,2*m-1:2m)'} \cdot \hat{T} + \texttt{empty\_vtx(:,3*(m-1) + 1)'} \mapsto T_m,$$

The matrix `p_T_6` $\in \mathbb{R}^{6\times 2}$ was provided by the precomputed file `data.mat`, and it stores the coordinates of the 6 quadrature points in the reference element $\hat{T}$. In order to compute `vm`, we use three nested operations over the $6 \times 2 * \texttt{ll}$ matrix `p_T_6*BBm(:,1:2*ll)`. To better understand this, suppose we rewrite this matrix as follows:

$$\texttt{p\_T\_6*BBm(:,1:2*ll)} = [A_1, A_2, ..., A_{\texttt{ll}}],$$

where A_i is a 6×2 matrix and $i = 1, .., \texttt{ll}$. Then, after the application of `reshape( permute( reshape(` we obtain the 6*`ll` by 2 matrix $[A_1; A_2; ...; A_{\texttt{ll}}]$, which can be used as an input in `pdist2`. This trick was taken out from [2].

Next, we compute distances from all the quadrature nodes in `vl` to the ones in `vm`, and raise them to the power of $-(2 + 2s)$:

```
norms(:,1:ll) = reshape(pdist2(vl,vm(1:6*ll,:)),36,[]).^(-2-2*s);
```

Thereby, `norms` is a $36 \times \texttt{ll}$ matrix such that for $\texttt{m} \in \{1, ..., \texttt{ll}\}$,

$$\texttt{norms(:,m)} = \begin{pmatrix} \|\texttt{vl(1,:)} - \texttt{vm(6*m - 5,:)}\|^{-(2+2s)} \\ \vdots \\ \|\texttt{vl(6,:)} - \texttt{vm(6*m - 5,:)}\|^{-(2+2s)} \\ \|\texttt{vl(1,:)} - \texttt{vm(6*m - 4,:)}\|^{-(2+2s)} \\ \vdots \\ \|\texttt{vl(6,:)} - \texttt{vm(6*m - 4,:)}\|^{-(2+2s)} \\ \vdots \\ \vdots \\ \|\texttt{vl(1,:)} - \texttt{vm(6*m,:)}\|^{-(2+2s)} \\ \vdots \\ \|\texttt{vl(6,:)} - \texttt{vm(6*m,:)}\|^{-(2+2s)} \end{pmatrix},$$

where $\|\cdot\|$ denotes the usual euclidean distance in $\mathbb{R}^2$.

At this point, we have collected all the necessary information to compute $I^{i,j}_{\ell,m}$ for $\overline{T_\ell} \cap \overline{T_m} = \emptyset$ and i, j corresponding to any of the six vertices of these elements. We employ the pre-built matrices `phiA`, `phiB` and `phiD`, that contain the values of the nodal basis functions evaluated at the quadrature points of $\hat{T}$, multiplied by their respective weights, and stored in an appropriate way in order to perform an efficient vectorized operation. Details are provided in appendixes A.1.1 and A.3.2. The code proceeds:

```
ML(1:3,1:3,1:ll) =  reshape( phiA*norms(:,1:ll) , 3 , 3 , [] );
ML(1:3,4:6,1:ll) =  reshape( phiB*norms(:,1:ll) , 3 , 3 , [] );
ML(4:6,4:6,1:ll) =  reshape( phiD*norms(:,1:ll) , 3 , 3 , [] );
ML(4:6,1:3,1:ll) =  permute( ML(1:3,4:6,1:ll) , [2 1 3] ) ;
```

So, the matrix `ML` satisfies

$$I^{i,j}_{\ell,m} \approx 4|T_\ell||T_m|\,\texttt{ML(i,j,m)}.$$

The last step to complete the computations for the case $\overline{T_\ell} \cap \overline{T_m} = \emptyset$ is to add the calculated values in their corresponding stiffness matrix entries:

```
for m=1:ll
    order = [nodl t( empty(m) , : )];
    K(order,order) = K(order,order) +...
    ( 8*area(empty(m))*area(l) ).*ML(1:6,1:6,m);
end
```

The vector `order` collects the local indices of the vertices of T_ℓ and T_m, given as explained in Remark A.1.1. Recall that $I^{i,j}_{\ell,m} = I^{i,j}_{m,\ell}$ and that we are summing over the elements listed in `empty`. In particular, this means that $\ell < m$. We multiply `ML(1:6,1:6,m)` by `8*area(empty(m))*area(l)` instead of by `4*area(empty(m))*area(l)` in order to avoid carrying the redundant computation of $I^{i,j}_{m,\ell}$.

3.4.3 Vertex-touching elements

In order to compute $I^{i,j}_{\ell,m}$ for the indices m corresponding to elements sharing a vertex with T_ℓ, we use the pre-built variables `vpsi1`, `vpsi2` and `p_cube` as input in the function `vertex_quad`. Let us mention once more that `vpsi1` and `vpsi2` contain the nodal basis in the reference element $\hat{T}$ evaluated at quadrature points, multiplied by their respective weight and properly stored. Moreover, the variable `p_cube` stores quadrature nodes in the unit cube $[0,1]^3$. Further details about `vertex_quad` and the auxiliary pre-built data can be found in appendixes A.1.2 and A.3.3, respectively. We compute the integrals and add the resulting values to `K` as follows:

```
for m=vertex
    nodm = t(m,:);
    nod_com = intersect(nodl, nodm);
    order = [nod_com nodl(nodl~=nod_com) nodm(nodm~=nod_com)];
    K(order,order) = K(order,order) ...
    + 2.*vertex_quad(nodl,nodm,nod_com,p,s,vpsi1,vpsi2,...
    area(l),area(m),p_cube);
end
```

Here, we store in `nodm` the indices of the vertices of T_m, whereas `nod_com` dentoes the index of the vertex shared by T_ℓ and T_m. The first entry of `order` is the index of this common vertex, followed by the nodes of T_ℓ different from it, and then by the indices of the remaining two nodes of T_m. Observe that, unlike the previous case, here there are involved five nodal basis, so the output of `vertex_quad` is a 5 by 5 array, such that:

$$\texttt{vertex\_quad}_{ij} \approx I_{\ell,m}^{i,j}.$$

3.4.4 Edge-touching elements

Proceeding similarly, we compute next the case where $\overline{T_\ell} \cap \overline{T_m}$ is an edge. Now there are only 4 nodal basis functions involved, and the local numbering is such that the first two nodes correspond to the endpoints of the shared edge, the third is the one in T_ℓ but not in T_m and the last one is the node in T_m but not in T_ℓ. Using the pre-built variables `epsi1`, `epsi2`, `epsi3`, `epsi4`,`epsi5` and `p_cube` as input in `edge_quad` (see appendixes A.1.3 and A.3.4), we proceed as in the previous case:

```
for m=edge
    nodm = t(m,:);
    nod_diff = [setdiff(nodl, nodm) setdiff(nodm, nodl)];
    order = [ nodl( nodl~=nod_diff(1) ) nod_diff  ];
    K(order,order) = K(order,order) +...
    2.*edge_quad(nodl,nodm,nod_diff,p,s,...
    epsi1,epsi2,epsi3,epsi4,epsi5,area(l),area(m),p_cube);
end
```

The indices of the two nodes not shared by T_ℓ and T_m are stored in `nod_diff`, and `order` has the nodes ordered as explained in the previous paragraph. The output of the function `edge_quad` is a 4 by 4 array satisfying

$$\texttt{edge\_quad}_{ij} \approx I_{\ell,m}^{i,j}.$$

3.4.5 Discrete solution

Once the main loop is concluded, the stiffness matrix `K` and the right hand side vector `b` have been computed, and thus it is possible to calculate the FE solution `uh` of the system (3.2.2):

```
uh(nf) = ( K(nf,nf)\b(nf) )./cns; % Solving linear system
```

The entries of `K` and `b` needed are only the ones corresponding to free nodes. The nodes belonging to $\partial\Omega$ and to the auxiliary domain $B \setminus \Omega$ are excluded, as the discrete solution `uh` is set to vanish on them.

Finally, `uh` is displayed, and the auxiliary domain is excluded from the representation:

```
trimesh(t(1:nt-nt_aux , :), p(1,:),p(2,:),uh);
```

3.5 Numerical Experiments

In order to illustrate the performance of the code, in this section we show the results we obtained in an example problem. Explicit solutions for (0.0.2) are scarce, but it is possible to obtain a family of them if Ω is a ball. Other numerical experiments carried with this code can be found in [3] and in [20] (for the eigenvalue problem in several domains).

According to the theory given in [3, 20] convergence in the energy norm is expected to occur with order $\frac{1}{2}$ with respect to the mesh size parameter h, or equivalently, of order $-\frac{1}{2n}$ with respect to the number of degrees of freedom. Moreover, using duality arguments, it is expected to have order of convergence $s+\frac{1}{2}$ (resp. $-\frac{s+1/2}{n}$) for $0 < s \leq 1/2$ and 1 (resp. $-\frac{1}{n}$) for $s > 1/2$ in the $L^2(\Omega)$-norm with respect to h (resp. number of degrees of freedom).

We first construct non-trivial solutions for (0.0.2) if Ω is a ball. Consider the Jacobi polynomials $P_k^{(\alpha,\beta)}\colon [-1,1] \to \mathbb{R}$, given by

$$P_k^{(\alpha,\beta)}(z) = \frac{\Gamma(\alpha+k+1)}{k!\,\Gamma(\alpha+\beta+k+1)} \sum_{m=0}^{k} \binom{k}{m} \frac{\Gamma(\alpha+\beta+k+m+1)}{\Gamma(\alpha+m+1)} \left(\frac{z-1}{2}\right)^m,$$

and the weight function $\omega^s : \mathbb{R}^n \to \mathbb{R}$,

$$\omega^s(x) = (1 - \|x\|^2)_+^s.$$

In [32, Theorem 3] it is shown how to construct explicit eigenfunctions for an operator closely related to the FL by using $P_k^{(s,n/2-1)}$. To be more precise, the authors prove the following result.

Theorem 3.5.1. *Let $B(0,1) \subset \mathbb{R}^n$ the unitary ball. For $s \in (0,1)$ and $k \in \mathbb{N}$, define*

$$\lambda_{k,s} = \frac{2^{2s}\,\Gamma(1+s+k)\Gamma\left(\frac{n}{2}+s+k\right)}{k!\,\Gamma\left(\frac{n}{2}+k\right)}$$

and $p_k^{(s)}\colon \mathbb{R}^n \to \mathbb{R}$,

$$p_k^{(s)}(x) = P_k^{(s,\,n/2-1)}(2\|x\|^2 - 1)\chi_{B(0,1)}(x).$$

Then the following equation holds

$$(-\Delta)^s \left(\omega^s p_k^{(s)}(x)\right) = \lambda_{k,s}\, p_k^{(s)}(x) \text{ in } B(0,1).$$

A family of explicit solutions is available by using this theorem. As a first example, we analyze the solution with $k = 0$. This gives a right hand side equal to a constant. Namely, consider

$$\begin{cases} (-\Delta)^s u = 1 & \text{in } B(0,1) \subset \mathbb{R}^2, \\ u = 0 & \text{in } B(0,1)^c. \end{cases} \tag{3.5.1}$$

We have run the code for a wide range of parameters s, while keeping the radius of the auxiliary ball B equal to 1.1. Orders of convergence in the L^2 and energy norm[4] are shown in Table 3.3; these results are in accordance with the theory.

As a second example we illustrate, in Table 3.4, that in problem (3.5.1) the radius R of the auxiliary ball B does not substantially affect the error of the scheme. This suggests that it is preferable to maintain the exterior ball's radius as small as possible. Since in this problem the domain Ω is itself a ball, for comparison, we also included the output of the code without resorting to the exterior ball (the row corresponding to $R = 1.0$). The table clearly shows that the CPU time grows linearly with respect to the number of elements $N_{\tilde{\mathcal{T}}} - N_{\mathcal{T}}$ used in the auxiliary domain. Taking into account that the final size of the linear system (3.2.2) involved in each case is the same, the computational cost is, essentially, increased only during the assembling routine. Since considering an auxiliary domain involves only the computation of the interaction between inner and outer nodes, a linear behavior of the type described above is clearly expected.

As a third example we return to the setting of Theorem 3.5.1. We consider $k = 2$ and compute the order of convergence in $L^2(\Omega)$ for $s = 0.25$ and $s = 0.75$. We summarize our numerical results in Figure 3.2. These are in accordance with the predicted rates of convergence. Finally, in Figure 3.3 the FE solution, for $s = 0.75$ and $k = 2$, computed with a mesh of about 14000 triangles is displayed.

Finally, we would like to mention just a few more facts: our numerical experiments suggest that the condition number of K behaves like $\sim N_{\mathcal{T}}^s$ while over the 99% of the CPU time is devoted to the assembly routine. Actually, the expected complexity for assembling K is quadratic in the number of elements, and this seems to be the case in our tests.

Resumen del Capítulo

Este capítulo está dedicado a la descripción e implementación del método de elementos finitos para el problema elíptico

$$\begin{cases} (-\Delta)^s u = f & \text{in } \Omega, \\ u = 0 & \text{in } \Omega^c. \end{cases}$$

[4]A discussion about how to compute errors in the energy norm can be found in [3].

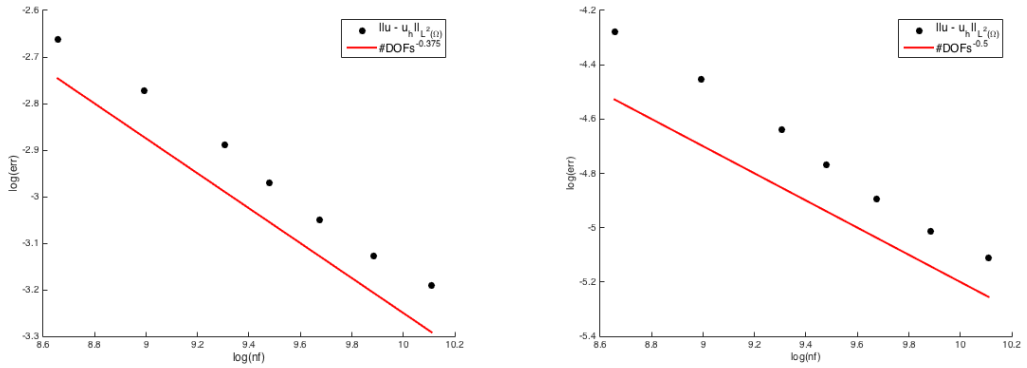

Figure 3.2: Computational rate of convergence in the $L^2(\Omega)$-norm for the problem with solution given by Theorem 3.5.1, for $k = 2$. The left panel corresponds to $s = 0.25$ and the right to $s = 0.75$. The *asymptotic* rate for $s = 0.25$ is $\approx (\#\text{DOFs})^{-3/8}$, whereas for $s = 0.75$ it is $\approx (\#\text{DOFs})^{-1/2}$, in agreement with theory.

En las secciones 3.1 y 3.2 se describe la formulación débil del problema y se establece el método de elementos finitos en base a esta. En las secciones 3.4 y 3.3 se brinda una descripción exhaustiva de la implementación del método en lenguaje *MATLAB*®, mientras que en la Sección 3.5 se muestran experimentos numéricos contrastando los órdenes de convergencia experimentales con los teóricos.

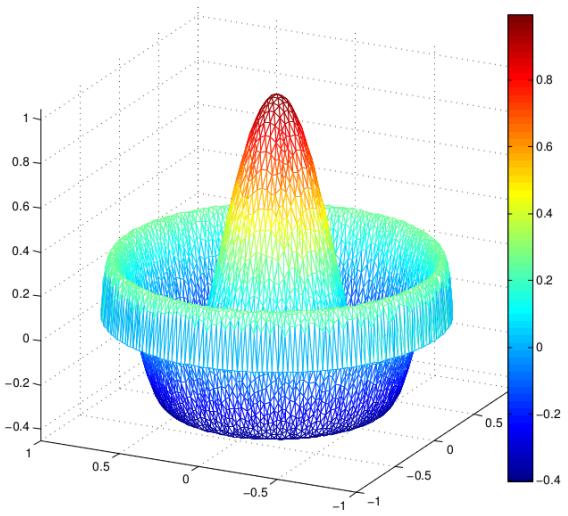

Figure 3.3: FE solution with a mesh containing about 14000 triangles. With $s = 0.75$, we use $f(x) = \lambda_{2,0.75}\, p_2^{(0.75)}(x)$ as a source term (see Theorem 3.5.1).

Table 3.2: Variables stored in `data.mat`

Name	Size	Used as input in function:	Description
`p_cube`	27x3	`vertex_quad` `edge_quad`	Quadrature points over $[0,1]^3$
`p_T_6`	6x2	None (used in non-touching case)	Quadrature points over $\hat{T}$
`p_T_12`	12x2	`comp_quad`	Quadrature points over $\hat{T}$
`p_I`	9x1	`comp_quad` `triangle_quad`	Quadrature points over $[0,1]$
`w_I`	9x1	`comp_quad`	Quadrature weights associated to `p_I`
`phiA` `phiB` `phiD`	9x36	None (used in non-touching case)	See Appendix A.3.2
`vpsi1` `vpsi2`	25x27	`vertex_quad`	See Appendix A.3.3
`epsi1` `epsi2` `epsi3` `epsi4` `epsi5`	16x27	`edge_quad`	See Appendix A.3.4
`tpsi1` `tpsi2` `tpsi3`	9x9	`triangle_quad`	See Appendix A.3.5
`cphi`	9x12	`comp_quad`	See Appendix A.3.6

Table 3.3: Computational rates of convergence for problem (3.5.1) with respect to the mesh size, measured in the $L^2(\Omega)$ and energy norms.

Value of s	Order in $L^2(\Omega)$	Order in $\widetilde{H}^s(\Omega)$
0.1	0.621	0.500
0.2	0.721	0.496
0.3	0.804	0.492
0.4	0.880	0.491
0.5	0.947	0.492
0.6	1.003	0.496
0.7	1.046	0.501
0.8	1.059	0.494
0.9	0.999	0.467

Table 3.4: The $L^2(\Omega)$ and $\widetilde{H}^s(\Omega)$ errors for different values of R in problem (3.5.1) with $s = 0.5$. In all the cases we are using a fixed and regular triangulation $\mathcal{T}$ of Ω, with $N_{\mathcal{T}} = 4228$. The computations were performed with $MATLAB^{®}$ version 2015a in Windows 10, Intel i7 Processor, RAM 8Gb.

R	$N_{\tilde{\mathcal{T}}}$	CPU time (sec.)	Error in $\|\cdot\|_{L^2(\Omega)}$	Error in $\|\cdot\|_{\widetilde{H}^s(\Omega)}$
1.0	4228	80.3	0.0164	0.1314
1.1	4980	100.7	0.0167	0.1345
1.4	8218	206.6	0.0167	0.1351
1.7	12370	344.7	0.0167	0.1352
2.0	17170	511.9	0.0167	0.1354

Chapter 4

Numerical approximations for linear evolution problems

This chapter introduces and analyzes a finite element scheme for linear evolution problems involving fractional-in-time and in-space differentiation operators up to order two. The discrete scheme we develop is based on piecewise linear elements for the space variable, taking advantage of the ideas displayed in the previous chapter, and a convolution quadrature for the time component. We illustrate the method's performance with numerical experiments in one- and two-dimensional domains.

A numerical scheme, based on standard Galerkin finite element approximations for the space variable and a convolution quadrature for the time component, is proposed and analyzed in Section 4.1. An error analysis for this scheme is carried out in Section 4.2. Finally, in Section 4.3 we present some numerical examples that illustrate the accuracy of our convergence estimates as well as the qualitative behavior of the solutions.

4.1 Numerical scheme

In this section we devise a discrete scheme to approximate (0.0.3). To this end, standard Galerkin finite elements are utilized in the spatial discretization (following [3]) and a convolution quadrature is used for the time variable (following [45]).

4.1.1 Semi discrete scheme

For an appropriate treatment, it is convenient to derive the numerical scheme in two steps. In first place we discretize in space, and afterwards in time. We follow the ideas developed in [45], taking advantage of the fact that, from the theoretical point of view,

minor changes are required to handle the fractional Laplacian instead of its classical counterpart.

Let $\mathcal{T}_h$ be a shape regular and quasi-uniform admissible simplicial mesh of Ω, and let $X_h \subset \widetilde{H}^s(\Omega)$ be the piecewise linear finite element space associated with $\mathcal{T}_h$, namely,

$$X_h := \{u_h \in C(\overline{\Omega})\colon u_h\big|_T \in \mathcal{P}^1 \ \forall T \in \mathcal{T}_h,\ u_h\big|_{\partial\Omega} = 0\}.$$

The semidiscrete problem reads: find $u_h\colon [0,T] \to X_h$ such that

$$\begin{cases} ({}^C\partial_t^\alpha u_h, w) + \langle u_h, w\rangle_{H^s(\mathbb{R}^n)} &= (f,w)\,, \quad \forall w \in X_h, \\ u_h(0) &= v_h, \\ u_h'(0) &= b_h, \text{ if } \alpha \in (1,2]. \end{cases} \tag{4.1.1}$$

Here, $v_h = P_h v$, $b_h = P_h b$, and P_h denotes the $L^2(\Omega)$ projection on X_h.

Observe that, defining the discrete fractional Laplacian $A_h : X_h \to X_h$ as the unique operator that satisfies

$$(A_h w, v) = \langle w, v\rangle_{H^s(\mathbb{R}^n)}, \text{ for all } w, v \in X_h,$$

and considering $f_h := P_h f$, we may rewrite (4.1.1) as

$$\begin{cases} {}^C\partial_t^\alpha u_h + A_h u_h &= f_h, \\ u_h(0) &= v_h, \\ u_h'(0) &= b_h, \text{ if } \alpha \in (1,2]. \end{cases} \tag{4.1.2}$$

4.1.2 Convolution Quadrature Rule

The aim of this section is to describe a numerical approximation technique for convolutions that plays an important role in the assemblage of the numerical scheme we propose. We give an overview of the main ideas and refer the reader to [56, 57] for further details.

Dividing $[0,T]$ uniformly with a time step size $\tau = T/N$, and letting $t = n\tau$ ($n \in \{1,\dots,N\}$), we seek for a numerical approximation of the convolution integral

$$k * g(t) = \int_0^t k(r) g(t-r)\, dr \tag{4.1.3}$$

by means of a finite sum

$$\sum_{j=0}^{n} \omega_j g(t - j\tau). \tag{4.1.4}$$

The weights $\{\omega_j\}_{j\in\mathbb{N}_0}$ are obtained as the coefficients of the power series

$$K\left(\frac{\delta(\xi)}{\tau}\right) = \sum_{j=0}^{\infty} \omega_j \xi^j,$$

where K denotes the Laplace transform of the kernel k, and $\delta(\xi)$ is the quotient of the generating polynomials of a linear multistep method.

To obtain the weights in (4.1.4), suppose that we extend the kernel k by zero over $r \leq 0$ and that for all $r > 0$ it satisfes

$$|k(r)| \leq Cr^{\mu-1}e^{cr}, \tag{4.1.5}$$

for some $c, \mu > 0$. Then, the inversion formula

$$k(r) = \frac{1}{2\pi i}\int_{\Gamma} K(z)e^{zr}dz \tag{4.1.6}$$

holds, where Γ is a contour lying in the sector of analyticity of K, parallel to its boundary and oriented with an increasing imaginary part. Furthermore, defining $\Sigma_\theta := \{z \in \mathbb{C} : |\arg(z)| \leq \theta\}$, $\theta \in (\pi/2, \pi)$, it holds that K is analytic in Σ_θ and satisfies

$$|K(z)| \leq C|z|^{-\mu} \quad \forall z \in \Sigma_\theta. \tag{4.1.7}$$

This condition is in turn equivalent to (4.1.5).

Replacing (4.1.6) in (4.1.3) and switching the order of integration gives

$$\int_0^t k(r)g(t-r)dr = \frac{1}{2\pi i}\int_{\Gamma} K(z)\int_0^t e^{zr}g(t-r)\,dr\,dz. \tag{4.1.8}$$

Since the inner integral in the right-hand side is the solution of the ordinary differential equation $y' = zy+g$, with $y(0) = 0$, we can obtain a numerical estimation by using some multistep method. For simplicity, suppose we utilize Backward Euler discretization (BE), that gives the scheme

$$\frac{y_n - y_{n-1}}{\tau} = zy_n + g_n.$$

Multiplying by ξ^n both sides of the equality, and summing over n, we obtain

$$\frac{(1-\xi)}{\tau}\mathbf{y}(\xi) = z\mathbf{y}(\xi) + \mathbf{g}(\xi), \tag{4.1.9}$$

where $\mathbf{y}(\xi) := \sum_{n=0}^{\infty} y_n\xi^n$ and $\mathbf{g}(\xi) := \sum_{n=0}^{\infty} g_n\xi^n$. Defining $\delta(\xi) := (1-\xi)$, from (4.1.9) we deduce

$$\mathbf{y}(\xi) = \left(\frac{\delta(\xi)}{\tau} - z\right)^{-1}\mathbf{g}(\xi).$$

Thus, the numerical approximation of y at time $n\tau$ is given by the n-th coefficient of the power series $\left(\frac{\delta(\xi)}{\tau} - z\right)^{-1}\mathbf{g}(\xi)$.

In order to obtain the desired numerical approximation of (4.1.3) we utilize the former expression, fix ξ and integrate in z the right hand side in (4.1.8). Using Cauchy's integral formula gives

$$\frac{1}{2\pi i}\int_\Gamma K(z)\left(\frac{\delta(\xi)}{\tau}-z\right)^{-1}\mathbf{g}(\xi)\,dz = K\left(\frac{\delta(\xi)}{\tau}\right)\cdot\mathbf{g}(\xi).$$

Therefore, the numerical approximation of (4.1.3) at $t=n\tau$ is given by the n-th coefficient of the power series $K\left(\frac{\delta(\xi)}{\tau}\right)\cdot\mathbf{g}(\xi)$. Finally, noticing that the coefficients of the series are the Cauchy product of the sequences $\{\omega_n\}_{n\in\mathbb{N}_0}$ and $\{g(n\tau)\}_{n\in\mathbb{N}_0}$, where $\{\omega_n\}$ are the coefficients of the power series expansion of $K\left(\frac{\delta(\xi)}{\tau}\right)$, we obtain (4.1.4).

Given a complex valued function K, analytic in Σ_θ and satisfying (4.1.7), we use the transfer function notation for (4.1.3),

$$K(z)g(t) := k*g(t) = \int_0^t k(r)g(t-r)\,dr,$$

where k is given by (4.1.6), and the notation

$$K\left(\frac{\delta(\xi)}{\tau}\right)g(t) := \sum_{j=0}^{n}\omega_j g(t-j\tau)$$

for the discrete approximation.

Next, we generalize the definition of the Convolution Quadrature Rule to operators that satisfy (4.1.7) with a negative value of μ. Indeed, let m be a positive integer such that $\mu+m>0$, setting $\tilde{K}(z) := z^{-m}K(z)$ we define

$$K(z)g(t) := \frac{\partial^m}{\partial t^m}\tilde{k}*g(t) = \frac{\partial^m}{\partial t^m}\int_0^t \tilde{k}(r)g(t-r)\,dr,$$

with $\tilde{k}$ the kernel associated with $\tilde{K}$. All the results and estimates that are achieved in the former case are still true upon this generalization (see [56, Section 5]). This is convenient because we are interested in the particular case of $K(z)=z^\alpha$, that delivers

$$z^\alpha g(t) := \frac{\partial^m}{\partial t^m}\int_0^t \frac{1}{r^{\alpha-m+1}}g(t-r)\,dr = \partial_t^\alpha g(t).$$

with m a positive integer such that $m-1\leq\alpha<m$. Considering this, we set the notation $K(\partial_t) := K(z)$ and $K(\overline{\partial_\tau}) := K(\delta(\xi)/\tau)$.

The following important result (cf. [56, Theorem 5.2]) bounds the error for the Convolution Quadrature Rule in case g is smooth on $t>0$, but has an asymptotic expansion in fractional powers of t at $t=0$.

Lemma 4.1.1. *Let K be a complex valued or operator valued function which is analytic in the sector Σ_θ, with $\theta \in (\pi/2, \pi)$, and bounded by*

$$\|K(z)\| \leq M|z|^{-\mu} \ \forall z \in \Sigma_\theta,$$

for some $\mu, M \in \mathbb{R}$. Then for $g(t) = Ct^{\beta-1}$, the operator ∂_τ satisfies

$$\|(K(\partial_t) - K(\overline{\partial_\tau}))g(t)\| \leq \begin{cases} ct^{\mu-1}\tau^\beta, & 0 < \beta \leq 1, \\ ct^{\mu+\beta-2}\tau, & \beta \geq 1. \end{cases}$$

Finally, another useful property of the operator ∂_τ is the associativity. That is, let K_1, K_2 be operators as in Lemma 4.1.1, and k an analytic function, we have

$$K_1(\partial_t)K_2(\partial_t) = (K_1K_2)(\partial_t) \quad \text{and } K_1(\partial_t)(k * g) = (K_1(\partial_t)k) * g. \tag{4.1.10}$$

4.1.3 Fully discrete scheme

At this point, a suitable discretization of the Caputo differentiation operator is required to obtain a fully discrete scheme. To this end, we employ the convolution quadrature technique described in the previous section, which allows us to derive discrete estimations of an integral which involve singular kernels.

Upon dividing $[0, T]$ uniformly with a time step size $\tau = T/N$, and letting $t = n\tau$ ($n \in \{1, \ldots, N\}$), by means of the convolution quadrature rule we are able to estimate the Riemann-Liouville operator of a function g by

$$\partial_t^\alpha g(t) \approx \sum_{j=0}^{n} \omega_j g(t - j\tau) =: \overline{\partial_\tau}^\alpha g(t), \tag{4.1.11}$$

where the weights $\{\omega_j\}_{j\in\mathbb{N}_0}$ are obtained as the coefficients of the power series

$$\left(\frac{1-\xi}{\tau}\right)^\alpha = \sum_{j=0}^{\infty} \omega_j \xi^j.$$

We are now able to suitably discretize the Caputo differentiation operator. To this end, we need to reformulate (0.0.3) using the Riemann-Liouville derivative instead of the Caputo one. It is well-known that these two operators are related by (see, for example, [31, Theorem 3.1])

$${}^C\partial_t^\alpha u(t) = \partial_t^\alpha \left(u(t) - \sum_{k=0}^{\lfloor\alpha\rfloor} \frac{u^{(k)}(0)}{k!} t^k \right), \tag{4.1.12}$$

under suitable regularity assumptions on u (see 2.1.5).

Thus, we rewrite (4.1.2) for the *fractional diffusion* case as

$$\begin{cases} \partial_t^\alpha(u_h - v_h) + A_h u_h &= f_h \\ u_h(0) &= v_h, \end{cases}$$

and for the *fractional diffusion-wave* case as

$$\begin{cases} \partial_t^\alpha(u_h - v_h - tb_h) + A_h u_h &= f_h \\ u_h(0) &= v_h \\ u_h'(0) &= b_h. \end{cases}$$

Replacing the Riemann-Liouville derivative by its discrete version given by (4.1.11), and that we will denote by $\overline{\partial_\tau}^\alpha$, we formulate the fully discrete problem as: find $U_h^n \in X_h$, with $n = \{1, \ldots, N\}$, such that

$$\begin{cases} \overline{\partial_\tau}^\alpha U_h^n + A_h U_h^n &= \overline{\partial_\tau}^\alpha v_h + F_h^n \\ U_h^0 &= v_h, \end{cases} \tag{4.1.13}$$

or

$$\begin{cases} \overline{\partial_\tau}^\alpha U_h^n + A_h U_h^n &= \overline{\partial_\tau}^\alpha v_h + (\overline{\partial_\tau}^\alpha t) b_h + F_h^n \\ U_h^0 &= v_h, \end{cases} \tag{4.1.14}$$

for *fractional diffusion* and *fractional diffusion-wave* problems respectively, where $F_h^n = P_h f(t_n)$.

In order to obtain a better error estimation in the *diffusion-wave* case, it is necessary to replace F_h^n with a corrected term $G_h^n := \overline{\partial_\tau}\partial_t^{-1} f_h(t_n)$.

For the sake of the reader's convenience, we conclude this section by giving the vectorial form of the fully discrete scheme. Let $\{\varphi_i\}_{i=1,\ldots,\mathcal{N}}$ be the Lagrange nodal basis that generates X_h. Let U^n, F^n and $G^n \in \mathbb{R}^{\mathcal{N}}$, $n = 0, \ldots, N$ be such that $U_h^n = \sum_{i=1}^{\mathcal{N}} U_i^n \varphi_i$, $F_h^n = \sum_{i=1}^{\mathcal{N}} F_i^n \varphi_i$ and $G_h^n = \sum_{i=1}^{\mathcal{N}} G_i^n \varphi_i$, where U_h^n denotes the solution of the fully discrete problem. Then we formulate (4.1.13) and (4.1.14), respectively, in the following vectorial equations:

$$M^{-1} \cdot (\omega_0 M + K) \cdot U^n = \left(\sum_{j=0}^{n} \omega_j \right) U^0 - \sum_{j=1}^{n} \omega_j U^{n-j} + F^n$$

and

$$\begin{aligned} M^{-1} \cdot (\omega_0 M + K) \cdot U^n = &\left(\sum_{j=0}^{n} \omega_j \right) U^0 + \left(\sum_{j=0}^{n} \omega_j \tau(n-j) \right) v_h \\ &- \sum_{j=1}^{n} \omega_j U^{n-j} + G^n. \end{aligned}$$

Above, $M, K \in \mathbb{R}^{\mathcal{N}\times\mathcal{N}}$ are the mass and stiffness matrices, respectively. Namely, $M_{i,j} = (\varphi_i, \varphi_j)$ and $K_{i,j} = \langle \varphi_i, \varphi_j \rangle_{H^s(\mathbb{R}^n)}$.

There are several options to compute the coefficients $\{\omega_j\}_{j\in\mathbb{N}_0}$. Recalling that

$$\left(\frac{1-\xi}{\tau}\right)^{\alpha} = \sum_{j=0}^{\infty} \omega_j \xi^n, \tag{4.1.15}$$

Fast Fourier Transform can be used for an efficient computation of $\{\omega_j\}_{j\in\mathbb{N}_0}$ (see [71, Section 7.5]) . Alternatively, a useful recursive expression is given also in [71, formula (7.23)]:

$$\omega_0 = \tau^{-\alpha}, \quad \omega_j = \left(1 - \frac{\alpha+1}{j}\right)\omega_{j-1}, \quad \forall j > 0.$$

For the numerical experiments we exhibit in Section 4.3 we have taken advantage of this identity.

4.2 Error bounds

This section shows error estimates for the numerical scheme discussed in Section 4.1. The derivation of the error bounds can be carried out following the guidelines from [45] and [47].

We start by defining the discrete analogue to operators E^α and F^α. Let $\{\phi_{h,1}, ..., \phi_{h,N}\} \subset X_h$ be an orthonormal base of egienfunctions of A_h, then we define

$$E_h^\alpha(t)v := \sum_{k=1}^{N} E_{\alpha,1}(-\lambda_{h,k}t^\alpha)\phi_{h,k}(v, \phi_{h,k})_{L^2(\Omega)}, \tag{4.2.1}$$

and

$$F_h^\alpha(t)v := \sum_{k=1}^{N} t^{\alpha-1}E_{\alpha,\alpha}(-\lambda_{h,k}t^\alpha)\phi_{h,k}(v, \phi_{h,k})_{L^2(\Omega)}. \tag{4.2.2}$$

Discrete analogues to Lemma 2.0.2 and Lemma 2.0.3 (using E_h^α and F_h^α instead of E^α and F^α) can be easily proved.

4.2.1 L^2 and elliptic projection

We start with some estimations on the elliptic or Ritz projection $R_h : \widetilde{H}^s(\Omega) \to X_h$. This operator is defined as the one that satisfies

$$\langle R_h u, \varphi\rangle_s = (Au, \varphi)_{L^2(\Omega)}, \quad \forall \varphi \in X_h,$$

and we have the following estimation.

Lemma 4.2.1. *Let $\psi \in \dot{H}^\theta(\Omega)$, with $\theta \in [0,2]$, then*

$$\|(R_h - I)\psi\|_{L^2(\Omega)} \leq h^{\gamma(1+\theta/2)}\|\psi\|_{\theta,s}, \tag{4.2.3}$$
$$\|(R_h - I)\psi\|_{1,s} \leq h^{\gamma\theta/2}\|\psi\|_{\theta,s}, \tag{4.2.4}$$

with $\gamma = \min\{s, 1/2 - \varepsilon\}$.

Proof. From [19] Proposition 3.3.2 and equation (3.3.3), taking $r = 0$ and $r = -s$, we can assert that

$$\begin{aligned}
\|(R_h - I)\psi\|_{L^2(\Omega)} &\leq Ch^{2\gamma}\|A\psi\|_{L^2(\Omega)} = Ch^{2\gamma}\|\psi\|_{2,s},\\
\|(R_h - I)\psi\|_{L^2(\Omega)} &\leq Ch^{\gamma}\|\psi\|_{L^2(\Omega)} = Ch^{\gamma}\|\psi\|_{0,s},\\
\|(R_h - I)\psi\|_{1,s} &\leq C\|\psi\|_{L^2(\Omega)} = C\|\psi\|_{0,s},\\
\|(R_h - I)\psi\|_{1,s} &\leq Ch^{\gamma}\|A\psi\|_{L^2(\Omega)} = Ch^{\gamma}\|\psi\|_{2,s},
\end{aligned}$$

From this, and using standard interpolation arguments (see [59, Theorem 4.36] for instance) we can obtain (4.2.3) and (4.2.4). □

We end this section with some estimates for P_h.

Lemma 4.2.2 (cf. [46, Lemma 2.1])**.** *For a quasi-uniform mesh, and $\theta \in [0,1]$ we have*

$$\|(P_h - I)\psi\|_{1,\theta} \leq h^{2-\theta}\|\psi\|_{H^2(\Omega)}, \quad \forall \psi \in H^2(\Omega) \cap H_0^1(\Omega), \tag{4.2.5}$$
$$\|(P_h - I)\psi\|_{1,\theta} \leq h^{1-\theta}\|\psi\|_{H^1(\Omega)}, \quad \forall \psi \in H_0^1(\Omega), \tag{4.2.6}$$
$$\|(P_h - I)\psi\|_{1,\theta} \leq h^{-\theta}\|\psi\|_{L^2(\Omega)}, \quad \forall \psi \in L^2(\Omega). \tag{4.2.7}$$

4.2.2 Discrete norm and inverse inequality

Let $(\lambda_{h,k}, \phi_{h,k})$, with $k = \{1, ..., \mathcal{N}\}$, be an eigen-pair of the operator A_h. Another important tool in the error estimation is the following discrete analogue of the norm $\|\cdot\|_{\theta,s}$. For every $u \in X_h$ we define

$$|||u|||_{\theta,s}^2 := \sum_{k=1}^{\mathcal{N}} \lambda_{h,k}^\theta (u, \phi_{h,k})_{L^2(\Omega)}^2.$$

It can be shown that both norms $|||\cdot|||_{\theta,s}$ and $\|\cdot\|_{\theta,s}$ are equivalents in the finite dimensional space X_h with constants independent of the discrete parameters. Indeed, this assertion can be easily checked for $\theta = 1, 0$, and the case $\theta \in (0,1)$ follows by means of interpolation arguments.

Also we have an inverse inequality [48, Lemma 3.3].

Lemma 4.2.3. *There exists a constant C, independent of h, such that for all $\psi \in X_h$ and for any $p > q$*

$$|||\psi|||_{p,s} \leq Ch^{s(q-p)}|||\psi|||_{q,s}. \tag{4.2.8}$$

Proof. It is well known that for a quasi uniform triangulation $\mathcal{T}_h$ the inverse inequality

$$|\psi|_{H^s(\mathbb{R}^n)} \leq Ch^{-s}\|\psi\|_{L^2(\Omega)},$$

holds for any $\psi \in X_h$. From this, observing that $|\phi_{h,k}|_{H^s(\mathbb{R}^n)} = (A_h\phi_{h,k}, \phi_{h,k})^{1/2}_{L^2(\Omega)} = \lambda^{1/2}_{h,k}$, we can conclude that $\max_{1\leq k\leq \mathcal{N}} \lambda_{h,k} \leq h^{-2s}$. Then we have

$$|||\psi|||^2_{p,s} \leq C\big(\max_{1\leq k\leq \mathcal{N}} \lambda^{p-q}_{h,k}\big) \sum_{k=1}^{\mathcal{N}} \lambda^q_{h,k}(\psi, \phi_{h,k})^2_{L^2(\Omega)} \leq Ch^{2s(q-p)}|||\psi|||^2_{q,s},$$

and (4.2.8) follows. □

4.2.3 Error bounds for the semi-discrete scheme

Here we focus only on the *diffusion-wave* case ($1 < \alpha < 2$), where the error bounds becomes more laborious. Of course, ideas used for this case can be straightforwardly applied for the case $0 < \alpha < 1$.

In order to establish the error bounds, we first set an integral representation of u for the homogeneous case $f = 0$. Define the sector $\Sigma_\theta := \{z \in \mathbb{C}, z \neq 0, \text{ such that } |\arg(z)| < \theta\}$, then $u(t) : [0, T] \to L^2(\Omega)$ can be analytically extended to Σ_θ (see [74, Theorem 2.3]). Applying the Laplace transform in (0.0.3) we obtain

$$z^\alpha \hat{u}(z) + A\hat{u}(z) = z^{\alpha-1}v + z^{\alpha-2}b,$$

where A is the fractional Laplacian with homogeneous Dirichlet conditions. Therefore, via the Laplace inversion formula, we write the integral representation

$$u(t) = \frac{1}{2\pi i}\int_{\Gamma_{\theta,\delta}} e^{zt}(z^\alpha I + A)^{-1}(z^{\alpha-1}v + z^{\alpha-2}b)\, dz, \tag{4.2.9}$$

where $\Gamma_{\theta,\delta} = \{z \in \mathbb{C} : |z| = \delta, |\arg(z)| \leq \theta\} \cup \{z \in \mathbb{C} : z = re^{\pm i\theta}, r \geq \delta\}$.

Recalling (2.0.8), if we choose θ such that $\pi/2 < \theta < \min\{\pi, \pi/\alpha\}$, then $z^\alpha \in \Sigma_{\theta'}$ with $\theta' = \alpha\theta$ for all $z \in \Sigma_\theta$. Considering θ in this way, there exists a constant C depending only on θ and α such that

$$\|(z^\alpha + A)^{-1})\|_{L^2(\Omega)} \leq C|z|^{-\alpha}. \tag{4.2.10}$$

As in (4.2.9), we can write an analogous expression for u_h,

$$u_h(t) = \frac{1}{2\pi i} \int_{\Gamma_{\theta,\delta}} e^{zt} (z^\alpha I + A_h)^{-1} (z^{\alpha-1} v_h + z^{\alpha-2} b_h)\, dz. \tag{4.2.11}$$

The following technical result can be proved analogously to [14, Lemma 3.3].

Lemma 4.2.4. *Let $\varphi \in \widetilde{H}^s(\Omega)$, and $z \in \Sigma_\theta$ with $\pi/2 < \theta < \min\{\pi, \pi/\alpha\}$. Then there exists a positive constant $c(\theta)$ such that*

$$|z^\alpha| \, \|\varphi\|^2_{L^2(\Omega)} + |\varphi|^2_{H^s(\mathbb{R}^n)} \leq c \left| z^\alpha \|\varphi\|^2_{L^2(\Omega)} + |\varphi|^2_{H^s(\mathbb{R}^n)} \right|.$$

The next lemma sets an error estimate between $(z^\alpha I + A)^{-1} f$ and its discrete approximation $(z^\alpha I + A_h)^{-1} P_h f$, analogous to [14, Lemma 3.4].

Lemma 4.2.5. *Let $f \in L^2(\Omega)$, $z \in \Sigma_\theta$, $\omega := (z^\alpha I + A)^{-1} f$, $\omega_h := (z^\alpha I + A_h)^{-1} P_h f$. Then there exists a positive constant $C(s, n, \theta)$ such that*

$$\|\omega - \omega_h\|_{L^2(\Omega)} + h^\gamma |\omega - \omega_h|_{H^s(\mathbb{R}^n)} \leq C h^{2\gamma} \|f\|_{L^2(\Omega)}.$$

As before, $\gamma = \min\{s, 1/2 - \varepsilon\}$, with $\varepsilon > 0$ arbitrary small.

Proof. We consider first the case $s \geq 1/2$. By definition of ω and ω_h, it holds that

$$\begin{aligned} z^\alpha(\omega, \varphi) + \langle \omega, \varphi \rangle_{H^s(\mathbb{R}^n)} &= (f, \varphi), \quad \forall \varphi \in \widetilde{H}^s(\Omega), \\ z^\alpha(\omega_h, \varphi) + \langle \omega_h, \varphi \rangle_{H^s(\mathbb{R}^n)} &= (f, \varphi), \quad \forall \varphi \in X_h. \end{aligned}$$

If we set $e_h := \omega - \omega_h$ and subtract these two expressions, we derive

$$z^\alpha(e_h, \varphi) + \langle e_h, \varphi \rangle_{H^s(\mathbb{R}^n)} = 0, \quad \forall \varphi \in X_h. \tag{4.2.12}$$

Applying Lemma 4.2.4 and this identity, we arrive to

$$\begin{aligned} |z^\alpha| \, \|e_h\|^2_{L^2(\Omega)} + |e_h|^2_{H^s(\mathbb{R}^n)} &\leq c \left| z^\alpha(e_h, e_h) + \langle e_h, e_h \rangle_{H^s(\mathbb{R}^n)} \right| \\ &= c \left| z^\alpha(e_h, \omega - \varphi) + \langle e_h, \omega - \varphi \rangle_{H^s(\mathbb{R}^n)} \right| \quad \forall \varphi \in X_h. \end{aligned}$$

Taking $\varphi = \Pi_h \omega$ in the previous expression, where Π_h is a suitable quasi-interpolation operator (see, for example, [3, Section 4.1]), we deduce

$$\begin{aligned} &|z^\alpha| \|e_h\|^2_{L^2(\Omega)} + |e_h|^2_{H^s(\mathbb{R}^n)} \\ &\quad \leq c \left(|z^\alpha| \, \|e_h\|_{L^2(\Omega)} h^{1/2-\varepsilon} |\omega|_{H^s(\mathbb{R}^n)} + |e_h|_{H^s(\mathbb{R}^n)} h^{1/2-\varepsilon} |\omega|_{H^{s+1/2-\varepsilon}(\mathbb{R}^n)} \right), \end{aligned} \tag{4.2.13}$$

where we have used the fact that $s \geq 1/2$ implies that $h^s \leq h^{1/2-\varepsilon}$.

On the other hand, if we choose $\varphi = \omega$ in Lemma 4.2.4, we obtain

$$\begin{aligned} |z^\alpha| \, \|\omega\|^2_{L^2(\Omega)} + |\omega|^2_{H^s(\mathbb{R}^n)} &\leq c \left| z^\alpha(\omega,\omega) + \langle \omega, \omega \rangle_{H^s(\mathbb{R}^n)} \right| \\ &= c \, |(f,\omega)| \leq c \|f\|_{L^2(\Omega)} \|\omega\|_{L^2(\Omega)}. \end{aligned}$$

Consequently,

$$\|\omega\|_{L^2(\Omega)} \leq c \, |z|^{-\alpha} \, \|f\|_{L^2(\Omega)} \quad \text{and} \quad |\omega|_{H^s(\mathbb{R}^n)} \leq c \, |z|^{-\alpha/2} \, \|f\|_{L^2(\Omega)}. \tag{4.2.14}$$

From Proposition 1.2.1, we know that for the case $z = 0$ the estimate $|\omega|_{H^{s+1/2-\varepsilon}(\mathbb{R}^n)} \leq \|f\|_{L^2(\Omega)}$ holds. Utilizing this estimate with $-z^\alpha \omega + f$ instead of f, we obtain

$$|\omega|_{H^{s+1/2-\varepsilon}(\mathbb{R}^n)} \leq \| - z^\alpha \omega + f\|_{L^2(\Omega)} \leq c \|f\|_{L^2(\Omega)},$$

where in the last inequality we used (4.2.14). Combining this with (4.2.13), we derive

$$|z^\alpha| \, \|e_h\|^2_{L^2(\Omega)} + |e_h|^2_{H^s(\mathbb{R}^n)} \leq c h^{1/2-\varepsilon} \|f\|_{L^2(\Omega)} \left(z^{\alpha/2} \|e_h\|_{L^2(\Omega)} + |e_h|_{H^s(\mathbb{R}^n)} \right).$$

This implies that

$$|z^\alpha| \, \|e_h\|^2_{L^2(\Omega)} + |e_h|^2_{H^s(\mathbb{R}^n)} \leq c h^{1-2\varepsilon} \|f\|^2_{L^2(\Omega)}, \tag{4.2.15}$$

and gives the bound for $|e_h|_{H^s(\mathbb{R}^n)}$. Next, we aim to estimate $\|e_h\|^2_{L^2(\Omega)}$. For this purpose, we proceed via the following duality argument. Given $\varphi \in L^2(\Omega)$, define

$$\psi := (z^\alpha + A)^{-1} \varphi \text{ and } \psi_h := (z^\alpha + A_h)^{-1} P_h \varphi.$$

Thus, we write

$$\|e_h\|_{L^2(\Omega)} = \sup_{\varphi \in L^2(\Omega)} \frac{|(e_h, \varphi)|}{\|\varphi\|_{L^2(\Omega)}} = \sup_{\varphi \in L^2(\Omega)} \frac{\left| z^\alpha(e_h, \psi) + \langle e_h, \psi \rangle_{H^s(\mathbb{R}^n)} \right|}{\|\varphi\|_{L^2(\Omega)}}.$$

We aim to bound the supremum in the identity above. Resorting to (4.2.12) and the Cauchy-Schwarz inequality, we bound

$$\begin{aligned} \left| z^\alpha(e_h, \psi) + \langle e_h, \psi \rangle_{H^s(\mathbb{R}^n)} \right| &= \left| z^\alpha(e_h, \psi - \psi_h) + \langle e_h, \psi - \psi_h \rangle_{H^s(\mathbb{R}^n)} \right| \\ &\leq z^{\alpha/2} \|e_h\|_{L^2(\Omega)} z^{\alpha/2} \|\psi - \psi_h\|_{L^2(\Omega)} + |e_h|_{H^s(\mathbb{R}^n)} |\psi - \psi_h|_{H^s(\mathbb{R}^n)} \\ &\leq \left(z^{\alpha/2} \|e_h\|_{L^2(\Omega)} + |e_h|_{H^s(\mathbb{R}^n)} \right) \left(z^{\alpha/2} \|\psi - \psi_h\|_{L^2(\Omega)} + |\psi - \psi_h|_{H^s(\mathbb{R}^n)} \right). \end{aligned}$$

Finally, applying (4.2.15) we arrive at

$$\left| z^\alpha(e_h, \psi) + \langle e_h, \psi \rangle_{H^s(\mathbb{R}^n)} \right| \leq h^{1-2\varepsilon} \|f\|_{L^2(\Omega)} \|\varphi\|_{L^2(\Omega)},$$

from where we can derive the desired inequality.

The analysis of the case $s \leq 1/2$ can be carried out in analogously. Indeed, using that $h^s \geq h^{1/2-\varepsilon}$ we obtain, instead of (4.2.13), the inequality

$$\begin{aligned} |z^\alpha| \, \|e_h\|^2_{L^2(\Omega)} &+ |e_h|^2_{H^s(\mathbb{R}^n)} \\ &\leq c \left(\|e_h\|_{L^2(\Omega)} h^s |\omega|_{H^s(\mathbb{R}^n)} + |e_h|_{H^s(\mathbb{R}^n)} h^s |\omega|_{H^{s+1/2-\varepsilon}(\mathbb{R}^n)} \right), \end{aligned}$$

and proceeding as before we arrive at the desired estimate. □

Homogeneous case

At this point, we are able to give an error estimation for the case $f \equiv 0$.

Theorem 4.2.6. *Let $1 < \alpha < 2$, u be the solution of (0.0.3) with $v \in \widetilde{H}^q(\Omega)$, $b \in \widetilde{H}^r(\Omega)$ $q, r \in [0, 2s]$, and $f = 0$; and let u_h be the solution of (4.1.1) with $v_h = P_h v$, $b_h = P_h b$, and $f_h = 0$. Writing $e_h(t) = u(t) - u_h(t)$, there exists a positive constant $C = C(s, n)$ such that*

$$\|e_h(t)\|_{L^2(\Omega)} + h^\gamma |e_h(t)|_{H^s(\mathbb{R}^n)} \leq Ch^{2\gamma} \left(t^{-\alpha\left(\frac{2s-q}{2s}\right)} \|v\|_{H^q(\mathbb{R}^n)} + t^{1-\alpha\left(\frac{2s-r}{2s}\right)} \|b\|_{H^r(\mathbb{R}^n)} \right).$$

Proof. First, suppose v and $b \in L^2(\Omega)$. Combining (4.2.9) and (4.2.11), we can obtain an integral representation for e_h,

$$e_h(t) = \frac{1}{2\pi i} \int_{\Gamma_{\theta,\delta}} e^{zt} \left(z^{\alpha-1}(w^v + w_h^v) + z^{\alpha-2}(w^b + w_h^b) \right) dz, \tag{4.2.16}$$

where $w^v = (z^\alpha I + A)^{-1} v$, $w_h^v = (z^\alpha I + A_h)^{-1} P_h v$, $w^b = (z^\alpha I + A)^{-1} b$, $w_h^b = (z^\alpha I + A_h)^{-1} P_h b$. Using Lemma 4.2.5 and choosing $\delta = 1/t$ in the definition of $\Gamma_{\theta,\delta}$ we have

$$\begin{aligned}
|e_h(t)|_{H^s(\mathbb{R}^n)} &\leq Ch^\gamma \left(\int_{-\theta}^{\theta} e^{\cos\psi} t^{-\alpha} d\psi + \int_{1/t}^{\infty} e^{rt\cos\theta} r^{\alpha-1} dr \right) \|v\|_{L^2(\Omega)} \\
&\quad + Ch^\gamma \left(\int_{-\theta}^{\theta} e^{\cos\psi} t^{1-\alpha}\, d\psi + \int_{1/t}^{\infty} e^{rt\cos\theta} r^{\alpha-2}\, dr \right) \|b\|_{L^2(\Omega)} \\
&\leq Ch^\gamma (t^{-\alpha}\|v\|_{L^2(\Omega)} + t^{1-\alpha}\|b\|_{L^2(\Omega)}).
\end{aligned}$$

With the same idea we can obtain the estimate for $\|e_h\|_{L^2(\Omega)}$, and this shows the assertion for $v, b \in L^2(\Omega)$.

Now, for $v, b \in H^{2s}(\mathbb{R}^n)$, first we set $v_h = R_h v$ and $b_h = R_h b$. Then $e_h(t) = u(t) - u_h(t)$ can be written as

$$\begin{aligned}
e_h(t) =& \frac{1}{2\pi \mathrm{i}} \int_{\Gamma_{\theta,\delta}} e^{zt} z^{\alpha-1} \left((z^\alpha I + A)^{-1} - (z^\alpha I + A_h)^{-1} R_h \right) v\, dz \\
&+ \frac{1}{2\pi \mathrm{i}} \int_{\Gamma_{\theta,\delta}} e^{zt} z^{\alpha-2} \left((z^\alpha I + A)^{-1} - (z^\alpha I + A_h)^{-1} R_h \right) b\, dz.
\end{aligned}$$

Using the identity $z^\alpha (z^\alpha I + A)^{-1} = I - (z^\alpha I + A)^{-1} A$, we have

$$\begin{aligned}
e_h(t) =& \frac{1}{2\pi \mathrm{i}} \left(\int_{\Gamma_{\theta,1/t}} e^{zt} z^{-1} (w^v(z) - w_h^v(z))\, dz + \int_{\Gamma_{\theta,1/t}} e^{zt} z^{-1} (v - R_h v)\, dz \right) \\
&+ \frac{1}{2\pi \mathrm{i}} \left(\int_{\Gamma_{\theta,1/t}} e^{zt} z^{-2} (w^b(z) - w_h^b(z))\, dz + \int_{\Gamma_{\theta,1/t}} e^{zt} z^{-2} (b - R_h b)\, dz \right) := \text{(i)} + \text{(ii)},
\end{aligned}$$

where $w^v(z) = (z^\alpha I + A)^{-1}Av$, $w_h^v(z) = (z^\alpha I + A_h)^{-1}A_h R_h v$, and $w^b(z)$ and $w_h^b(z)$ are defined analogously. Now Lemma 4.2.5 and the relation $A_h R_h = P_h A$ yield

$$\|w^v(t) - w_h^v(t)\|_{L^2(\Omega)} + h^\gamma |w^v(t) - w_h^v(t)|_{H^s(\mathbb{R}^n)} \le Ch^{2\gamma}\|Av\|_{L^2(\Omega)}.$$

Then, we can estimate the first term (i)

$$\begin{aligned}\|(\mathrm{i})\|_{L^2(\Omega)} &\le Ch^{2\gamma}\|Av\|_{L^2(\Omega)}\left|\frac{1}{2\pi \mathrm{i}}\int_{\Gamma_{\theta,\delta}} e^{zt}z^{-1}\,dz\right| \\ &\le Ch^{2\gamma}\|Av\|_{L^2(\Omega)}\left(\int_{1/t}^{\infty} e^{rt\cos\theta}r^{-1}\,dr + \int_{-\theta}^{\theta} e^{\cos\psi}\,d\psi\right) \le Ch^{2\gamma}\|v\|_{H^{2s}(\mathbb{R}^n)}.\end{aligned}$$

The second term (ii) can be estimated in a similar way:

$$\|(\mathrm{ii})\|_{L^2(\Omega)} \le Ch^{2\gamma}\|Ab\|_{L^2(\Omega)}\left|\frac{1}{2\pi \mathrm{i}}\int_{\Gamma} e^{zt}z^{-2}\,dz\right| \le Ch^{2\gamma}t\|b\|_{H^{2s}(\mathbb{R}^n)},$$

and the $L^2(\Omega)$-error estimate follows. The estimate in $H^s(\mathbb{R}^n)$ norm can be obtained analogously. Finally, for the choice $v_h = P_h v$ and $b_h = P_h b$, we have

$$E^\alpha(t)v - E_h^\alpha(t)P_h v = E(t)v - E_h^\alpha(t)R_h v + E_h^\alpha(t)(R_h v - P_h v),$$

The first term is already bounded. For the second one we have

$$\|E_h^\alpha(t)(P_h v - R_h v)\|_{p,s} \le C\|P_h v - R_h v\|_{p,s} \le Ch^{2\gamma-\gamma p}\|v\|_{H^{2s}(\mathbb{R}^n)}, \quad p = 0, 1.$$

where in the first inequality we have used Lemma 2.0.2, and lemmas 4.2.1 and 4.2.2 (combined with classical interpolation techniques) in the second step. The estimate for $b \in H^{2s}(\mathbb{R}^n)$ follows analogously. These estimates along with standard interpolation arguments complete the proof of the theorem. □

Non-homogeneous case

To complete the error estimate for the semi-discrete scheme, it still remains to analyze the case $v \equiv b \equiv 0$ and $f \not\equiv 0$. A proper generalization of [47, Theorem 3.2] can be carried out following the guidelines outlined in that work.

Theorem 4.2.7. *Let $1 < \alpha < 2$, $f \in L^\infty(0, T; L^2(\Omega))$, and let u and u_h be the solutions of (0.0.3) and (4.1.1) respectively, with $f_h = P_h f$, and all the initial data equal to zero. Then, there exists a positive constant $C = C(s, n)$ such that*

$$\|u - u_h\|_{L^2(\Omega)} \le Ch^{2\gamma}|\log h|^2\|f\|_{L^\infty([0,T];L^2(\Omega))}.$$

Proof. Recalling the results of Section 2.3, we know that if $v \equiv b \equiv 0$ then

$$u(t) = \int_0^t F^\alpha(t-s) f(t)\, ds.$$

So we can estimate

$$\|u(t)\|_{2-\varepsilon,s} \leq \int_0^t \|F^\alpha(t-s) f(t)\|_{2-\varepsilon,s}\, ds \leq \int_0^t (t-s)^{\varepsilon\alpha/2-1} \|f(t)\|_{L^2(\Omega)}\, ds \tag{4.2.17}$$

$$\leq C\varepsilon^{-1} t^{\varepsilon\alpha/2} \|f\|_{L^\infty([0,T];L^2(\Omega))},$$

where in the second inequality we have used Lemma 2.0.2.

Now, splitting $u - u_h$ as

$$u - u_h = (u - P_h u) + (P_h u - u_h) = a(t) + c(t),$$

and using the relation $A_h R_h = P_h A$ we can obtain the following equation for $a(t)$:

$${}^C\partial_t^\alpha a + A_h a = A_h(R_h u - A_h u), \tag{4.2.18}$$

with $a(0) \equiv \partial_t a(0) \equiv 0$.

Using 4.2.1 and (4.2.17) we can easily estimate

$$\|c(t)\|_{L^2(\Omega)} \leq h^{2\gamma-\gamma\varepsilon/2} \|u(t)\|_{2-\varepsilon,s} \leq h^{2\gamma-\varepsilon} \|u(t)\|_{2-\varepsilon,s} \tag{4.2.19}$$

$$\leq Ch^{2\gamma-\varepsilon}\varepsilon^{-1} t^{\varepsilon\alpha/2} \|f\|_{L^\infty([0,T];L^2(\Omega))},$$

for all $t > 0$.

On the other hand, using (4.2.18) we can write

$$a(t) = \int_0^t F^\alpha(t-s) A_h(R_h u - A_h u)\, ds,$$

and from this we can estimate

$$\|a(t)\|_{L^2(\Omega)} \leq \int_0^t \|F^\alpha(t-s) A_h(R_h u - A_h u)\|_{L^2(\Omega)}\, ds = \int_0^t \|F^\alpha(t-s)(R_h u - A_h u)\|_{2,s}\, ds$$

$$\leq C \int_0^t (t-s)^{\alpha\varepsilon/2-1} \|(R_h u - A_h u)\|_{\varepsilon,s}\, ds \leq C \int_0^t (t-s)^{\alpha\varepsilon/2-1} |||(R_h u - A_h u)|||_{\varepsilon,s}\, ds,$$

where in the third step we have used Lemma 2.0.2 with $p = 2$ and $q = \varepsilon$. Further, using the inverse estimation from Lemma 4.2.3 for $\|\!|R_h u - P_h u|\!\|_{\varepsilon,s}$, and then Lemma 4.2.1 on $(R_h u - u)$ and $(u - P_h u)$ we obtain

$$\|a(t)\|_{L^2(\Omega)} \leq Ch^{-s\varepsilon} \int_0^t (t-s)^{\alpha\varepsilon/2-1} \|(R_h u - A_h u)\|_{L^2(\Omega)}\, ds \tag{4.2.20}$$

$$\leq Ch^{2\gamma-2\varepsilon} \int_0^t (t-s)^{\alpha\varepsilon/2-1} \|u\|_{2-\varepsilon,s}\, ds \leq C\varepsilon^{-1} h^{2\gamma-2\varepsilon} \|f\|_{L^\infty([0,T],L^2(\Omega))} \int_0^t (t-s)^{\alpha\varepsilon/2-1} t^{\varepsilon\alpha/2}\, ds$$

$$\leq C\varepsilon^{-1} h^{2\gamma-2\varepsilon} \|f\|_{L^\infty([0,T],L^2(\Omega))},$$

where in the third step we have used estimation (4.2.17). Finally, we can obtain the statement of the theorem taking $\varepsilon = |\log h|$ in the last inequality.

□

4.2.4 Error bounds for the fully-discrete scheme

Considering all the theory displayed up to this point, error estimates for the fully-discrete scheme can be derived in the same way as in [45].

Theorem 4.2.8. *Let u be the solution of problem (0.0.3) with $v \in \widetilde{H}^q(\Omega)$, $b \in \widetilde{H}^r(\Omega)$ $q, r \in [0, 2s]$, and $f = 0$; and let U_h^n be the solution of (4.1.13) or (4.1.14) with $v_h = P_h v$, $b_h = P_h b$, and $F_h^n = 0$. Then, there exists a positive constant $C = C(s, n)$ such that*

- *If $0 < \alpha < 1$, then*

$$\|u(t_n) - U_h^n\|_{L^2(\Omega)} \leq C \left(t_n^{\alpha\left(\frac{q}{2s}\right)-1} \tau + t_n^{-\alpha\left(\frac{2s-q}{2s}\right)} h^{s+\gamma} \right) \|v\|_{H^q(\mathbb{R}^n)}.$$

- *If $1 < \alpha < 2$, then*

$$\|u(t_n) - U_h^n\|_{L^2(\Omega)} \leq C \left(t_n^{\alpha\left(\frac{q}{2s}\right)-1} \tau + t_n^{-\alpha\left(\frac{2s-q}{2s}\right)} h^{s+\gamma} \right) \|v\|_{H^q(\mathbb{R}^n)}$$
$$+ C \left(t_n^{\alpha\left(\frac{r}{2s}\right)} \tau + t_n^{1-\alpha\left(\frac{2s-r}{2s}\right)} h^{2\gamma} \right) \|b\|_{H^r(\mathbb{R}^n)}.$$

Proof. In view of Theorem 4.2.6, it suffices to bound $U_h^n - u_h(t_n)$. To this end, we denote for $z \in \Sigma_\theta$, $\theta \in (\pi/2, \pi)$, $G(z) = z^\alpha (z^\alpha I + A_h)^{-1}$. Then by (4.1.13) and (4.1.14), we have

$$U_h^n - u_h(t_n) = (G(\overline{\partial_\tau}) - G(\partial_t)) v_h. \tag{4.2.21}$$

From (4.2.10) we have $G(z) \leq C$ for $z \in \Sigma_\theta$. Hence, for $v \in L^2(\Omega)$, (4.2.21), Lemma 4.1.1 (with $\mu = 0$ and $\beta = 1$), and the $L^2(\Omega)$ stability of P_h we obtain

$$\|u_h(t_n) - U_h^n\|_{L^2(\Omega)} \leq C\tau t_n^{-1} \|v_h\|_{L^2(\Omega)} \leq Ct_n^{-1} \tau \|v\|_{L^2(\Omega)}. \tag{4.2.22}$$

For $v \in H^{2s}(\mathbb{R}^n)$, we first consider $v_h = R_h v$. Using the relation $G(z) = I - (z^\alpha I + A_h)^{-1} A_h$, with $G_s(z) = (z^\alpha I + A_h)^{-1}$, we have $U_h^n - u_h(t_n) = (G_s(\overline{\partial_\tau}) - G_s(\partial_t)) A_h v_h$. Using (4.2.10) and Lemma 4.1.1 (with $\mu = \alpha$ and $\beta = 1$) gives

$$\|u_h(t_n) - U_h^n\|_{L^2(\Omega)} \leq C\tau t_n^{\alpha-1} \|A_h v_h\|_{L^2(\Omega)} \leq c\tau t_n^{\alpha-1} \|v\|_{H^{2s}(\mathbb{R}^n)},$$

where the last step we have used $A_h R_h = P_h A$. The estimate holds also for the choice $v_h = P_h v$ in view of the $L^2(\Omega)$ stability of the scheme (4.2.22), and repeating the final argument in the proof of Theorem 4.2.6. The assertion now follows from interpolation. The case of $1 < \alpha < 2$ is analogous, and hence the proof is omitted. □

Remark 4.2.9. In the previous theorem –and in Theorem 4.2.6 as well – we wrote the orders of convergence in term of various Sobolev norms of the data. For clarity, hypotheses in theorems 2.1.3 and 2.3.2 just involved either L^2 or H^s norms of the data. For instance, assuming that $v \in \widetilde{H}^s(\Omega)$ is such that $(-\Delta)^s v \in L^2(\Omega)$ and $b \in \widetilde{H}^s(\Omega)$, the conclusions of Theorem 4.2.8 read

$$\begin{aligned}
\|u(t_n) - U_h^n\|_{L^2(\Omega)} &\leq C\left(t_n^{\alpha-1}\tau + h^{s+\gamma}\right) \|(-\Delta)^s v\|_{L^2(\Omega)} \quad \text{if } 0 < \alpha < 1, \\
\|u(t_n) - U_h^n\|_{L^2(\Omega)} &\leq C\left(t_n^{\alpha-1}\tau + h^{s+\gamma}\right) \|(-\Delta)^s v\|_{L^2(\Omega)} \\
&\quad + C\left(t_n^{\frac{\alpha}{2}}\tau + t_n^{1-\frac{\alpha}{2}} h^{2\gamma}\right) |b|_{H^s(\mathbb{R}^n)} \qquad \text{if } 1 < \alpha < 2.
\end{aligned}$$

We emphasize that, as stated in Remark 1.2.3, the identity $\|(-\Delta)^s v\|_{L^2(\Omega)} \leq C|v|_{H^{2s}(\mathbb{R}^n)}$ holds for all $v \in \widetilde{H}^{2s}(\Omega)$.

Finally, we state the order of convergence of the fully-discrete scheme for the problems with a non-null source term.

Theorem 4.2.10. *Let u be the solution of* (0.0.3) *with homogeneous initial data and with $f \in L^\infty(0,T;L^2(\Omega))$; and let U_h^n be the solution of* (4.1.13) *or* (4.1.14) *with $f_h = P_h f$. Then, there exists a positive constant $C = C(s,n)$ such that*

- *For $0 < \alpha < 1$, if $\int_0^t (t-s)^{\alpha-1} \|f'(s)\|_{L^2(\Omega)} ds < \infty$ for $t \in (0,T]$, then*

$$\begin{aligned}
\|u(t_n) - U_h^n\|_{L^2(\Omega)} \leq C\Big(&h^{2\gamma}\ell_h^2 \|f\|_{L^\infty([0,T];L^2(\Omega))} + t_n^{\alpha-1}\tau \|f(0)\|_{L^2(\Omega)} \\
&+ \tau \int_0^{t_n} (t_n - s)^{\alpha-1} \|f'(s)\|_{L^2(\Omega)}\Big).
\end{aligned}$$

- *If $1 < \alpha < 2$, then*

$$\|u(t_n) - U_h^n\|_{L^2(\Omega)} \leq C(h^{2\gamma}\ell_h^2 + \tau) \|f\|_{L^\infty([0,T];L^2(\Omega))}.$$

Proof. Defining $G(z) = (z^\alpha I + A_h)^{-1}$, the semidiscrete solution u_h and fully discrete solution U_h^n can be written as $u_h = G(\partial_t) f_h$ and $U_h^n = G(\overline{\partial_\tau}) f_h$, respectively. Using the splitting $f_h(t) = f_h(0) + (1 * f_h')(t)$ and the associativity property (4.1.10), we have

$$\begin{aligned} u_h(t_n) - U_h^n &= \left(G(\partial_t) - G(\overline{\partial_\tau})\right) \left(f_h(0) + (1 * f_h')(t_n)\right) \\ &= \left(G(\partial_t) - G(\overline{\partial_\tau})\right) f_h(0) + \left((G(\partial_t) - G(\overline{\partial_\tau}))1\right) * f_h'(t_n)) := \text{(i)} + \text{(ii)}. \end{aligned}$$

Then Lemma 4.1.1 (with $\mu = \alpha$ and $\beta = 1$) gives us a bound for the first term (i)

$$\|\text{(i)}\|_{L^2(\Omega)} \le c\tau t_n^{\alpha-1} \|f_h(0)\|_{L^2(\Omega)} \le c\tau t_n^{\alpha-1} \|f(0)\|_{L^2(\Omega)}.$$

Again, by Lemma 4.1.1 and the L^2 stability of P_h we have

$$\begin{aligned} \|\text{(ii)}\|_{L^2(\Omega)} &\le \int_0^{t_n} \| \left((G(\partial_t) - G(\overline{\partial_\tau}))1\right) (t_n - s) f_h'(s)\|_{L^2(\Omega)} \, ds \\ &\le c\tau \int_0^{t_n} (t_n - s)^{\alpha-1} \|f_h'(s)\|_{L^2(\Omega)} \, ds \le c\tau \int_0^{t_n} (t_n - s)^{\alpha-1} \|f'(s)\|_{L^2(\Omega)} \, ds. \end{aligned}$$

This shows the first assertion. For the scheme (4.1.14) (using the corrected term $G_h^n = \overline{\partial_\tau} \partial_t^{-1} f_h(t_n)$ as source) with $v = b = 0$, we have $U_h^n = G(z) g_h$ with $g_h = \partial_t^{-1} f_h$ and $G(z) = z(z^\alpha I + A_h)^{-1}$. Hence the relation $g_h = 1 * f_h$, the convolution property (4.1.10) and Lemma 4.1.1 with $\mu = \alpha - 1$ and $\beta = 1$ yield

$$\|u_h(t_n) - U_h^n\|_{L^2(\Omega)} \le c\tau \int_0^{t_n} (t_n - s)^{\alpha-2} \|f(s)\|_{L^2(\Omega)} \, ds \le c_T \tau \|f\|_{L^\infty(0,T;L^2(\Omega))},$$

from which follows the second assertion. □

4.3 Numerical experiments

This section exhibits the results of numerical tests for discretizations of problems posed in one- and two-dimensional domains. Numerical solutions of (0.0.3) were obtained by applying the scheme described in Section 4.1. The experiments in two-dimensional geometries were carried out with a code based on the one presented in Chapter 3.

4.3.1 Explicit Solutions

In Section (3.5) it is shown how some families of non-trivial solutions for the fractional Poisson problem can be constructed. Here we recall these results in order to be applied to the evolution equation in the cases in which Ω corresponds to *a*) $(-1, 1) \subset \mathbb{R}$ and, more generally, *b*) $B(0, 1) \subset \mathbb{R}^n$.

We recall that for $n \geq 1$, the function $\omega^s : \mathbb{R}^n \to \mathbb{R}$, is defined as

$$\omega^s(x) = (1 - |x|^2)_+^s.$$

Then,

$$u(x) := \omega^s(x) g_k^{(s)}(x)$$

solves

$$\begin{cases} (-\Delta)^s u = f & \text{in } \Omega, \\ u = 0 & \text{in } \Omega^c, \end{cases}$$

with $f(x) = \lambda_s^k g_k^{(s)}(x)$, where in case a)

$$\lambda_s^k = \frac{\Gamma(2s + k + 1)}{k!} \qquad g_k^{(s)}(x) := C_k^{(s+1/2)}(x),$$

and in case b)

$$\lambda_s^k = \frac{2^{2s}\,\Gamma(1 + s + k)\Gamma\left(\frac{n}{2} + s + k\right)}{k!\,\Gamma\left(\frac{n}{2} + k\right)} \qquad g_k^{(s)}(x) := P_k^{(s,\, n/2-1)}(2|x|^2 - 1).$$

Above, $C_k^{(s+1/2)}$ and $P_k^{(s,\, n/2-1)}$ denote a Gegenbauer and a Jacobi polynomial [1], respectively.

Next, let $h(t)$ be a function such that ${}^C\partial_t^\alpha h(t)$ can be easily computed. By means of separation of variables we can construct explicit solutions of the fractional evolution problem of the form

$$u(x,t) = h(t) \cdot \omega^s(x) g_k^{(s)}(x).$$

4.3.2 Orders of convergence

In order to confirm the predicted convergence rate, we show the results we obtained in three example problems:

a. $u(x,t) = E_{\alpha,1}(-t^\alpha) \cdot \omega^s(x) C_3^{(s)}(x)$, $\Omega = (-1, 1)$;

b. $u(x,t) = \sin(t) \cdot \omega^s(x) C_3^{(s)}(x)$, $\Omega = (-1, 1)$;

c. $u(x,t) = E_{\alpha,1}(-t^\alpha) \cdot \omega^s(x) P_k^{(s,0)}(2|x|^2 - 1)$, $\Omega = B(0,1) \subset \mathbb{R}^2$.

For examples (a) and (b) we examine the time and spatial convergence over a fixed time $t = 0.1$. A fixed small time step is taking to see the spatial convergence and vice versa. For the computation of the Mittag-Leffler functions we have used the algorithm described in [36]. Our results are summarized in tables 4.1, 4.2, 4.3 and 4.4.

Example	$\alpha \setminus \tau$	0.01	0.005	0.0025	0.001	Rate (in τ)
(a)	0.5	4.227e-3	2.105e-3	1.055e-3	4.493e-4	0.98
(a)	1.5	2.512e-2	1.261e-2	6.349e-3	2.602e-3	0.99
(b)	1.5	4.867e-3	2.402e-3	1.188e-3	5.362e-4	0.96

Table 4.1: The $L^2(\Omega)$ error at time $t = 0.1$ with $s = 0.75$ using a uniform mesh with size $h = 1/5000$. The expected convergence rate in τ is 1.

Example	$\alpha \setminus$ mesh size h	1/250	1/500	1/1000	1/1500	Rate (in h)
(a)	0.5	8.837e-3	3.856e-3	1.781e-3	1.198e-3	1.12
(a)	1.5	9.978e-3	4.350e-3	1.967e-3	1.252e-3	1.16
(b)	0.5	1.162e-3	5.158e-4	4.010e-3	1.640e-4	1.09
(b)	1.5	8.453e-4	3.644e-4	1.632e-4	1.035e-4	1.17

Table 4.2: The $L^2(\Omega)$ error at time $t = 0.1$ with $s = 0.75$ using $\tau = 1/5000$. The expected convergence rate in h is 1.

The experimental orders of convergence (e.o.c.) are in agreement with the theory in the case $s > 1/2$ while our numerical examples exhibit e.o.c. (in space) higher than those predicted if $s < 1/2$ (see Tables 4.3 and 4.4). This behavior seems to be due to the fact that the extra regularity of the data present in our examples can not be exploited in our arguments; the actual solutions are more regular than what is predicted by theorems 2.1.3 and 2.3.2.

4.3.3 Qualitative aspects in $\mathbb{R}^2$

Finally, we present experiments that illustrate some qualitative effects of the fractional derivatives. In Figure 4.1, we fix $s = 0.5$, and show the evolution in time for different values of the parameter α, ranging from *fractional diffusion* to *fractional diffusion-wave*. Memory effects are present for $\alpha = 0.5$, while the solution oscillates for $\alpha = 1.5$.

Figure 4.2, in turn, displays the effect of moving the parameters α and s for a fixed time. It can be seen that increasing the spatial differentiation order s leads to a faster spreading of the initial condition. Apparent differences can be noticed among the three different problems with $\alpha = 2s$ exhibited along the diagonal of the figure.

Our third example, in Figure 4.3, exhibits the persistence of a singularity along the time due to the *memory* induced by the fractional in-time derivative. In that experiment, we have set $\alpha = 0.99$ and $s = 0.9$. Notice that the solution vanishes to 0 as time increases, but even though the differentiation parameters are both close to 1, which corresponds to the classical heat equation, the singular behavior of the initial condition persists in time.

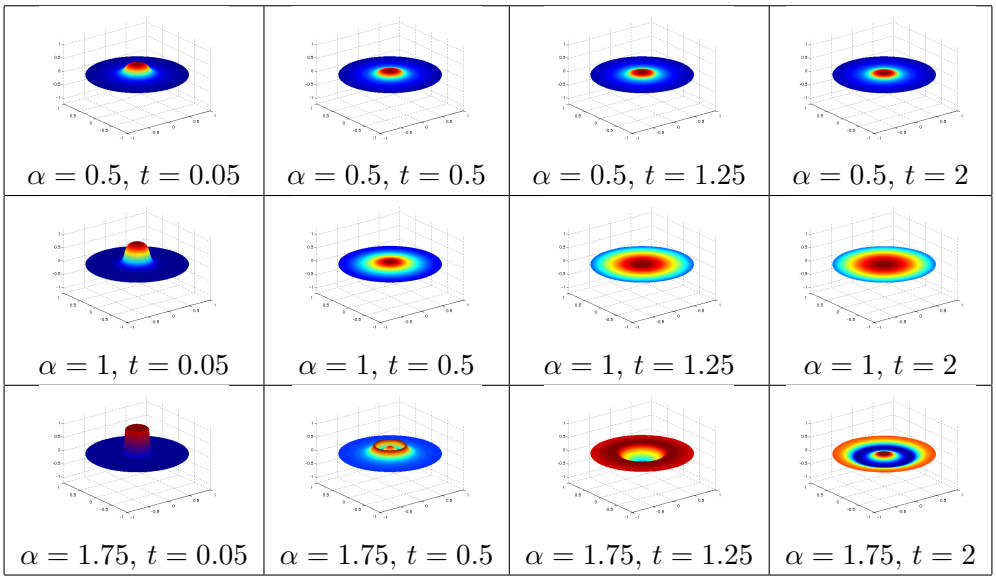

Figure 4.1: In this example we set $\Omega = B(0,1)$, $s = 0.5$ and the initial conditions $v(x) = \chi_{B(0,r)}$ with $r = 0.275$, and $b \equiv 0$ for $\alpha > 1$. The evolution in time is displayed for several values of α.

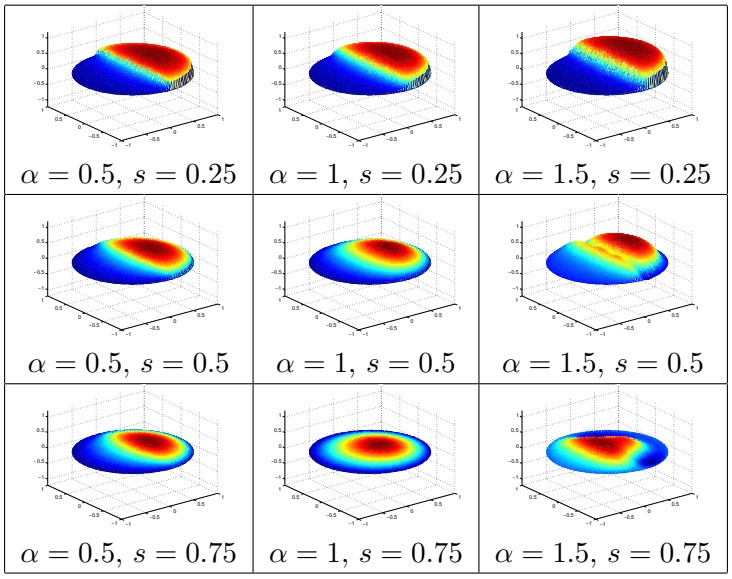

Figure 4.2: Effect of considering various α and s at time $t = 0.05$. In this example, $\Omega = B(0,1)$ and the initial data are $v(x,y) = \chi_{\{y>0\}}(x,y)$ and $b \equiv 0$ for $\alpha > 1$.

Example	$\alpha\backslash$ mesh size h	1/250	1/500	1/1000	1/1500	Rate (in h)
(a)	0.5	8.571e-2	4.999e-2	2.924e-2	2.139e-2	0.77
(a)	1.5	1.125e-1	6.596e-2	3.859e-2	2.818e-2	0.77
(b)	0.5	1.171e-2	6.845e-3	4.010e-3	2.937e-3	0.77
(b)	1.5	1.154e-2	6.811e-3	4.014e-3	2.943e-3	0.76

Table 4.3: The $L^2(\Omega)$ error at time $t = 0.1$ with $s = 0.25$ using $\tau = 1/5000$. The expected convergence rate in h is 0.5.

Mesh size h	$s = 0.25$	$s = 0.75$
0.1	1.790e-1	5.673e-2
0.05	1.102e-1	2.342e-2
0.03	7.077e-2	1.054e-2
0.02	5.206e-2	6.255e-3

Table 4.4: The $L^2(\Omega)$ error at time $t = 0.02$ with $s \in \{0.25, 0.75\}$ and $\alpha = 0.8$, using $\tau = 1/5000$ for example (c). The observed rates are 0.77 and 1.38, respectively.

4.3.4 Qualitative behaviour in $\mathbb{R}$

Explicit expressions for the fundamental solutions of the problem

$$\begin{cases} {}^C\partial_t^\alpha u &= (-\Delta)^s u \text{ in } \mathbb{R} \times (0, T], \\ u(0) &= v \text{ in } \mathbb{R}, \end{cases} \tag{4.3.1}$$

can be derived following the guidelines exposed by Mainardi, Luchko and Pagnini in [60]. In that work, the authors have studied fundamental solutions for the problem (4.3.7) with $0 < s \leq 1$ and $0 < \alpha \leq 2$ (including asymmetric kernels), and explicit expressions suitable for computational representations are provided.

Here, we are going to restrict ourselves to three special cases:

- Space-fractional Diffusion ($0 < s \leq 1$, $\alpha = 1$)
- Time-fractional Diffusion ($s = 1$, $0 < \alpha \leq 1$)
- Neutral fractional Diffusion ($0 < s = \alpha \leq 1$)

Indeed, defining $\nu = \frac{\alpha}{2s}$, the fundamental solution (or Green function) $G_{\alpha,\beta}(x, t)$ can be expressed as:

$$G_{s,\alpha}(x, t) = t^{-\nu} K_{s,\alpha}(x/t^\nu), \tag{4.3.2}$$

where $K_{s,\alpha}(x)$ is referred as the reduced Green function.

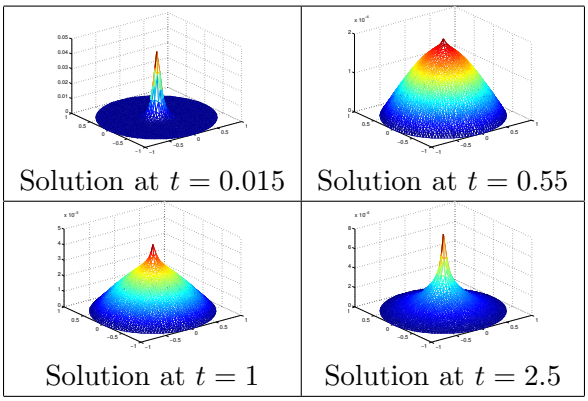

Figure 4.3: The effect of a fractional derivative in time: observe the persistence of the singularity along the time, even for $\alpha \sim 1$. In this example we set $\Omega = B(0,1)$, $\alpha = 0.99$, $s = 0.9$ and $v(0,0) = 1$ and $v(x) = 0$ for any other node of the mesh.

For the space-fractional diffusion case, the reduced Green function is a Lévy strictly stable distribution, that is

$$G_{s,1}(x,t) = t^{-1/2s} L_{2s,0}(x/t^{1/2s}), \tag{4.3.3}$$

where $L_{2s,0}(x)$ denote a symmetric Lévy $2s$-stable distribution.

For the second case, i.e. $s = 1$, $0 < \alpha \leq 1$, the fundamental solution can be expressed by means of the so-called M function $M_{\frac{\alpha}{2}}$ (of the Wright type),

$$G_{1,\alpha}(x,t) = \frac{1}{2} t^{-\alpha/2} M_{\frac{\alpha}{2}}(x/t^{\alpha/2}), \tag{4.3.4}$$

where,

$$M_\gamma(z) = \frac{1}{\pi} \sum_{n=1}^{\infty} \frac{(-z)^{n-1}}{(n-1)!} \Gamma(\gamma n) \sin(\pi \gamma n),$$

with $\gamma \in (0,1)$ and $\forall z \in \mathbb{C}$.

Finally, for the case $s = \alpha$ we have an explicit expression of the reduced Green function,

$$K_{s,2s}(x) = \frac{1}{\pi} \frac{|x|^{2s-1} \sin(s\pi)}{1 + 2|x|^{2s} \cos(s\pi) + |x|^{4s}}, \text{ with } x \neq 0, \tag{4.3.5}$$

and

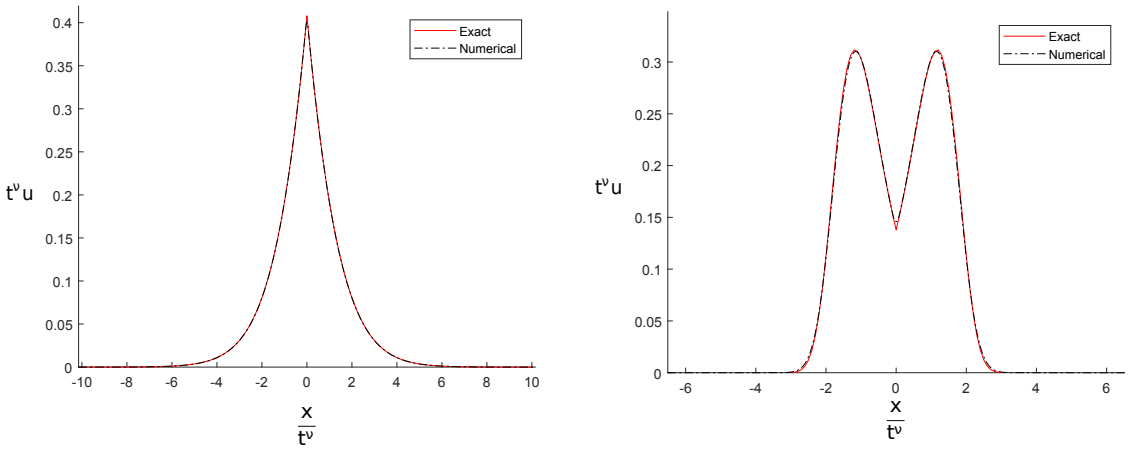

Figure 4.4: Time-fractional diffusion case: The numerical solution with initial data $12.5 I_{[-0.04,0.04]}$ at time $t = 0.3$ in black-dashed, and the exact solution for a Dirac-delta type initial datum is shown in red. Here, $s = 1$ in both case while $\alpha = 0.5$ in the left figure and $\alpha = 1.5$ in the right figure.

$$\lim_{x\to 0} K_{s,2s}(x) = \begin{cases} +\infty & 0 < s < \frac{1}{2}, \\ \frac{1}{\pi} & s = \frac{1}{2}, \\ 0 & \frac{1}{2} < s < 1. \end{cases} \tag{4.3.6}$$

Recalling that a Green function for the parabolic problem (4.3.7) can be understood as the solution with initial data $v = \delta(x)$, being δ a Dirac Delta function, the aim of the numerical experiment in this section is to compare the fundamental solution's behavior with its numerical counterpart, starting from a suitable domain and initial condition.

Indeed, we apply our numerical method to solve the problem

$$\begin{cases} {}^C\partial_t^\alpha u &= (-\Delta)^s u \text{ in } [-10,10]\times(0,0.3], \\ u(0) &= 12.5 \cdot I_{[-0.04,0.04]} \text{ in } [-10,10]. \end{cases} \tag{4.3.7}$$

The obtained numerical solutions are shown in figures (4.4)-(4.6). Here, we have used a 2000 nodes space discretization, and a time step $\delta t = 0.01$. Numerical solutions are shown in black-dashed, and the explicit solutions, computed from equations (4.3.3)-(4.3.5), are indicated in red. Solutions are displayed properly rescaled, following the relation (4.3.2).

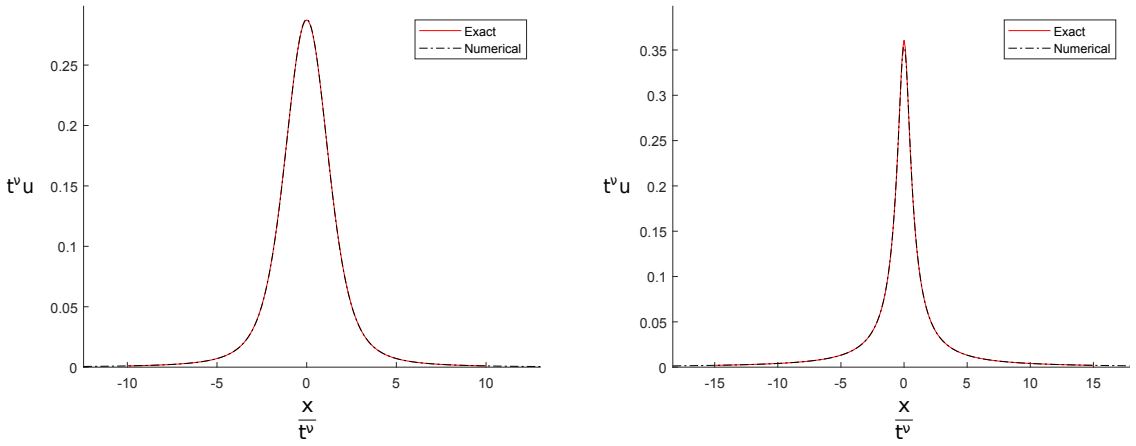

Figure 4.5: Space-fractional diffusion case: The numerical solution with initial data $12.5I_{[-0.04,0.04]}$ at time $t = 0.3$ is displayed in black-dashed, and the exact solution for a Dirac-delta type initial data is shown in red. Here, $\alpha = 1$ in both cases, $s = 0.75$ in the left one, and $s = 0.4$ in the other case.

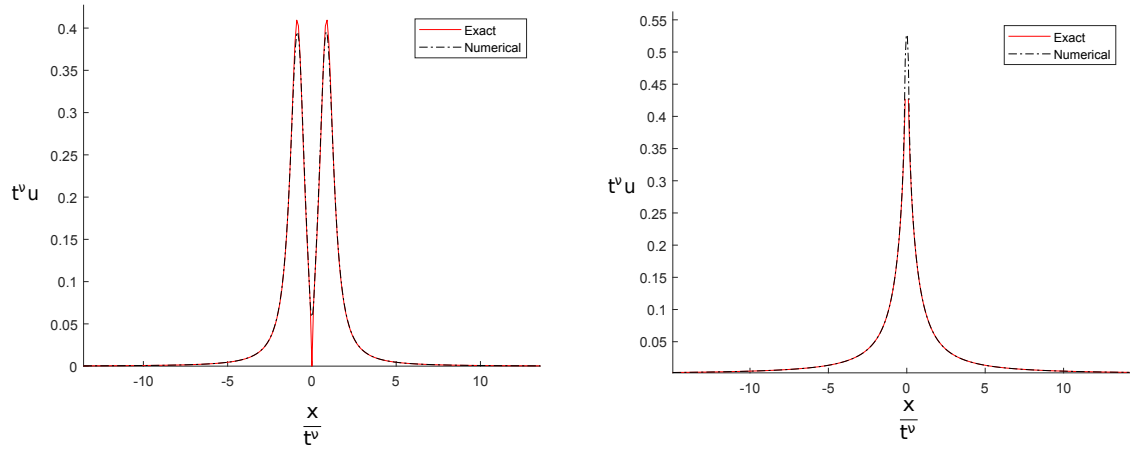

Figure 4.6: Neutral diffusion case: The numerical solution with initial data $12.5I_{[-0.04,0.04]}$ at time $t = 0.3$ is presented in black-dashed, and the exact solution for a Dirac-delta type initial data is indicated in red. Here we have used the parameters $s = 0.75$, $\alpha = 1.5$ in the first case, and $s = 0.4$, $\alpha = 0.8$ in the last one.

Resumen del Capítulo

En este capítulo se propone y analiza un método numérico para la resolución de la ecuación

$$ {}^{C}\partial_t^{\alpha} u + (-\Delta)^s u = f \text{ in } \Omega \times (0,T), $$

con $\alpha \in (0,2]$.

La Sección 4.1 está dedicada la descripción del método numérico utilizado, el cual hace uso de elementos finitos en la discretización espacial y cuadraturas de convolución en temporal. En la Sección 4.2 se obtienen estimaciones para el error de aproximación, mientras que en la Sección 4.3 se exponen experimentos numéricos verificando los órdenes de convergencia obtenidos en la sección anterior, así como también pruebas numéricas explorando el comportamiento cualitativo de las soluciones.

Chapter 5

Numerical approximation for the fractional Allen-Cahn Equation

In this chapter our study will be focused on the development of numerical techniques for the so-called fractional Allen-Cahn equation, that can be established as: find u such that

$$\begin{cases} {}^{C}\partial_t^{\alpha} u + \varepsilon^2(-\Delta)^s u &= f(u) \text{ in } \Omega \times (0,T], \\ u(0) &= v \text{ in } \Omega, \\ u &= 0 \text{ in } \Omega^c \times [0,T], \end{cases} \tag{5.0.1}$$

where Ω is a bounded domain in $\mathbb{R}^n$ with a sufficiently smooth boundary, $f(u) = u - u^3$, $v \in L^2(\Omega)$, $0 < \alpha \leq 1$ and ε^2 close to zero.

The classical Allen-Cahn equation was originally introduced to model the motion of phase boundaries in crystalline solids [13]. In this context, the unknown function u represent the density of the components, describing full concentration of one of them where $u = 1$ (or -1). Notably, the original formulation of the phase-field models [24] contemplates nonlocal interactions, which have been subsequently simplified and approximated by local models. Recently, theoretical aspects and numerical techniques have been developed for space and time non-local versions of this equation, most of them based on finite differences or spectral methods. Here, we can cite [55, 41, 78, 54, 42, 11]. Also, numerical techniques have been considered for non-local versions of related phase separation models, like the Cahn-Hilliard equation. In this way we can mention [9, 10].

In order to make use of the theory developed in Section 2.2, since f does not satisfy conditions (2.2.2) and (2.2.3), we are going to employ a truncated source term. That is, all the analysis will be made for the problem

$$\begin{cases} {}^C\partial_t^\alpha u + \varepsilon^2(-\Delta)^s u &= g(u) \text{ in } \Omega \times (0,T], \\ u(0) &= v \text{ in } \Omega, \\ u &= 0 \text{ in } \Omega^c \times [0,T], \end{cases} \tag{5.0.2}$$

where $g : \mathbb{R} \to \mathbb{R}$ and

- $g \in C^2(\mathbb{R})$,
- $g \equiv f$, in $[-1-\delta_0, 1+\delta_0]$, for some $\delta_0 > 0$,
- $|g|, |g'|, |g''| < B$ for some $B > 0$.

The goal is to prove that if u is a solution of (5.0.2) with $\|v\|_{L^\infty(\Omega)} \leq 1$, then $\|u\|_{L^\infty(\Omega)} \leq 1$ for all time, and then formulations (5.0.2) and (5.0.1) are equivalent. This is carried out through the analysis of the semi-discrete in time scheme in Section 5.2.3.

5.1 FEM discretization

5.1.1 Semi-discrete Scheme

In view of the weak formulation for the semilinear problem 2.2.1, and using the same finite element setting as in the linear case (Section 4.1), the semi-discrete problem may be set as: find $u_h \colon [0,T] \to X_h$ such that

$$\begin{cases} ({}^C\partial_t^\alpha u_h, w) + \varepsilon^2 \langle u_h, w \rangle_{H^s(\mathbb{R}^n)} &= (g(u_h), w), \quad \forall w \in X_h, \\ u_h(0) &= v_h. \end{cases} \tag{5.1.1}$$

We recall that $v_h = P_h v$, and P_h denotes the $L^2(\Omega)$ projection on X_h. Also, using the discrete operator A_h, we may rewrite (5.1.1) as

$$\begin{cases} {}^C\partial_t^\alpha u_h + \varepsilon^2 A_h u_h &= P_h g(u_h), \\ u_h(0) &= v_h. \end{cases} \tag{5.1.2}$$

5.1.2 Fully discrete scheme

Arguing as in the linear case, using identity (4.1.12) and replacing the Riemann-Liouville derivative by its discrete version given by (4.1.4), we can formulate the fully discrete problem as: find $U_h^n \in X_h$, with $n = \{1, \ldots, N\}$, such that

$$\begin{cases} \overline{\partial_\tau}^\alpha U_h^n + A_h U_h^n &= \overline{\partial_\tau}^\alpha v_h + P_h g(U_h^n) \\ U_h^0 &= v_h, \end{cases} \tag{5.1.3}$$

For the sake of the reader's convenience, we include a vectorized form of the fully discrete scheme. Let $\{\varphi_i\}_{i=1,\dots,\mathcal{N}}$ be the Lagrange nodal basis that generates X_h. Let $U^n \in \mathbb{R}^{\mathcal{N}}$, $n = 0, \dots, N$ be such that $U_h^n = \sum_{i=1}^{\mathcal{N}} U_i^n \varphi_i$, where U_h^n denotes the solution of the fully discrete problem. Then, we may formulate (5.1.3) in the following vectorized non-linear equation:

$$M^{-1} \cdot (\omega_0 M + K) \cdot U^n = \left(\sum_{j=0}^{n} \omega_j \right) U^0 - \sum_{j=1}^{n} \omega_j U^{n-j} + g(U^n).$$

Where M and K are the mass and stiffness matrices respectively. That is, $M_{i,j} = (\varphi_i, \varphi_j)$ and $K_{i,j} = \langle \varphi_i, \varphi_j \rangle_{H^s(\mathbb{R}^n)}$. Of course, the computation and assembly of the stiffness matrix in dimension greater than one can be carried out by means of the ideas exposed in Chapter 3.

Since (5.1.3) is not a linear equation, it is not clear a priori that there exists a solution. In that way, next result gives us existence and uniqueness for problem (5.1.3).

Theorem 5.1.1. *There exists τ small enough, such that problem* (5.1.3) *has a unique solution $U_h^n \in X_h$ for all $n \in \{1, ..., n\}$.*

Proof. Recalling that $\omega_0 = \tau^{-\alpha}$, dividing equation (5.1.3) by ω_0 at both sides, we obtain

$$(I + \tau^\alpha A_h) U_h^n = \left(\sum_{j=0}^{n} \tilde{\omega}_j \right) U_h^0 - \sum_{j=1}^{n} \tilde{\omega}_j U_h^{n-j} + \tau^\alpha P_h f(U_h^n).$$

Observe that, since $(A_h w, w) > 0$ for all $w \in X_h$, it is true that

$$\|(I + \tau^\alpha A_h)^{-1}\|_{L^2(\Omega)} \leq 1,$$

for all $\tau > 0$. Now, suppose by induction, that we have a solution $U_h^m \in X_h$ for all $m < n$, and define $T : X_h \to X_h$ as

$$T(w) = (I + \tau^\alpha A_h)^{-1} \Big(\left(\sum_{j=0}^{n} \tilde{\omega}_j \right) U_h^0 - \sum_{j=1}^{n} \tilde{\omega}_j U_h^{n-j} + \tau^\alpha P_h f(w) \Big).$$

Applying a fixed point argument, if T is a contraction over X_h, then problem (5.1.3) will have a unique solution. To this end, suppose that we have u and $w \in X_h$. Then, using $|g'| < B$ we have

$$\begin{aligned} \|T(u) - T(w)\|_{L^2(\Omega)} &= \|(I + \tau^\alpha A_h)^{-1} \Big(\tau^\alpha P_h (g(u) - g(w)) \Big) \|_{L^2(\Omega)} \\ &\leq \tau^\alpha \|g(u) - g(w)\|_{L^2(\Omega)} \leq B \tau^\alpha \|u - w\|_{L^2(\Omega)}. \end{aligned}$$

Taking $\tau < B^{-\alpha}$, we have that T is a contraction, and problem (5.1.3) has a unique solution.

□

5.2 Error estimation

The error estimation for the numerical scheme presented in the previous section can be obtained in a similar way to the linear case. For the sake of simplicity we are going to consider $\varepsilon^2 = 1$ throughout this section.

5.2.1 Error estimation for the semidiscrete scheme

First, we give an error estimation for the semi-discrete scheme.

Theorem 5.2.1. *Let u and u_h be the the exact and the semi-discrete solution of* (2.2.4) *and* (5.1.1) *respectively. And let $v \in L^2(\Omega)$ and $v_h = P_h v$ with $\|v\|_{L^2(\Omega)} \leq R$. Then there exists a positive constant $C = C(R,T)$ such that*

$$\|u(t) - u_h(t)\|_{L^2(\Omega)} \leq Ch^{2\gamma}(t^{-\alpha} + |\log h|^2)\ , t \in (0,T]. \tag{5.2.1}$$

With γ as in Theorem 4.2.6.

Proof. We can write the solution and its semi-discrete approximation as

$$u = E^\alpha(t)v + \int_0^t F^\alpha(t-s)g(u(s))\,ds,$$

and

$$u_h = E_h^\alpha(t)v_h + \int_0^t F_h^\alpha(t-s)g(u_h(s))\,ds,$$

respectively. Then, defining $e = u - u_h$, we have

$$e(t) = \big(E^\alpha - E_h^\alpha P_h\big)(t)v + \int_0^t F_h^\alpha(t-s)P_h\big(\,g(u(s)) - g(u_h(s))\,\big)\,ds$$

$$+ \int_0^t \big(F^\alpha - F_h^\alpha P_h\big)(t-s)g(u(s))\,ds.$$

Using Theorem 4.2.6 in the first term; $|g|, |g'| \leq B$, and (2.0.6) in the second term; Theorem 4.2.7 with $f = g(u)$ and $|g| < B$ in the last term, we have

$$\|e(t)\|_{L^2(\Omega)} \leq Ckt^{-\alpha}h^{2\gamma} + CB\int_0^t (t-s)^{\alpha-1}\|e(s)\|_{L^2(\Omega)}\,ds + Ch^{2\gamma}|\log h|^2$$

Then, applying Lemma 2.2.2 we derive (5.2.1).

□

5.2.2 Error estimation for the fully discrete scheme

Consider the discrete problem of find $V_h^n \in X_h$, $n \in \{1, ..., N\}$, $V_h^0 = 0$ such that

$$\sum_{j=0}^{n} \omega_j V_h^{n-j} = -A_h V_h^n + f_h^n, \tag{5.2.2}$$

with $f_h^n \in X_h$, for all $n \in \{1, ..., N\}$. Recalling that $\omega_0 = \tau^{-\alpha}$, and defining $E = (I + \tau^\alpha A_h)^{-1}$, we can rewrite (5.2.2) as

$$V_h^n = E\Big(\sum_{j=1}^{n} -\tau^\alpha \omega_j V_h^{n-j} + \tau^\alpha f_h^n\Big). \tag{5.2.3}$$

If we define $\{\tilde{\omega}_n\}_{n\in\mathbb{N}}$ as the coefficients of the series expansion of $(1-\xi)^\alpha$, from the definition of $\{\omega_n\}_{n\in\mathbb{N}}$ (4.1.15) we have $\tilde{\omega}_n = \tau^\alpha \omega_n$ for all $n \in \mathbb{N}$. And we can write V_h^n as a function of f_h^n in a recursive expression

$$V_h^n = \sum_{j=1}^{n} E_{n-j} f_h^j, \quad n > 0, \tag{5.2.4}$$

with E_n recursively defined as

$$E_0 = \tau^\alpha E, \quad E_n = E\Big(\sum_{j=0}^{n-1} -\tilde{\omega}_{n-j} E_j\Big). \tag{5.2.5}$$

As we have observed in the proof of Theorem 5.1.1, we have

$$\|E\|_{L^2(\Omega)} = \|(I + \tau^\alpha A_h)^{-1}\|_{L^2(\Omega)} < 1.$$

Then, from (5.2.5), and recalling that $-\tilde{\omega}_j > 0$ for $j \geq 1$, we have

$$\|E_0\|_{L^2(\Omega)} \leq \tau^\alpha, \quad \|E_n\|_{L^2(\Omega)} \leq \sum_{j=0}^{n-1} -\tilde{\omega}_{n-j} \|E_j\|_{L^2(\Omega)}. \tag{5.2.6}$$

Defining the sequence

$$c_0 = 1, \quad c_n = \sum_{j=0}^{n-1} -\tilde{\omega}_{n-j} c_j, \tag{5.2.7}$$

it is possible to check that

$$\|E_n\|_{L^2(\Omega)} \leq \tau^\alpha c_n. \tag{5.2.8}$$

In order to bound the error, it will be useful to know about the asymptotic behavior of $\{c_n\}_{n\in\mathbb{N}}$. This is analyzed in the next lemma.

Lemma 5.2.2. *Let $\{\tilde{\omega}_n\}_{n\in\mathbb{N}_0}$ be the coefficients of the power series expansion of $(1-\xi)^\alpha$, with $\alpha \in (0,1)$, and $\{c_n\}_{n\in\mathbb{N}_0}$ the sequence recursively defined in (5.2.7). Then, $c_n \in O(n^{\alpha-1})$.*

Proof. From the definition of $\{\tilde{\omega}_n\}_{n\in\mathbb{N}_0}$, we know that

$$(1-\xi)^\alpha = \sum_{j=0}^{\infty} \tilde{\omega}_j \xi^j.$$

Then, defining $g(\xi) = 1-(1-\xi)^\alpha$, and recalling that $w_0 = 1$, we have

$$g(\xi) = \sum_{j=1}^{\infty} -\tilde{\omega}_j \xi^j.$$

Now, defining $f(\xi) = \sum_{j=0}^{\infty} c_j \xi^j$, from the definition of $\{c_n\}_{n\in\mathbb{N}_0}$, and using the Cauchy product for power series, the following equality can be easily checked,

$$f(\xi)\frac{g(\xi)}{\xi} = \frac{f(\xi)-c_0}{\xi}. \tag{5.2.9}$$

Recalling that $c_0 = 1$, and $-\tilde{\omega}_1 = \alpha$, from (5.2.9) we can obtain an explicit expression for f,

$$f(\xi) = (1-\xi)^{-\alpha}. \tag{5.2.10}$$

It is well known that series expansion of f is

$$f(\xi) = \sum_{j=0}^{\infty} (-1)^j \binom{-\alpha}{j} \xi^j.$$

Then

$$c_n = (-1)^n \binom{-\alpha}{n}, \tag{5.2.11}$$

where

$$\binom{-\alpha}{n} = \frac{\Gamma(1-\alpha)}{\Gamma(1+n)\Gamma(1-n-\alpha)}. \tag{5.2.12}$$

Finally, by means of basic Gamma function properties, we can check that $\binom{-\alpha}{n} \in O(n^{\alpha-1})$, and hence $\{c_n\}_{n\in\mathbb{N}_0} \in O(n^{\alpha-1})$.

□

At this point, we are able to obtain a bound for the error.

Theorem 5.2.3. *Let u and $U_h^n = U_h(t_n)$ be the solution of (5.0.2) and (5.1.3) respectively. Consider $v \in L^2(\Omega)$ and $v_h = P_h v$ with $\|v\|_{L^2(\Omega)} \leq R$. Then, under the condition $0 < \tau^\alpha < \delta < 1$, there exists a positive constant $C = C(R, T, \alpha, \delta)$ such that*

$$\|u(t_n) - U_h(t_n)\|_{L^2(\Omega)} \leq Ch^{2\gamma}(t_n^{-\alpha} + |\log h|^2) + C\tau t_n^{-1}, \qquad t_n \in [0, T]. \tag{5.2.13}$$

Proof. In view of Theorem 5.2.1, we only need to estimate $\|u_h(t_n) - U_h(t_n)\|_{L^2(\Omega)}$, with u_h the semi-discrete solution. Defining the function $G(z) = (z^\alpha I + A_h)^{-1}$, analytic in a sector Σ_θ with $\theta \in (\pi/2, \pi)$ (see Section 4.1.2), from the semi-discrete and fully discrete scheme we have

$$u_h = G(\partial_t)\partial_t^\alpha v_h + G(\partial_t)P_h g(u_h),$$

and

$$U_h = G(\overline{\partial_\tau})\overline{\partial_\tau}^{\,\alpha} v_h + G(\overline{\partial_\tau})P_h g(U_h).$$

Subtracting both expressions we obtain an equation for $e_h := u_h - U_h$,

$$\begin{aligned} e_h &= (G(\partial_t)\partial_t^\alpha - G(\overline{\partial_\tau})\overline{\partial_\tau}^{\,\alpha} P_h)v + G(\partial_t)P_h g(u_h) - G(\overline{\partial_\tau})P_h g(U_h) = \\ &(G(\partial_t)\partial_t^\alpha - G(\overline{\partial_\tau})\overline{\partial_\tau}^{\,\alpha} P_h)v_h + (G(\partial_t) - G(\overline{\partial_\tau}))P_h g(u_h) + G(\overline{\partial_\tau})P_h(g(u_h) - g(U_h)) \\ &= (i) + (ii) + (iii). \end{aligned} \tag{5.2.14}$$

The norm of the first term (i) can be approximated by means of Lemma 4.1.1. That is, taking $\mu = 0, \beta = 1$ in that lemma, we obtain

$$\|(i)\|_{L^2(\Omega)} \leq Ct_n^{-1}\tau\|v_h\|_{L^2(\Omega)} \leq Ct_n^{-1}\tau,$$

with $C = C(R)$.

For the second term, using property (4.1.10), we can split (ii) as follow

$$\begin{aligned} (ii) &= \big(G(\partial_t) - G(\overline{\partial_\tau})\big)\big(\, P_h g(u_h(0)) + (1 * P_h \partial_t g(u_h(t_n))\,\big) \\ &= \big(G(\partial_t) - G(\overline{\partial_\tau})\big)P_h g(u_h(0)) + (\big(G(\partial_t) - G(\overline{\partial_\tau})\big)1) * P_h \partial_t g(u_h(t_n)) \\ &= I + II. \end{aligned}$$

Using Lemma 4.1.1 with $\mu = \alpha, \beta = 1$, along with the fact that $|g| < B$, we can estimate

$$\|I\|_{L^2(\Omega)} \leq Ct_n^{\alpha-1}\tau.$$

On the other hand, noticing that estimation (2.2.16) can be easily extended to $\partial_t u_h$ in order to get $\|\partial_t u_h\|_{L^2(\Omega)} \leq C t^{\alpha/2-1}$ (since $v_h \in \widetilde{H}^s(\Omega)$); using again Lemma 4.1.1, the fact that $|g'| < B$, and writing $\partial_t g(u_h(t)) = g'(u_h(t))\partial_t u_h$, we have

$$\|II\|_{L^2(\Omega)} \leq \int_0^{t_n} \|\big(\big(G(\partial_t) - G(\overline{\partial_\tau})\big)1\big)(t_n - s)g'(u_h(s))\partial_t u_h(s)\|_{L^2(\Omega)}\, ds$$

$$\leq C\tau \int_0^{t_n} (t_n - s)^{\alpha-1} \|\partial_t u_h(s)\|_{L^2(\Omega)}\, ds \leq C\tau \int_0^{t_n} (t_n - s)^{\alpha-1} s^{\alpha/2-1}\, ds$$

$$\leq C\tau t_n^{\frac{3}{2}\alpha-1},$$

where in the last inequality we have estimated the integral in terms of the beta function $B(\alpha/2, \alpha)$, as in Theorem 2.2.1.

Now, we observe that the last term (iii) is a solution for (5.2.2), with $f_h^n = P_h(g(u_h) - g(U_h))$. Then, in view of (5.2.4) and (5.2.8), and using again that $|g'| < B$, we have

$$\|(iii)\|_{L^2(\Omega)} \leq \tau^\alpha \sum_{j=1}^{n} c_{n-j} \|e_h(t_j)\|_{L^2(\Omega)},$$

where $\{c_n\}_{n\in\mathbb{N}}$ is the sequence defined in (5.2.7).

Using that

$$C\tau(t_n^{-1} + t_n^{\frac{3}{2}\alpha-1} + t_n^{\alpha-1}) \leq C\tau t_n^{-1},$$

with $C = C(T)$, we can derive the following

$$\|e_h(t_n)\|_{L^2(\Omega)} \leq C\tau t_n^{-1} + \tau^\alpha \sum_{j=1}^{n} c_{n-j} \|e_h(t_j)\|_{L^2(\Omega)}.$$

Now, recalling that $0 < \tau^\alpha < \delta < 1$, we have

$$\|e_h(t_n)\|_{L^2(\Omega)} \leq C\tau t_n^{-1} + C\tau^\alpha \sum_{j=1}^{n-1} c_{n-j} \|e_h(t_j)\|_{L^2(\Omega)},$$

with $C = C(\delta)$. We can apply a discrete Gronwall type inequality to the former expression, and get

$$\|e_h(t_n)\|_{L^2(\Omega)} \leq C\tau t_n^{-1} e^{(C\tau^\alpha \sum_{j=1}^{n-1} c_{n-j})}. \tag{5.2.15}$$

Now, from Lemma 5.2.2, we know that $c_n \sim n^{\alpha-1}$, and hence $\tau^\alpha \sum_{j=1}^{n} c_{n-j} \lesssim \tau^\alpha n^\alpha \leq \tau^\alpha N^\alpha = T^\alpha$. From this, (5.2.15), and (5.2.1), we can derive (5.2.13).

□

5.2.3 L^∞ bounds

In order to prove that the solution remains bounded between 1 and -1, we are going to define first the semi-discrete in time problem. That is, find $U^n \in \widetilde{H}^s(\Omega)$, with $n \in \{1, ..., N\}$, such that

$$\begin{cases} \overline{\partial_\tau}^\alpha U^n + AU^n &= \overline{\partial_\tau}^\alpha v + g(U^n) \\ U^0 &= v. \end{cases} \tag{5.2.16}$$

Before giving an existence result, we set the following auxiliary lemma.

Lemma 5.2.4. *Let $\{a_j\}_{j\in\mathbb{N}}$ and $\{b_j\}_{j\in\mathbb{N}}$ be two sequences of real numbers, with $\{a_j\}_{j\in\mathbb{N}}$ non-increasing and positive valued. Suppose*

$$\sum_{j=0}^{n-1} a_j(b_{n-j} - b_{n-j-1}) < 0,$$

for some $n \geq 2$. Then there exists $j_0 < n$ such that $b_{j_0} > b_n$.

Proof. Suppose $b_j \leq b_n$ for all $j < n$. Since $a_{j-1} \geq a_j > 0$ we have

$$0 > \sum_{j=0}^{n-1} a_j(b_{n-j} - b_{n-j-1}) \geq a_1(b_n - b_{n-2}) + \sum_{j=2}^{n-1} a_j(b_{n-j} - b_{n-j-1})$$

$$\geq a_2(b_n - b_{n-3}) + \sum_{j=3}^{n-1} a_j(b_{n-j} - b_{n-j-1}) \geq ... \geq a_{n-1}(b_n - b_0) \geq 0,$$

and the contradiction came from the assumption $b_j \leq b_n$ for all $j < n$. Then there exists $j_0 < n$ such that $b_{j_0} > b_n$ and the lemma is proved.

□

The proof of the existence and uniqueness of solutions for problem (5.2.16) is similar to the one given for the fully discrete case. For the solutions of this problem, we have the following result.

Theorem 5.2.5. *Consider the semi-discrete in time scheme* (5.2.16) *with $U^0 \in L^\infty(\Omega)$, then there exists $\tau > 0$ small enough such that* (5.2.16) *has a unique solution U^n, $n \in \{0, ..., N\}$, with $U^n \in C^s(\mathbb{R}^n)$ for all $n > 0$. Moreover if $|U^0(x)| \leq 1$ for all $x \in \Omega$, then $|U^n(x)| \leq 1$ for all $x \in \Omega$ and $n \in \{1, ...N\}$.*

Proof. Suppose we have a solution with the desired properties for all $m < n$. From (5.2.16) we have the identity

$$U^n = (I + \tau^\alpha A)^{-1}\Big(\left(\sum_{j=0}^{n} \tilde{\omega}_j\right) U^0 - \sum_{j=1}^{n} \tilde{\omega}_j U^{n-j} + \tau^\alpha g(U^n)\Big), \tag{5.2.17}$$

where $\tilde{\omega}_j := \tau^\alpha \omega_j$.

First we want to show that there exists $U^n \in L^2(\Omega)$ that satisfies equation 5.2.17. In order to do that, we define the map $T : L^2(\Omega) \to L^2(\Omega)$

$$T(u) := (I + \tau^\alpha A)^{-1}\Big(\left(\sum_{j=0}^{n} \omega_j\right) U^0 - \sum_{j=1}^{n} \omega_j U^{n-j} + \tau^\alpha g(u)\Big).$$

We want to show that T is a contraction in $L^2(\Omega)$. From the fact that A is a maximal monotone operator (see [22]), we know that $\|(I + \tau^\alpha A)\|_{L^2(\Omega)} \leq 1$. Let u and $v \in L^2(\Omega)$, we can estimate

$$\|T(u) - T(v)\|_{L^2(\Omega)} = \|(I + \tau^\alpha A)^{-1}\tau^\alpha \big(g(u) - g(v)\big)\|_{L^2(\Omega)}$$

$$\leq \tau^\alpha \|g(u) - g(v)\|_{L^2(\Omega)} \leq \tau^\alpha C \|u - v\|_{L^2(\Omega)}.$$

Then, for a small τ we have that T is a contraction. Hence, there exists a unique solution $U^n \in L^2(\Omega)$ for (5.2.17), and the relation

$$AU^n = \left(\sum_{j=0}^{n} \omega_j\right) U^0 - \sum_{j=1}^{n} \omega_j U^{n-j} + g(U^n) \tag{5.2.18}$$

is satisfied. Since the right hand side belongs to $L^\infty(\Omega)$, applying Theorem 1.2.4, we can conclude that $U^n \in C^s(\mathbb{R}^n) \cap C^{2s}(\Omega_\rho)$ for all $0 < \rho < \rho_0$.

Now, we want to see that if the initial data is regular enough, then the solution remains bounded between 1 and -1. Suppose $|U^m(x)| \leq 1$ for all $x \in \Omega$, for all $m < n$. The semi-discrete in time scheme gives us the relation

$$\sum_{j=0}^{n} \omega_j U^{n-j} - \left(\sum_{j=0}^{n} \omega_j\right) U^0 = -AU^n + g(U^n),$$

which can be rewritten as

$$\sum_{j=0}^{n-1} a_j (U^{n-j} - U^{n-j-1}) = -AU^n + g(U^n),$$

with $a_n = \sum_{j=0}^{n} \omega_j$. Suppose there exists some x_0 such that U^n achieves its maximum on that point, and $U^n(x_0) > 1$. Recall that $\|U^m\|_{L^\infty(\Omega)} \leq 1$ for all $m < n$. Assuming

$U^m \in C^2(\Omega) \cap C^s(\mathbb{R}^n)$ for all $m < n$ it is possible to show that $U^n \in C^2(\Omega) \cap C^s(\mathbb{R}^n)$ (see Remark 5.2.6). Using this, we can show that $AU^n(x_0) = (-\Delta)^s U^n(x_0) \geq 0$ (see [33, Lemma 3.9]). Then, from the fact that $U^n(x_0) > 1$, we have $g(U^n(x_0)) < 0$, which implies

$$\sum_{j=0}^{n-1} a_j (U^{n-j}(x_0) - U^{n-j-1}(x_0)) < 0.$$

Observing the fact that $\{a_n\}$ is a positive valued and decreasing sequence, we can apply Lemma 5.2.4 to show that there exists $m_0 < n$, such that $U^{m_0}(x_0) > U^n(x_0)$, and then $1 \geq U^{m_0}(x_0) > U^n(x_0) > 1$. The contradiction came from the assumption that $U^n(x_0) > 1$.

Now we want to see that the same bound holds for less regular initial data. To this end, applying a density argument, suppose U^n is a solution for (5.2.16) with $U^0 \in L^\infty(\Omega)$, $\|U^0\|_{L^\infty(\Omega)} \leq 1$. Consider $\{U_k^0\}_{k\in\mathbb{N}} \subset C_c^\infty(\Omega)$, with $\|U_k^0\|_{L^\infty(\Omega)} \leq 1$ for all k, and $U_k^0 \to U^0$ in $L^2(\Omega)$.

Let U_k^n be the solution of (5.2.16) with initial data U_k^0. Calling $e_k^n = U^n - U_k^n$, we have the equation

$$e_k^n = (I + \tau^\alpha A)^{-1}\Big(\left(\sum_{j=0}^{n} \tilde{\omega}_j \right) e_k^0 - \sum_{j=1}^{n} \tilde{\omega}_j e_k^{n-j} + \tau^\alpha \big(g(U^n) - g(U_k^n) \big) \Big),$$

and taking norms we obtain

$$\|e_k^n\|_{L^2(\Omega)} \leq \|e_k^0\|_{L^2(\Omega)} + \sum_{j=1}^{n} -\tilde{\omega}_j \|e_k^{n-j}\|_{L^2(\Omega)} + \tau^\alpha C \|e_k^n\|_{L^2(\Omega)}. \tag{5.2.19}$$

Choosing τ such that $\tau^\alpha C < 1$, recalling that $0 < \sum_{j=1}^{n} -\tilde{\omega}_j < 1$, and applying a Gronwall type inequality we have

$$\|e_k^n\|_{L^2(\Omega)} \leq \|e_k^0\|_{L^2(\Omega)} \frac{e^{1/1-\tau^\alpha C}}{1 - \tau^\alpha C} = C \|e_k^0\|_{L^2(\Omega)},$$

with $C = C(\tau, \alpha, C)$, and then, $\|e_k^n\|_{L^2(\Omega)} \to 0$.

Since $\|U_k^0\|_{L^\infty(\Omega)} \leq 1$, then $\|U_k^n\|_{L^\infty(\Omega)} \leq 1$ for all k, and for all $n \in \{1, ..., N\}$. Hence, for a fixed n, we can construct a sub-sequence $\{U_{k_j}^n\}_{j\in\mathbb{N}}$, such that $U_{k_j}^n \to U^n$ a.e. , and conclude that $\|U^n\|_{L^\infty(\Omega)} \leq 1$.

□

Remark 5.2.6. Suppose we have $U^m \in C^2(\Omega) \cap C^s(\mathbb{R}^n)$ for all $m < n$. If we take a fixed $\rho' > 0$ and $\rho = 2\rho'$ in Theorem 1.2.5, a repeated application of this result, along with the fact that $g \in C^2(\mathbb{R})$, implies that $U^n \in C^{2+2s}(\Omega_{k\rho_0})$ for some $k \in \mathbb{N}$, only

depending on s. Since ρ_0 can be arbitrary small, we can assert that $U^n \in C^2(\Omega)$, and then, $U^n \in C^2(\Omega) \cap C^s(\mathbb{R}^n)$.

Finally, proceeding analogously as in Theorem 5.2.3, we can derive the following error estimation.

Theorem 5.2.7. *Let u and $U^n = U(t_n)$ be the solution of (5.0.2) and (5.2.16) respectively, with $v \in L^2(\Omega)$, $\|v\|_{L^2(\Omega)} \leq R$. Then, under the condition $0 < \tau^\alpha < \delta < 1$, there exists a positive constant $C = C(R, T, \alpha, \delta)$ such that*

$$\|u(t_n) - U(t_n)\|_{L^2(\Omega)} \leq C t_n^{-1} \tau, \quad t_n \in [0, T]. \tag{5.2.20}$$

Now, consider $\|v\|_{L^\infty(\Omega)} \leq 1$, a family of nested subdivisions of [0,T] with $\tau = T/N_k$ with $k \in \mathbb{N}$, and a fixed $t_n \in (0, T]$. Let $U_k(t_n)$ be the solution of (5.2.16), and u the solution of (2.2.4), using 5.2.7 we have that $U_k(t_n) \to u(t_n)$ in $L^2(\Omega)$. So, we can extract a sub-sequence $\{U_{k_j}(t_n)\}_{j \in \mathbb{N}}$ such that $U_k(t_n) \to u(t_n)$ a.e. . Using 5.2.5, we know that $\|U_k(t_n)\|_{L^\infty(\Omega)} \leq 1$, and then, $\|u(t_n)\|_{L^\infty(\Omega)} \leq 1$. We can summarize this observation in the following result.

Theorem 5.2.8. *Let u a solution of (2.2.5) with $\|v\|_{L^\infty(\Omega)} \leq 1$. Then $\|u(t)\|_{L^\infty(\Omega)} \leq 1$ for all $t \in (0, T]$.*

This theorem implies that all the analysis displayed up to here remains valid replacing g by f and therefore to the Allen-Cahn equation (2.2.1).

5.3 Asymptotic behavior with $s \to 0$

Considering now the usual derivative in time ($\alpha = 1$), the Allen-Cahn equation can be understood as a gradient flow in L^2, minimizing the free energy functional

$$F_s(u) = \frac{\varepsilon^2}{2} |u|^2_{H^s(\mathbb{R}^n)} + \int_\Omega W(u), \tag{5.3.1}$$

with $W(u) = \frac{(u^2-1)^2}{4}$ (see for example [9]). It is well known that the size of ε affects the interface width of the minimizers of F_s. That is, interface width tends to zero with $\varepsilon \to 0$. This fact can be easily derived from expression (5.3.1), observing that the right term, which penalizes the variation of u, tends to lose relevance as ε goes to zero, forcing the minimizer u to take values into the set of minimizers of W, that is values belonging to $\{1, -1\}$. However, since $\varepsilon > 0$, the right term promote the minimization of the interface length (for $n \geq 2$), which implies that the limit behavior cannot be understood as the minimization of F_s with $\varepsilon = 0$. In [76], Savin and Valdinoci show, by means of Γ-convergence theory, that the limit behavior of the problem of minimizing

F_s tends to a minimal surface problem if $s \in [1/2, 1)$, and to a non-local version of the minimal surface problem for $s \in (0, 1/2)$.

In our case, numerical experiments (see Figure 5.2) show that the interface width tends to become thinner when the parameter s goes to zero, suggesting that (as in the case $\varepsilon \to 0$) a minimizer of F_s should approximate a binary function when $s \to 0$. Motivated by the previous observation, the aim of this section is to analyze the asymptotic behavior of the minimizers of F_s with s tending to zero. To this end, we are going to follow the ideas displayed in [76], and study the Γ-convergence of a suitable modification of the functional F_s.

5.3.1 Γ-convergence when $s \to 0$.

Since Γ-convergence may not be a usual concept in numerical analysis, we start this section by giving its definition and basic properties, and we refer to [21] for further details.

Let X be a topological space, and $\{F_n\}_{\in \mathbb{N}}$, $F_n : X \to [-\infty, +\infty]$, a sequence of functionals. Then, we say that F_n Γ-converge to $F : X \to [-\infty, +\infty]$, if the following conditions holds:

- For every sequence $\{x_n\}_{n\in\mathbb{N}} \subset X$ such that $x_n \to x$, then
$$F(x) \leq \liminf_{n\to\infty} F_n(x_n).$$
- For every $x \in X$, there exists a sequence x_n converging to x such that
$$F(x) \geq \limsup_{n\to\infty} F_n(x_n).$$

Also, we define a complementary concept. We say that the family $\{F_n\}$ has the equi-coerciveness property if for all $c \in \mathbb{R}$ exists a compact set K_c in such a way that $\{F_n < c\} \subset K_c$ for all $n \in \mathbb{N}$.

These two concept allow us to say something about the limiting behavior of the minimizers of F_n in terms of the minimizers of F. That is, if x_n is a minimizer of F_n, then every cluster point of $\{x_n\}_{n\in\mathbb{N}}$ (if exists) is a minimizer of F. This can be summarized as follow

$$\text{Equi-coerciveness} + \Gamma\text{-convergence} \Rightarrow \text{Convergence of minimizers}$$

In order to study the Γ-convergence of F_s, we must set an appropriate domain X for F_s,

$$X = \{u \in L^\infty(\mathbb{R}^n) \text{ with } |u| \leq 1, \text{ and } u \equiv 0 \text{ in } \Omega^c\}.$$

And we are going to consider this space furnished with the norm $\|\cdot\|_{L^1(\Omega)}$. Note that if $u \in X$ but $u \notin \tilde{H}^s(\Omega)$, then we can define $F_s(u) = +\infty$.

From the definition of F_s, and supposing $\varepsilon^2 < 1$, we have

$$F_s(u) = \frac{\varepsilon^2}{2}|u|^2_{H^s(\mathbb{R}^n)} - \frac{\varepsilon^2}{2}\|u\|^2_{L^2(\Omega)} + \frac{\varepsilon^2}{2}\|u\|^2_{L^2(\Omega)} + \int_\Omega W(u)$$

$$= \frac{\varepsilon^2}{2}\big(|u|^2_{H^s(\mathbb{R}^n)} - \|u\|^2_{L^2(\Omega)}\big) + \int_\Omega \big(W(u) + \frac{\varepsilon^2}{2}u^2\big),$$

and, denoting $\mathcal{F}[u](\xi)$ as the Fourier transform of u, we know from [30] and Plancharel's identity that

$$|u|^2_{H^s(\mathbb{R}^n)} = \|\mathcal{F}[u]|\xi|^s\|^2_{L^2(\mathbb{R}^n)} = \int_{\mathbb{R}^n} \mathcal{F}^2[u](\xi)|\xi|^{2s}\, d\xi,$$

and

$$\|u\|^2_{L^2(\Omega)} = \int_{\mathbb{R}^n} \mathcal{F}^2[u](\xi)\, d\xi.$$

Then we have

$$|u|^2_{H^s(\mathbb{R}^n)} - \|u\|^2_{L^2(\Omega)} = \int_{\mathbb{R}^n} \big(|\xi|^{2s} - 1\big)\mathcal{F}^2[u](\xi)\, d\xi,$$

so we can rewrite F_s as

$$F_s = \frac{\varepsilon^2}{2}\int_{\mathbb{R}^n} \big(|\xi|^{2s} - 1\big)\mathcal{F}^2[u](\xi)\, d\xi + \int_\Omega \tilde{W}(u),$$

with $\tilde{W}(s) = W(s) + \frac{\varepsilon^2}{2}s$.

Since we have $\varepsilon^2 < 1$, $\tilde{W}(s)$ is a double-well type potential with minimizers $\pm\sqrt{1-\varepsilon^2}$.

Noticing that $\tilde{W}(\pm\sqrt{1-\varepsilon^2}) = k_\varepsilon > 0$, we define a new auxiliary functional $\tilde{F}_s$

$$\tilde{F}_s = \frac{1}{2s}\big(F_s - \int_\Omega k_\varepsilon\big),$$

and, for sake of simplicity, we redefine $\tilde{W}$ as

$$\tilde{W}(s) = W(s) + \frac{\varepsilon^2}{2}s - k_\varepsilon,$$

so now $\tilde{W}(\pm\sqrt{1-\varepsilon^2}) = 0$.

Fixing s and ε, it is easy to check that $u \in X$ is a minimizer of F_s if and only if u is a minimizer of $\tilde{F}_s$. So we focus our study on the asymptotic behavior of $\tilde{F}_s$.

Defining the functional

$$F_0(u) = \begin{cases} \int_{\mathbb{R}^n} \ln|\xi| \mathcal{F}^2[u](\xi)\, d\xi, & \text{if } u \equiv \sqrt{1-\varepsilon^2}\big(I_E - I_{E^c}\big) \\ +\infty, & \text{in other case,} \end{cases} \tag{5.3.2}$$

with $E \subset \Omega$ and $E^c = \Omega \setminus E$, we have the following theorem.

Theorem 5.3.1. *Let $\tilde{F}_s$ and F_0 defined as before, then $\tilde{F}_s \xrightarrow{\Gamma} F_0$.*

Proof. Let $u_s \to u$ with $s \to 0$ in X, and suppose w.l.o.g, that s takes values in a discrete set. First, we want to see

$$\liminf_{s\to 0} \tilde{F}_s(u_s) \geq F_0(u). \tag{5.3.3}$$

Indeed, suppose that $l = \liminf_{s\to 0} \tilde{F}_s(u_s) \leq +\infty$, in other case there is nothing to prove. If we choose a suitable sub-sequence of u_s such that $u_s \to u$ a.e. and $\tilde{F}_s(u_s) \to l$, then

$$l = \liminf_{s\to 0} \tilde{F}_s(u_s) \geq \liminf_{s\to 0} \int_{\mathbb{R}^n} \frac{|\xi|^{2s}-1}{2s} \mathcal{F}^2[u_s](\xi)\, d\xi + \liminf_{s\to 0} \frac{1}{2s} \int_\Omega \tilde{W}(u_s) \tag{5.3.4}$$

We first analyze the left term of the right hand side of (5.3.4). In this case we have

$$\liminf_{s\to 0} \int_{\mathbb{R}^n} \frac{|\xi|^{2s}-1}{2s} \mathcal{F}^2[u_s](\xi)\, d\xi \geq \liminf_{s\to 0} \int_{|\xi|>1} \frac{|\xi|^{2s}-1}{2s} \mathcal{F}^2[u_s](\xi)\, d\xi$$
$$+ \liminf_{s\to 0} \int_{|\xi|\leq 1} \frac{|\xi|^{2s}-1}{2s} \mathcal{F}^2[u_s](\xi)\, d\xi = (i) + (ii).$$

From the fact that $u_s \to u$ in $L^1(\mathbb{R}^n)$ norm, we have $\mathcal{F}[u_s] \to \mathcal{F}[u]$ point-wise, and we also have $(|\xi|^{2s}-1)/2s \to \ln|\xi|$. Then, using Fatou's Lemma, we get

$$(i) \geq \int_{|\xi|>1} \ln|\xi| \mathcal{F}^2[u](\xi)\, d\xi > 0$$

On the other hand, since $|\mathcal{F}[u_s](\xi)| \leq \|u_s\|_{L^1(\Omega)} \leq |\Omega|$, we can estimate the second term as follow

$$(ii) = -\limsup \int_{|\xi|\leq 1} \frac{1-|\xi|^{2s}}{2s} \mathcal{F}^2[u_s](\xi)\, d\xi \geq -\int_{|\xi|\leq 1} -\ln|\xi| \mathcal{F}^2[u](\xi)\, d\xi$$
$$= \int_{|\xi|\leq 1} \ln|\xi| \mathcal{F}^2[u](\xi)\, d\xi > -\infty, \tag{5.3.5}$$

where in the last inequality we have use the reverse Fatous's Lemma.

Hence, the first term on the right hand side of (5.3.4) must be a finite number. This implies that

$$0 \leq \liminf_{s\to 0} \frac{1}{2s} \int_\Omega \tilde{W}(u_s) < +\infty,$$

and thus, $\int_\Omega \tilde{W}(u_s) \to 0$ with $s \to 0$.

Since we have chosen u_s in such a way that $u_s \to u$ a.e., we have that $\tilde{W}(u) = 0$ a.e., then u must have the form

$$u = \sqrt{1-\varepsilon^2}(I_E - I_{E^c}).$$

Now, we can estimate

$$\liminf_{s\to 0} \tilde{F}_s(u_s) = \liminf_{s\to 0} \int_{\mathbb{R}^n} \frac{|\xi|^{2s}-1}{2s} \mathcal{F}^2[u_s](\xi)\, d\xi + \frac{1}{2s}\int_\Omega \tilde{W}(u_s)$$

$$\geq \int_{\mathbb{R}^n} \ln|\xi| \mathcal{F}^2[u](\xi)\, d\xi = F_0(u),$$

and (5.3.3) follow.

Finally we only need the to verify that if $u \in X$, then

$$F_0(u) \geq \limsup_{s\to 0} F_s(u) \tag{5.3.6}$$

To this end, suppose $u = \sqrt{1-\varepsilon^2}(I_E - I_{E^c})$, otherwise there is nothing to prove. In this case we have

$$F_s(u) = \int_{\mathbb{R}^n} \frac{|\xi|^{2s}-1}{2s} \mathcal{F}^2[u](\xi)\, d\xi.$$

The fact that $(|\xi|^{2s}-1)/2s \searrow \ln|\xi|$ with $s \to 0$, implies that $\tilde{F}_s(u)$ is decreasing in s. Then

$$\limsup_{s\to 0} \tilde{F}_s(u) = \lim_{s\to 0} \tilde{F}_s(u) = \lim_{s\to 0} \int_{\mathbb{R}^n} \frac{|\xi|^{2s}-1}{2s} \mathcal{F}^2[u](\xi)\, d\xi$$

$$= \lim_{s\to 0} \Big(\int_{|\xi|\leq 1} + \int_{|\xi|>1} \Big) \frac{|\xi|^{2s}-1}{2s} \mathcal{F}^2[u](\xi)\, d\xi.$$

Then, using Monotone Convergence Theorem on the integral over $|\xi| > 1$, and Dominated Convergence Theorem over $|\xi| \leq 1$, we have

$$\limsup_{s\to 0} \tilde{F}_s(u) = F_0(u),$$

which proves (5.3.6).

□

5.3.2 Equi-coerciveness of $\tilde{F}_s$

To complete the analysis we prove the equi-coerciveness of $\{\tilde{F}_s\}_s$.

Theorem 5.3.2. *Suppose $s_n \to 0$, and $\{u_n\}_{n\in\mathbb{N}} \subset X$, such that $\tilde{F}_{s_n}(u_n) \leq C$ for all $n \in \mathbb{N}$. Then there exists $u \in X$ and a subsequence $\{u_{n_j}\}_{j\in\mathbb{N}}$, such that $u_{n_j} \to u$ in X.*

Proof. First we observe that, as before, we have

$$\tilde{F}_{s_n}(u_n) = \int_{\mathbb{R}^n} \frac{|\xi|^{s_n} - 1}{2s_n} \mathcal{F}^2(u_n)[\xi]\, d\xi + \frac{1}{2s_n} \int_\Omega \tilde{W}(u_n)\, dx.$$

Since $(|\xi|^{2s} - 1)/2s \searrow \ln|\xi|$ and $\tilde{F}_{s_n}(u_n) \leq C$ for all $n \in \mathbb{N}$, we can assert that

$$\int_{\mathbb{R}^n} \ln|\xi| \mathcal{F}^2(u_n)[\xi]\, d\xi \leq C, \quad \forall n \in \mathbb{N}. \tag{5.3.7}$$

The fact that $u_n \in X$, implies $\|u_n\|_{L^1(\Omega)} \leq C_0$ for all $n \in \mathbb{N}$, and then

$$\int_{|\xi|\leq 1} \ln|\xi| \mathcal{F}^2(u_n)[\xi]\, d\xi \geq C_0^2 \int_{|\xi|\leq 1} \ln|\xi|\, d\xi \geq C_1. \tag{5.3.8}$$

Now we want to show that (5.3.7) implies that functions in the set $\{\mathcal{F}^2(u_n)\}_n$ keep a substantial part of their mass uniformly bounded. Namely, given $\eta > 0$, there exists $R > 0$ such that

$$\int_{|\xi|>R} \mathcal{F}^2(u_n)[\xi]\, d\xi \leq \eta, \quad \forall n \in \mathbb{N}. \tag{5.3.9}$$

By contradiction suppose that there exists $\eta_0 > 0$ such that for every $R > 0$ there is a number $m = m(R, \eta_0) \in \mathbb{N}$, in such a way that

$$\int_{|\xi|>R} \mathcal{F}^2(u_m)[\xi]\, d\xi > \eta_0.$$

Choosing $R > 0$ such that $\eta_0 \ln(R) + C_1 > C$, with C the constant in (5.3.7), and C_1 the one in (5.3.8) , we have

$$\int_{\mathbb{R}^n} \ln|\xi|\mathcal{F}^2(u_m)[\xi]\,d\xi > \int_{|\xi|>R} \ln|\xi|\mathcal{F}^2(u_m)[\xi]\,d\xi + \int_{|\xi|\leq 1} \ln|\xi|\mathcal{F}^2(u_m)[\xi]\,d\xi$$

$$> \ln(R)\eta_0 + C_1 > C,$$

which, in view of (5.3.7) results in a contradiction. Hence, assertion (5.3.9) holds.

On the other hand, the fact that $\{u_n\}_{n\in\mathbb{N}} \subset X$, implies that this sequence is uniformly bounded in $L^2(\Omega)$, and then, we can extract a weakly convergent subsequence $\{u_{n_j}\}_{j\in\mathbb{N}}$. Let $u \in L^2(\Omega)$ such that $u_{n_j} \rightharpoonup u$, our goal now is to show that $u_{n_j} \to u$ strongly in $L^2(\Omega)$, which implies strong convergence in $L^1(\Omega)$ since $|\Omega| < \infty$.

To this end, we only need to show that $\|u_{n_j}\|_{L^2(\Omega)} \to \|u\|_{L^2(\Omega)}$ or, equivalently, $\|\mathcal{F}(u_{n_j})\|_{L^2(\mathbb{R}^n)} \to \|\mathcal{F}(u)\|_{L^2(\mathbb{R}^n)}$. From (5.3.9), and the fact that $u \in L^2(\Omega)$, we can take R large enough, in such a way that

$$\int_{|\xi|>R} \mathcal{F}^2(u_{n_j})[\xi]\,d\xi < \eta, \quad \forall j \in \mathbb{N},$$

and

$$\int_{|\xi|>R} \mathcal{F}^2(u)[\xi]\,d\xi < \eta.$$

Then we have

$$\Big|\|\mathcal{F}(u_{n_j})\|^2_{L^2(\mathbb{R}^n)} - \|\mathcal{F}(u)\|^2_{L^2(\mathbb{R}^n)}\Big| \leq \tag{5.3.10}$$

$$\Big|\int_{|\xi|\leq R} \mathcal{F}^2(u_{n_j})[\xi]\,d\xi - \int_{|\xi|\leq R} \mathcal{F}^2(u)[\xi]\,d\xi\Big| + 2\eta.$$

Since u_{n_j} is supported in Ω, for all $j \in \mathbb{N}$, weak convergence implies $\mathcal{F}(u_{n_j})[\xi] \to \mathcal{F}(u)[\xi]$ for all $\xi \in \mathbb{R}^n$. And, as we have observed before, since $\|u_{n_j}\|_{L^1(\Omega)} \leq C_0$ for all $j \in \mathbb{N}$, $\mathcal{F}^2(u_{n_j})[\xi] \leq C_0^2$ for all $\xi \in \mathbb{R}^n$. Hence, we can apply the Dominated Convergence Theorem in (5.3.10) and say that there exists j_0 in such a way that if $j > j_0$ then

$$\Big|\|\mathcal{F}(u_{n_j})\|^2_{L^2(\mathbb{R}^n)} - \|\mathcal{F}(u)\|^2_{L^2(\mathbb{R}^n)}\Big| \leq 3\eta. \tag{5.3.11}$$

Since η can be arbitrary small, we have $\|u_{n_j}\|_{L^2(\Omega)} \to \|u\|_{L^2(\Omega)}$, and the statement of the theorem follows.

□

5.3.3 The case of the spectral fractional Laplacian

Besides (0.0.1), it is possible to define a related operator, usually called *spectral* fractional Laplacian, in the following way

$$(-\Delta)^s_\Omega u(x) := \sum_{i=1}^{\infty} \lambda_i^s (u, \varphi_i)_{L^2(\Omega)} \varphi_i(x), \tag{5.3.12}$$

with (λ_i^s, φ_i) eigenpair of the classical Laplacian with homogeneous Dirichlet boundary condition in Ω. The associated *spectral* semi-norm is defined as

$$|u|_s^2 := \sum_{i=1}^{\infty} \lambda_i^{2s} (u, \varphi_i)^2_{L^2(\Omega)}. \tag{5.3.13}$$

Ideas used in the proof of theorems 5.3.1 and 5.3.2 can be straightforwardly adapted in order to extend this results to the *spectral* case. That is, redefining (5.3.1) and (5.3.2) as

$$F_s(u) := \frac{\varepsilon^2}{2} |u|_s^2 + \int_\Omega W(u), \tag{5.3.14}$$

and

$$F_0(u) := \begin{cases} \sum_{i=1}^{\infty} \ln(\lambda_i)(u, \varphi_i)^2_{L^2(\Omega)} & \text{if } u \equiv \sqrt{1-\varepsilon^2}\big(I_E - I_{E^c}\big) \\ +\infty, & \text{in other case,} \end{cases} \tag{5.3.15}$$

respectively, with $E \subset \Omega$ and $E^c = \Omega \setminus E$, it is possible to prove that minimizers of F_s converge to minimizers of F_0.

From this, it can be observed that the minimization problems given by (5.3.2) and (5.3.15) present a similar behaviour, since both functionals prioritize *low frequency* functions. In order to make this point clear, consider first the minimization problem given by (5.3.15). With the purpose of minimize (5.3.15) we should find a set $E \subset \Omega$ in such a way that its associated characteristic function $u = \sqrt{1-\varepsilon^2}\big(I_E - I_{E^c}\big)$ can be well approximated using low frequency modes. That is, since $\ln(\lambda)$ is increasing as a function of λ, we need the largest values of $(u, \varphi_i)^2$ associated to small values of λ_i. A similar observation can be done about the minimization problem given by (5.3.2).

5.4 Numerical experiments

In this section, three numerical examples are presented in order to explore the behavior of the solution under fractional parameters s and α.

For the first example, we have used $\Omega = [-1, 1]$, a uniform mesh consisting of 3000 nodes, $s = 0.005$, $\alpha = 1$, $\varepsilon^2 = 0.5$, and the function $v = -0.5 I_{(-1,0)} + 0.5 I_{[0,1)}$ as the initial datum. Here, the aim is to obtain some experimental support for the ideas displayed in Section 5.3, that is, the behavior with a small parameter s. Numerical results are summarized in figure 5.1, and equilibrium values far from 1 and -1 can be

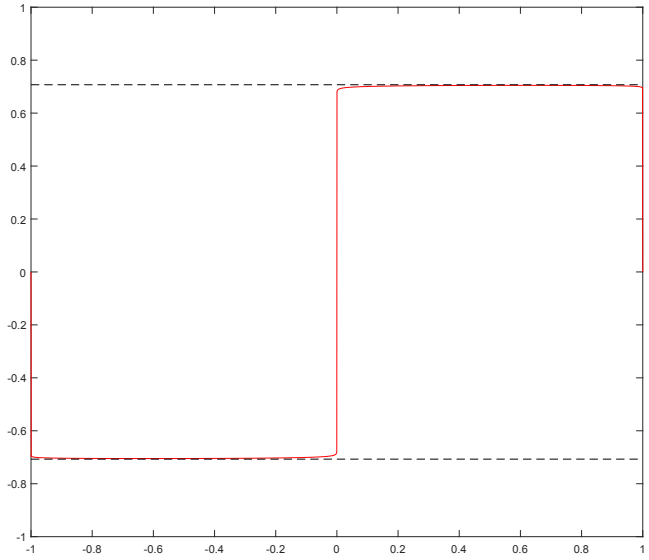

Figure 5.1: In red the solution of example 1 at $t = 50$, in black-dashed the values $\pm\sqrt{1-\varepsilon^2}$. It can be seen that the equilibrium states remain far from 1 and -1, unlike the behavior in the classic AC equation, and approach the values predicted in Section 5.3 (see (5.3.2)).

observed. Furthermore, equilibrium values seems to be placed near the values predicted in Section 5.3 or, in other words, the solution seems to approximate a minimizer of (5.3.2).

Example 2 and 3 (spinodal decomposition) are showed in figure 5.2 and 5.3 respectively. Here we have used Ω as the unitary ball, a uniform triangulation consisting of 16554 triangles, $\varepsilon^2 = 0.02$, and random noise as initial data. In example 2 (figure 5.2), the parameter α is fixed in 1, and results for several values of s are shown. Can be observed the fact that, as we have mentioned in Section 5.3, the smaller the parameter s, the thinner the interface. Finally, example 3 (figure 5.3) shows the behavior for fractional values of the parameter α, with $s = 1$.

Resumen del Capítulo

En este capítulo se aplican las técnicas desarrolladas en el capítulo anterior a una versión fraccionaria de la ecuación de Allen-Cahn,

$$ {}^{C}\partial_t^{\alpha} u + (-\Delta)^s u = f(u) \text{ in } \Omega \times (0,T), $$

con $s, \alpha \in (0,1]$, $f(u) = u - u^3$.

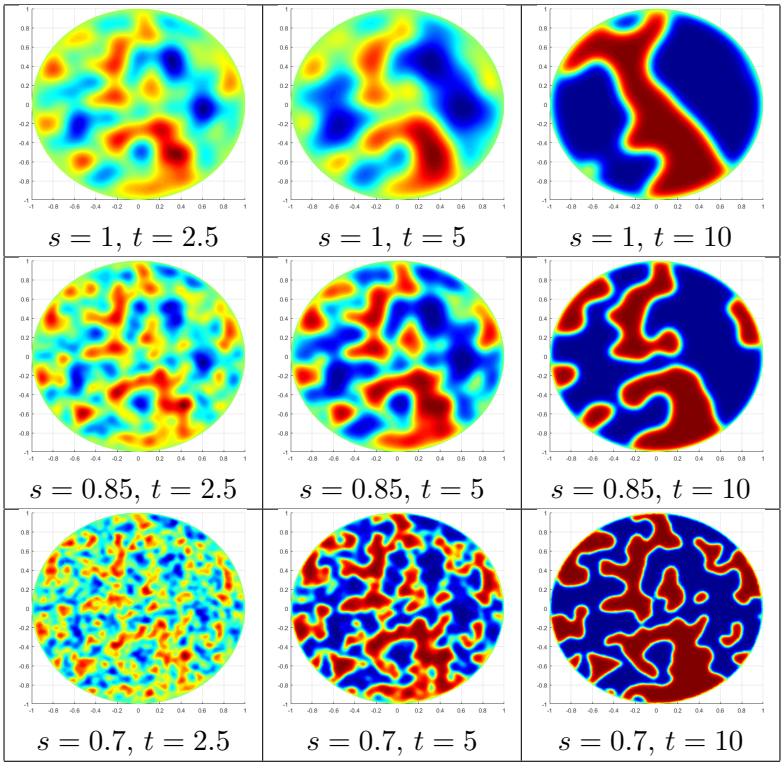

Figure 5.2: In this example we set $\Omega = B(0,1)$, $\alpha = 1$, and random noise as initial condition. The evolution in time is displayed for several values of s.

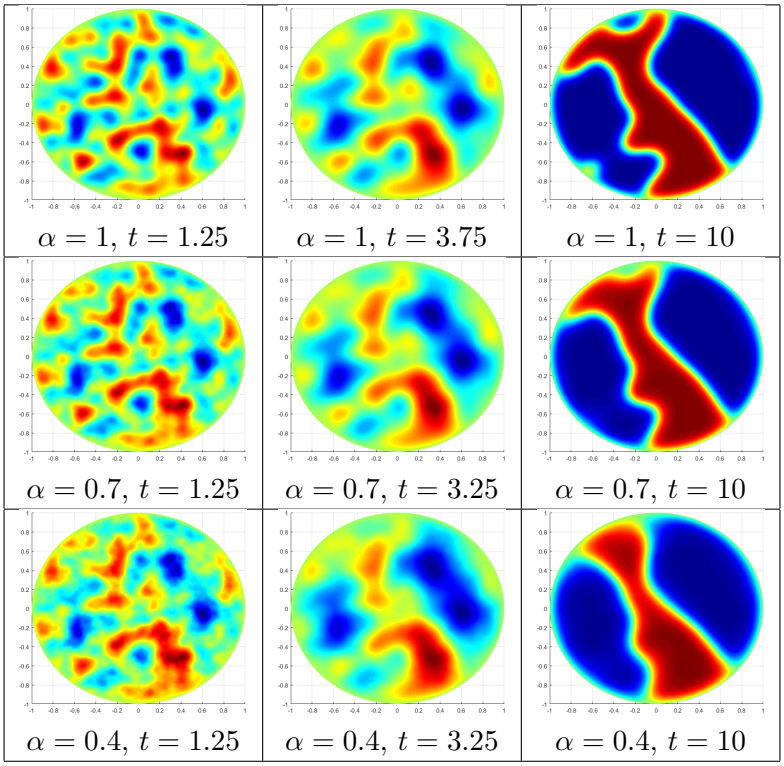

Figure 5.3: In this example we set $\Omega = B(0,1)$, $s = 1$, and random noise as initial condition. The evolution in time is displayed for several values of α.

En la Sección 5.1 se describe el método numérico propuesto (basado en el usado para el caso lineal), mientras que en la Sección 5.2 se obtienen estimaciones del error. En la Sección 5.3 se analiza el comportamiento asintótico de las soluciones con $\alpha = 1$ y $s \to 0^+$. Finalmente, en la Sección 5.4 se presentan experimentos numéricos explorando el comportamiento cualitativo de las soluciones.

Appendix A

Implementation details

A.1 Quadrature rules

Here we give details about how to compute the integrals $I^{i,j}_{\ell,m}$ and $J^{i,j}_{\ell}$ (see Section 3.2). In order to cope with $I^{i,j}_{\ell,m}$, we proceed according to whether $\overline{T_\ell} \cap \overline{T_m}$ is empty, a vertex, an edge or an element. Recall that $I^{i,j}_{\ell,m} = I^{i,j}_{m,\ell}$, so that we may assume $\ell \leq m$.

Consider two elements T_ℓ and T_m such that $\mathrm{supp}(\varphi_i), \mathrm{supp}(\varphi_j) \cap (T_\ell \cup T_m) \neq \emptyset$. Observe that if one of this intersections is empty, then $I^{i,j}_{\ell,m} = 0$. Moreover, it could be possible that one of the elements is disjoint with the support of both φ_i and φ_j, provided the other element intersects both supports and $I^{i,j}_{\ell,m} \neq 0$.

We are going to consider the reference element

$$\hat{T} = \{\hat{x} = (\hat{x}_1, \hat{x}_2) \colon 0 \leq \hat{x}_1 \leq 1,\, 0 \leq \hat{x}_2 \leq \hat{x}_1\},$$

whose vertices are

$$\hat{x}^{(1)} = \begin{pmatrix} 0 \\ 0 \end{pmatrix}, \quad \hat{x}^{(2)} = \begin{pmatrix} 1 \\ 0 \end{pmatrix}, \quad \hat{x}^{(3)} = \begin{pmatrix} 1 \\ 1 \end{pmatrix}.$$

The basis functions on $\hat{T}$ are, obviously,

$$\hat{\varphi}_1(\hat{x}) = 1 - \hat{x}_1, \quad \hat{\varphi}_2(\hat{x}) = \hat{x}_1 - \hat{x}_2, \quad \hat{\varphi}_3(\hat{x}) = \hat{x}_2.$$

Remark A.1.1. Given two elements T_ℓ and T_m, we provide a local numbering in the following way. If T_ℓ and T_m are disjoint, we set the first three nodes to be the nodes of T_ℓ and the following three nodes to be the ones of T_m. Else, we set the first node(s) to be the ones in the intersection, then we insert the remaining node(s) of T_ℓ and finally the one(s) of T_m (see Figure A.1). For simplicity of notation, when computing $I^{i,j}_{\ell,m}$ and $J^{i,j}_{\ell}$, we assume that i, j denote the local numbering of the basis functions involved; for example, if T_ℓ and T_m share only a vertex, then $1 \leq i, j \leq 5$.

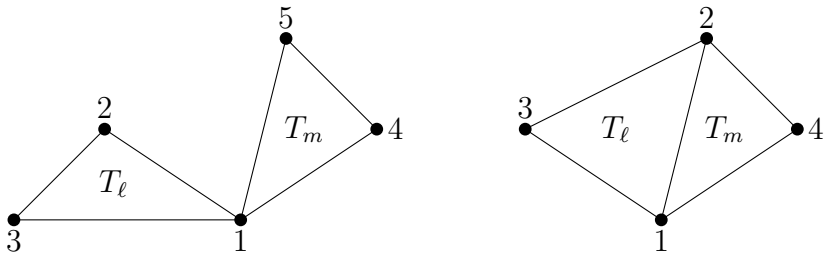

Figure A.1: Local numbering for elements with a vertex and an edge in common.

Consider the affine mappings

$$\begin{aligned} &\chi_\ell : \hat{T} \to T_\ell, && \chi_\ell(\hat{x}) = B_\ell \hat{x} + x_\ell^{(1)}, \\ &\chi_m : \hat{T} \to T_m, && \chi_m(\hat{x}) = B_m \hat{x} + x_m^{(1)}, \end{aligned}$$

where the matrices B_ℓ and B_m are such that $\hat{x}^{(2)}$ (resp. $\hat{x}^{(3)}$) is mapped respectively to the second (resp. third) node of T_ℓ and T_m in the local numbering defined above. Then, it is clear that

$$\begin{aligned} I_{\ell,m}^{i,j} &= 4|T_\ell||T_m| \int_{\hat{T}} \int_{\hat{T}} \frac{(\varphi_i(\chi_\ell(\hat{x})) - \varphi_i(\chi_m(\hat{y})))(\varphi_j(\chi_\ell(\hat{x})) - \varphi_j(\chi_m(\hat{y})))}{|\chi_\ell(\hat{x}) - \chi_m(\hat{y})|^{2+2s}} \, d\hat{x} \, d\hat{y} = \\ &= 4|T_\ell||T_m| \iiiint_{\hat{T}\times\hat{T}} F_{ij}(\hat{x}_1, \hat{x}_2, \hat{y}_1, \hat{y}_2) \, d\hat{x}_1 \, d\hat{x}_2 \, d\hat{y}_1 \, d\hat{y}_2. \end{aligned} \tag{A.1.1}$$

We discuss how to compute $I_{\ell,m}^{i,j}$ depending on the relative position of T_ℓ and T_m, and afterwards we tackle the computation of $J_\ell^{i,j}$.

A.1.1 Non-touching elements

This is the simplest case, since the integrand F_{ij} in (A.1.1) is not singular. Recall that

$$I_{\ell,m}^{i,j} = \int_{T_\ell} \int_{T_m} \frac{(\varphi_i(x) - \varphi_i(y))(\varphi_j(x) - \varphi_j(y))}{|x-y|^{2+2s}} \, dxdy, \quad 1 \le \ell, m \le N_{\tilde{\mathcal{T}}}.$$

Splitting the numerator in the integrand, we obtain

$$\begin{aligned} I_{\ell,m}^{i,j} = &\int_{T_\ell} \int_{T_m} \frac{\varphi_i(x)\varphi_j(x)}{|x-y|^{2+2s}} \, dxdy + \int_{T_\ell} \int_{T_m} \frac{\varphi_i(y)\varphi_j(y)}{|x-y|^{2+2s}} \, dxdy \\ &- \int_{T_\ell} \int_{T_m} \frac{\varphi_i(x)\varphi_j(y)}{|x-y|^{2+2s}} \, dxdy - \int_{T_\ell} \int_{T_m} \frac{\varphi_i(y)\varphi_j(x)}{|x-y|^{2+2s}} \, dxdy. \end{aligned}$$

Note that all the integrands depend on ℓ and m only through their denominators. Since $\varphi_i(x) = 0$ if $i = 1, 2, 3$ and $x \in T_m$ or if $i = 4, 5, 6$ and $x \in T_\ell$, given two

indices i, j, only one of the four integrals above is not null. Thus, we may divide the 36 interactions between the 6 basis functions involved into four 3 by 3 blocks, and write the local matrix `ML` as:

$$\texttt{ML} = \begin{pmatrix} A_{\ell,m} & B_{\ell,m} \\ C_{\ell,m} & D_{\ell,m} \end{pmatrix}, \tag{A.1.2}$$

where

$$A^{i,j}_{\ell,m} = \int_{T_\ell}\int_{T_m} \frac{\varphi_i(x)\varphi_j(x)}{|x-y|^{2+2s}}\,dxdy, \qquad B^{i,j}_{\ell,m} = -\int_{T_\ell}\int_{T_m} \frac{\varphi_i(x)\varphi_{j+3}(y)}{|x-y|^{2+2s}}\,dxdy$$
$$C^{i,j}_{\ell,m} = -\int_{T_\ell}\int_{T_m} \frac{\varphi_{i+3}(y)\varphi_j(x)}{|x-y|^{2+2s}}\,dxdy, \qquad D^{i,j}_{\ell,m} = \int_{T_\ell}\int_{T_m} \frac{\varphi_{i+3}(y)\varphi_{j+3}(y)}{|x-y|^{2+2s}}\,dxdy.$$

We use two nested Gaussian quadrature rules to estimate these integrals. These have 6 quadrature nodes each, making a total of 36 quadrature points. Let us denote by p_k and w_k $(k = 1, \ldots, 6)$ the quadrature nodes and weights in $\hat{T}$, respectively. Changing variables we obtain

$$A^{i,j}_{\ell,m} = 4|T_\ell||T_m| \int_{\hat{T}}\int_{\hat{T}} \frac{\hat{\varphi}_i(x)\hat{\varphi}_j(x)}{|\chi_\ell(x) - \chi_m(y)|^{2+2s}}\,dxdy,$$

and applying the quadrature rule twice, we derive:

$$A^{i,j}_{\ell,m} \approx 4|T_\ell||T_m| \sum_{q=1}^{6}\sum_{k=1}^{6} \frac{w_q\, w_k\, \hat{\varphi}_i(p_k)\hat{\varphi}_j(p_k)}{|\chi_\ell(p_k) - \chi_m(p_q)|^{2+2s}}. \tag{A.1.3}$$

Note that the right hand side summands only depend on i and j through their numerators, and on ℓ and m through their denominators. As our goal is to compute the whole block $A_{\ell,m}$ as efficiently as possible, we set the following definitions:

- The matrix $\Phi^A \in \mathbb{R}^9 \times \mathbb{R}^{36}$ stores the numerators involved in (A.1.3), corresponding to the 9 pairs of basis functions and the 36 pairs of quadrature nodes, respectively. Namely,

$$\Phi^A_{ij} = \hat{\varphi}_{[i-1]_3+1}(p_{\lceil \frac{j}{6} \rceil})\hat{\varphi}_{\lceil \frac{i}{3} \rceil}(p_{\lceil \frac{j}{6} \rceil}) w_{[j-1]_6+1} w_{\lceil \frac{j}{6} \rceil}, \tag{A.1.4}$$

  where $[m]_k$ denotes m modulo k and $\lceil \cdot \rceil$ is the ceiling function. Let us make this definition more explicit. The matrix Φ^A may be divided in 6 blocks,

$$\Phi^A = (\Phi^{A_1} \ldots \Phi^{A_6}),$$

where Φ^{A_k} is a 6×9 matrix:

$$\Phi^{A_k} = \begin{pmatrix} \hat{\varphi}_1(p_k)\hat{\varphi}_1(p_k)w_k w_1 & \hat{\varphi}_1(p_k)\hat{\varphi}_1(p_k)w_k w_2 & \dots & \hat{\varphi}_1(p_k)\hat{\varphi}_1(p_k)w_k w_6 \\ \hat{\varphi}_2(p_k)\hat{\varphi}_1(p_k)w_k w_1 & \hat{\varphi}_2(p_k)\hat{\varphi}_1(p_k)w_k w_2 & \dots & \hat{\varphi}_2(p_k)\hat{\varphi}_1(p_k)w_k w_6 \\ \hat{\varphi}_3(p_k)\hat{\varphi}_1(p_k)w_k w_1 & \hat{\varphi}_3(p_k)\hat{\varphi}_1(p_k)w_k w_2 & \dots & \hat{\varphi}_3(p_k)\hat{\varphi}_1(p_k)w_k w_6 \\ \hat{\varphi}_1(p_k)\hat{\varphi}_2(p_k)w_k w_1 & \hat{\varphi}_1(p_k)\hat{\varphi}_2(p_k)w_k w_2 & \dots & \hat{\varphi}_1(p_k)\hat{\varphi}_2(p_k)w_k w_6 \\ \hat{\varphi}_2(p_k)\hat{\varphi}_2(p_k)w_k w_1 & \hat{\varphi}_2(p_k)\hat{\varphi}_2(p_k)w_k w_2 & \dots & \hat{\varphi}_2(p_k)\hat{\varphi}_2(p_k)w_k w_6 \\ \hat{\varphi}_3(p_k)\hat{\varphi}_2(p_k)w_k w_1 & \hat{\varphi}_3(p_k)\hat{\varphi}_2(p_k)w_k w_2 & \dots & \hat{\varphi}_3(p_k)\hat{\varphi}_2(p_k)w_k w_6 \\ \hat{\varphi}_1(p_k)\hat{\varphi}_3(p_k)w_k w_1 & \hat{\varphi}_1(p_k)\hat{\varphi}_3(p_k)w_k w_2 & \dots & \hat{\varphi}_1(p_k)\hat{\varphi}_3(p_k)w_k w_6 \\ \hat{\varphi}_2(p_k)\hat{\varphi}_3(p_k)w_k w_1 & \hat{\varphi}_2(p_k)\hat{\varphi}_3(p_k)w_k w_2 & \dots & \hat{\varphi}_2(p_k)\hat{\varphi}_3(p_k)w_k w_6 \\ \hat{\varphi}_3(p_k)\hat{\varphi}_3(p_k)w_k w_1 & \hat{\varphi}_3(p_k)\hat{\varphi}_3(p_k)w_k w_2 & \dots & \hat{\varphi}_3(p_k)\hat{\varphi}_3(p_k)w_k w_6 \end{pmatrix}.$$

- The variable $d^m \in \mathbb{R}^{36}$ is a vector storing the distances between all the quadrature nodes involved:

$$d_k^m = \left|\chi_\ell(p_{[k-1]_6+1}) - \chi_m(p_{\lceil \frac{k}{6} \rceil})\right|^{-(2+2s)}. \tag{A.1.5}$$

  Namely, the vector d^m can be written as:

$$d^m = \begin{pmatrix} |\chi_\ell(p_1) - \chi_m(p_1)|^{-(2+2s)} \\ \vdots \\ |\chi_\ell(p_6) - \chi_m(p_1)|^{-(2+2s)} \\ |\chi_\ell(p_1) - \chi_m(p_2)|^{-(2+2s)} \\ \vdots \\ |\chi_\ell(p_6) - \chi_m(p_2)|^{-(2+2s)} \\ \vdots \\ \vdots \\ |\chi_\ell(p_1) - \chi_m(p_6)|^{-(2+2s)} \\ \vdots \\ |\chi_\ell(p_6) - \chi_m(p_6)|^{-(2+2s)} \end{pmatrix}.$$

With these two variables in hand, the computation of the integrals A^{ij} may be done in a vectorized mode. Defining $\hat{A}_{\ell,m} := \Phi^A \cdot d^m$, we obtain:

$$\begin{aligned} A_{\ell,m}^{[i-1]_3+1,\lceil \frac{i}{3} \rceil} &\approx 4|T_\ell||T_m|\hat{A}_{\ell,m}^i \\ &= 4|T_\ell||T_m| \sum_q \sum_k w_q w_k \frac{\hat{\varphi}_{[i-1]_3+1}(p_k)\hat{\varphi}_{\lceil \frac{i}{3} \rceil}(p_k)}{|\chi_\ell(p_k) - \chi_m(p_q)|^{2+2s}}, \ i \in \{1, ..., 9\}. \end{aligned}$$

Equivalently, using *MATLAB*® notation:

$$A_{\ell,m} \approx 4|T_\ell||T_m|\,\texttt{reshape}(\hat{A}_{\ell,m}\texttt{, 3 , 3}).$$

We apply the same ideas to computate the remaining blocks in (A.1.2). We define:

- a 9×36 matrix Φ^B, such that

$$\Phi^B_{ij} = \hat{\varphi}_{[i-1]_3+1}(p_{\lceil \frac{j}{n} \rceil})\hat{\varphi}_{\lceil \frac{i}{3} \rceil+3}(p_{[j-1]_n+1})w_{[j-1]_n+1}w_{\lceil \frac{j}{n} \rceil},$$

- a 9×36 matrix Φ^D, such that

$$\Phi^D_{ij} = \hat{\varphi}_{[i-1]_3+4}(p_{[j-1]_n+1})\hat{\varphi}_{\lceil \frac{i}{3} \rceil+3}(p_{[j-1]_n+1})w_{[j-1]_n+1}w_{\lceil \frac{j}{n} \rceil}.$$

Then, considering

$$\hat{B}_{\ell,m} := \Phi^B \cdot d^m,$$
$$\hat{D}_{\ell,m} := \Phi^D \cdot d^m,$$

we just need to multiply

$$B_{\ell,m} \approx 4|T_\ell||T_m|\texttt{reshape}(\hat{B}_{\ell,m}\texttt{, 3 , 3}),$$
$$D_{\ell,m} \approx 4|T_\ell||T_m|\texttt{reshape}(\hat{D}_{\ell,m}\texttt{, 3 , 3}).$$

Is simple to verify that $C_{\ell,m} = B'_{\ell,m}$, so that there is no need to make additional operations to compute the block $C_{\ell,m}$. Moreover, let us emphasize that the matrices Φ^A, Φ^B and Φ^D depend on the quadrature rule employed, but not on the elements under consideration; these are precomputed and stored in `data.mat`. We refer to Section A.3.2 for details on how this is done. However, in the main loop, the vector d^m needs to be calculated for every $1 \leq \ell \leq m \leq N_{\hat{\mathcal{T}}}$.

We obtain a matrix `ML` as follows:

$$\texttt{ML} \approx 4|T_\ell||T_m| \begin{pmatrix} \texttt{reshape}(\Phi^A \cdot d^m\texttt{, 3 , 3}) & \texttt{reshape}(\Phi^B \cdot d^m\texttt{, 3 , 3}) \\ \texttt{reshape}(\Phi^B \cdot d^m\texttt{, 3 , 3)'} & \texttt{reshape}(\Phi^D \cdot d^m\texttt{, 3 , 3}) \end{pmatrix}.$$

In addition, this vectorized approach gives us an efficient way to compute $I_{\ell,m}$ for several values of $m \in \{1, ..., N_{\tilde{\mathcal{T}}}\}$ at once. Indeed, suppose that want to calculate $I_{\ell,m}$ for $m \in \mathcal{S} \subseteq \{1, ..., N_{\tilde{\mathcal{T}}}\}$ (along the execution of the main code, $\mathcal{S}$ would contain the indices listed in `empty`). It is possible to compute $\hat{A}_{\ell,m}$, $\hat{B}_{\ell,m}$ and $\hat{D}_{\ell,m}$ for all $m \in \mathcal{S}$ using vectorized operations as follows:

$$\left(\hat{A}_{\ell,m_1}, ..., \hat{A}_{\ell,m_{\#\mathcal{S}}}\right) = \Phi^A \cdot (d^{m_1}, ..., d^{m_{\#\mathcal{S}}}),$$
$$\left(\hat{B}_{\ell,m_1}, ..., \hat{B}_{\ell,m_{\#\mathcal{S}}}\right) = \Phi^B \cdot (d^{m_1}, ..., d^{m_{\#\mathcal{S}}}),$$

$$\left(\hat{D}_{\ell,m_1},...,\hat{D}_{\ell,m_{\#\mathcal{S}}}\right) = \Phi^D \cdot (d^{m_1},...,d^{m_{\#\mathcal{S}}})\,.$$

Observe that, fixed ℓ and $\mathcal{S}$, the distances between interpolation points of the involved triangles are all the necessary information to obtain the estimation of the matrix `ML` (given by (A.1.2)), for $m \in \mathcal{S}$.

In order to perform an efficient computation of $(d^{m_1},...,d^{m_{\#\mathcal{S}}})$, we use the *MATLAB*® function `pdist2` in the following way:

$$(d^{m_1},...,d^{m_{\#\mathcal{S}}}) = \texttt{reshape(pdist2(}X^\ell, \begin{pmatrix} X^{m_1} \\ X^{m_2} \\ \vdots \\ X^{m_{\#\mathcal{S}}} \end{pmatrix} \texttt{), } n^2 \texttt{, [])}^{(-1-s)}.$$

Here, the vectors X^m are given by

$$X^m := \begin{pmatrix} \chi_m(p_1) \\ \vdots \\ \chi_m(p_6) \end{pmatrix}.$$

The computation of the matrix `ML` is carried in the main code, and it is implemented in Subsection 3.4.2.

A.1.2 Vertex-touching elements

In case $\overline{T_\ell} \cap \overline{T_m}$ consists of a vertex, define $\hat{z} = (\hat{x}, \hat{y})$, identify $\hat{z}$ with a vector in $\mathbb{R}^4$, and split the domain of integration in (A.1.1) into two components D_1 and D_2, where

$$D_1 = \{\hat{z}\colon 0 \le \hat{z}_1 \le 1,\, 0 \le \hat{z}_2 \le \hat{z}_1,\, 0 \le \hat{z}_3 \le \hat{z}_1,\, 0 \le \hat{z}_4 \le \hat{z}_3\},$$
$$D_2 = \{\hat{z}\colon 0 \le \hat{z}_3 \le 1,\, 0 \le \hat{z}_4 \le \hat{z}_3,\, 0 \le \hat{z}_1 \le \hat{z}_3,\, 0 \le \hat{z}_2 \le \hat{z}_1\}.$$

Let $\xi \in [0,1]$ and $\eta = (\eta_1, \eta_2, \eta_3) \in [0,1]^3$. We consider the mappings $T_h\colon [0,1] \times [0,1]^3 \to D_h,\ h = 1, 2,$

$$T_1(\xi,\eta) = \begin{pmatrix} \xi \\ \xi\eta_1 \\ \xi\eta_2 \\ \xi\eta_2\eta_3 \end{pmatrix}, \quad T_2(\xi,\eta) = \begin{pmatrix} \xi\eta_2 \\ \xi\eta_2\eta_3 \\ \xi \\ \xi\eta_1 \end{pmatrix},$$

having Jacobian determinants $|JT_1| = \xi^3\eta_2 = |JT_2|$.

We perform the calculations in detail only on D_1. Observe that if $i = 1$, which corresponds to the vertex in common between T_ℓ and T_m, then

$$\varphi_i(\chi_\ell(\xi, \xi\eta_1)) - \varphi_i(\chi_m(\xi\eta_2, \xi\eta_2\eta_3)) = -\xi(1-\eta_2).$$

Meanwhile, if the subindex i equals 2 or 3, it corresponds to one of the other two vertices of T_ℓ. Therefore, in those cases $\varphi_i(\chi_m(\xi\eta_2, \xi\eta_2\eta_3)) = 0$, and

$$\begin{aligned}\varphi_2(\chi_\ell(\xi, \xi\eta_1)) =& \xi(1-\eta_1),\\ \varphi_3(\chi_\ell(\xi, \xi\eta_1)) =& \xi\eta_1.\end{aligned}$$

Analogously, if $i \in \{4, 5\}$, then $\varphi_i(\chi_\ell(\xi, \xi\eta_1)) = 0$ and so

$$\begin{aligned}\varphi_4(\chi_m(\xi\eta_2, \xi\eta_2\eta_3)) =& -\xi\eta_2(1-\eta_3),\\ \varphi_5(\chi_m(\xi\eta_2, \xi\eta_2\eta_3)) =& -\xi\eta_2\eta_3.\end{aligned}$$

Thus, defining the functions $\psi_k^{(1)} \colon [0,1]^3 \to \mathbb{R}$ $(k \in \{1, \dots, 5\})$,

$$\begin{aligned}&\psi_1^{(1)}(\eta) = \eta_2 - 1, && \psi_2^{(1)}(\eta) = 1 - \eta_1, && \psi_3^{(1)}(\eta) = \eta_1,\\ &\psi_4^{(1)}(\eta) = -\eta_2(1-\eta_3), && \psi_5^{(1)}(\eta) = -\eta_2\eta_3,\end{aligned}$$

we may write

$$\begin{aligned}\int_{D_1} F_{ij}(\hat{z})\, d\hat{z} =& \int_{[0,1]} \int_{[0,1]^3} \frac{\psi_i^{(1)}(\eta)\psi_j^{(1)}(\eta)}{\left| B_\ell \begin{pmatrix} \xi \\ \xi\eta_1 \end{pmatrix} - B_m \begin{pmatrix} \xi\eta_2 \\ \xi\eta_2\eta_3 \end{pmatrix} \right|^{2+2s}} \xi^5 \eta_2\, d\eta\, d\xi\\ =& \left(\int_0^1 \xi^{3-2s} d\xi \right) \left(\int_{[0,1]^3} \frac{\psi_i^{(1)}(\eta)\psi_j^{(1)}(\eta)}{\left| d^{(1)}(\eta) \right|^{2+2s}} \eta_2\, d\eta \right)\\ =& \frac{1}{4-2s} \left(\int_{[0,1]^3} \frac{\psi_i^{(1)}(\eta)\psi_j^{(1)}(\eta)}{\left| d^{(1)}(\eta) \right|^{2+2s}} \eta_2\, d\eta \right),\end{aligned}$$

where we have defined the function

$$d^{(1)}(\eta) = B_\ell \begin{pmatrix} 1 \\ \eta_1 \end{pmatrix} - B_m \begin{pmatrix} \eta_2 \\ \eta_2\eta_3 \end{pmatrix}.$$

Observe that in the first line of last equation (or equivalently, in (A.1.1)), the integrand is singular at the origin. The key point in the identity above is that the singularity of the integral is explicitly computed. The function $d^{(1)}$ is not zero on $[0,1]^3$, and therefore the last integral involves a regular integrand that is easily estimated by means of a Gaussian quadrature rule.

In a similar fashion, the integrals over D_2 take the form

$$\int_{D_2} F_{ij}(\hat{z})\, d\hat{z} = \frac{1}{4-2s} \left(\int_{[0,1]^3} \frac{\psi_i^{(2)}(\eta)\psi_j^{(2)}(\eta)}{\left| d^{(2)}(\eta) \right|^{2+2s}} \eta_2\, d\eta \right),$$

where

$$\psi_1^{(2)}(\eta) = 1 - \eta_2, \qquad \psi_2^{(2)}(\eta) = \eta_2(1-\eta_3), \qquad \psi_3^{(2)}(\eta) = \eta_2\eta_3,$$

$$\psi_4^{(2)}(\eta) = \eta_1 - 1, \qquad \psi_5^{(2)}(\eta) = -\eta_1,$$

and

$$d^{(2)}(\eta) = B_\ell \begin{pmatrix} \eta_2 \\ \eta_2\eta_3 \end{pmatrix} - B_m \begin{pmatrix} 1 \\ \eta_1 \end{pmatrix}.$$

Based on the previous analysis, we describe the function `vertex_quad`. Let $p_1, ..., p_n \in [0,1]^3$ be a set of quadrature points and $w_1, ..., w_n$ their respective weights. In the code we present, we work with three nested three-point quadrature rules on $[0,1]$, making a total of 27 quadrature nodes in the unit cube. The data necessary to use this quadrature is supplied in the file `data.mat`, and in Appendix A.3.1.

Set $h \in \{1,2\}$. Then, applying the mentioned quadrature rule in the cube,

$$\int_{[0,1]^3} \frac{\psi_i^{(h)}(\eta)\psi_j^{(h)}(\eta)}{\left|d^{(h)}(\eta)\right|^{2+2s}} \eta_2 \, d\eta \approx \sum_{k=1}^{27} w_k \frac{\psi_i^{(h)}(p_k)\psi_j^{(h)}(p_k)}{\left|d^{(h)}(p_k)\right|^{2+2s}} p_{k,2},$$

where $p_{k,2}$ denotes the second coordinate of the point p_k. The right hand side only depends on ℓ and m through $d^{(h)}$. So, in order to compute $I_{\ell,m}^{i,j}$ using vectorized operations, we define the following variables, in analogy to (A.1.4) and (A.1.5):

- A 25×27 matrix Ψ^h satisfying

$$\Psi_{ij}^h = w_j \, \psi_{[i-1]_5+1}^{(h)}(p_j)\psi_{\lceil \frac{i}{5} \rceil}^{(h)}(p_j) \, p_{j,2}.$$

- A vector $d^h \in \mathbb{R}^{27}$, such that

$$d_k^h = \left|d^{(h)}(p_k)\right|^{-(2+2s)}.$$

Then, defining $\hat{I}_{\ell,m} := \Psi^1 \cdot d^1 + \Psi^2 \cdot d^2$, we obtain

$$\begin{aligned} I_{\ell,m}^{[i-1]_5+1,\lceil \frac{i}{5} \rceil} &\approx \frac{4|T_\ell||T_m|}{4-2s} \hat{I}_{\ell,m}^i \\ &= \sum_{h=1}^{2} \sum_{k=1}^{27} w_k \frac{\psi_{[i-1]_5+1}^{(h)}(p_k)\psi_{\lceil \frac{i}{5} \rceil}^{(h)}(p_k)}{\left|d^{(h)}(p_k)\right|^{2+2s}}, \quad i \in \{1, ..., 25\}. \end{aligned}$$

Equivalently, using *MATLAB*® notation:

$$I_{\ell,m} \approx \frac{4|T_\ell||T_m|}{4-2s} \texttt{reshape}(\hat{I}_{\ell,m}, \texttt{5 , 5}).$$

Given that the matrices Ψ^1 and Ψ^2 do not change along the execution, we only need to compute them once. These are precomputed and provided on the data file; explicit information regarding its entries is available on Appendix A.3.3.

So, the function `vertex_quad` computes the previous quadrature rule in the following way:

```
function ML = vertex_quad (nodl,nodm,sh_nod,p,s,psi1,psi2,areal,aream,p_c)
xm = p(1, nodm);
ym = p(2, nodm);
xl = p(1, nodl);
yl = p(2, nodl);
x = p_c(:,1);
y = p_c(:,2);
z = p_c(:,3);
local_l = find(nodl==sh_nod);
nsh_l = find(nodl~=sh_nod);
nsh_m = find(nodm~=sh_nod);
p_c = [xl(local_l), yl(local_l)];
Bl = [xl(nsh_l(1))-p_c(1) xl(nsh_l(2))-xl(nsh_l(1));
      yl(nsh_l(1))-p_c(2) yl(nsh_l(2))-yl(nsh_l(1))];
Bm = [xm(nsh_m(1))-p_c(1) xm(nsh_m(2))-xm(nsh_m(1));
      ym(nsh_m(1))-p_c(2) ym(nsh_m(2))-ym(nsh_m(1))];
ML = ( 4*areal*aream/(4-2*s) ).*reshape(...
     psi1*( sum( ([ones(length(x),1)  x]*(Bl')...
             - [y , y.*z]*(Bm') ).^2, 2 ).^(-1-s) ) +...
     psi2*( sum( ([ones(length(x),1)  x]*(Bm')...
             - [y , y.*z]*(Bl') ).^2, 2 ).^(-1-s) )...
     , 5 , 5);
end
```

In the code above, `nodl` and `nodm` are the vertex indices of T_ℓ and T_m respectively, `sh_nod` is the index of the shared node, `p` is an array that contains all the vertex coordinates, `areal` and `aream` denote $|T_\ell|$ and $|T_m|$ respectively, `s` is s, and `p_c` contains the coordinates of the quadrature points on $[0,1]^3$. This last variable is gathered form `data.mat`, where it is stored as `p_cube` (see Appendix A.3.1). In addition, `Bl` and `Bm` play the role of B_ℓ and B_m, and `psi1` and `psi2` are Ψ^1 and Ψ^2 respectively. As we mentioned, `psi1` and `psi2` have been pre-computed and stored on `data.mat` as `vpsi1` and `vpsi2` respectively (see Appendix A.3.3).

The output of `vertex_quad` is a 6×6 matrix `ML` that satisfies `ML(i,j)` $\approx I_{\ell,m}^{i,j}$.

A.1.3 Edge-touching elements

In this case, the parametrization of the elements we are considering is such that both χ_ℓ and χ_m map $[0,1] \times \{0\}$ to the common edge between T_ℓ and T_m. Therefore, if we consider $\hat{z} = (\hat{y}_1 - \hat{x}_1, \hat{y}_2, \hat{x}_2)$, the singularity of the integrand is localized at $\hat{z} = 0$:

$$I_{\ell,m}^{i,j} = 4|T_\ell||T_m| \int_0^1 \int_{-\hat{x}_1}^{1-\hat{x}_1} \int_0^{\hat{z}_1+\hat{x}_1} \int_0^{\hat{x}_1} F_{ij}(\hat{x}_1, \hat{z}_3, \hat{x}_1 + \hat{z}_1, \hat{z}_2)\, d\hat{z}\, d\hat{x}_1.$$

We decompose the domain of integration as $\cup_{k=1}^5 D_k$, where

$$D_1 = \{(\hat{x}_1, \hat{z}) \colon\ -1 \le \hat{z}_1 \le 0,\ 0 \le \hat{z}_2 \le 1 + \hat{z}_1,$$

$$
\begin{aligned}
&0 \le \hat{z}_3 \le \hat{z}_2 - \hat{z}_1,\ \hat{z}_2 - \hat{z}_1 \le \hat{x}_1 \le 1\},\\
D_2 = \{(\hat{x}_1, \hat{z})\colon\ &-1 \le \hat{z}_1 \le 0,\ 0 \le \hat{z}_2 \le 1 + \hat{z}_1,\\
&\hat{z}_2 - \hat{z}_1 \le \hat{z}_3 \le 1,\ \hat{z}_3 \le \hat{x}_1 \le 1\},\\
D_3 = \{(\hat{x}_1, \hat{z})\colon\ &0 \le \hat{z}_1 \le 1,\ 0 \le \hat{z}_2 \le \hat{z}_1,\\
&0 \le \hat{z}_3 \le 1 - \hat{z}_1,\ \hat{z}_3 \le \hat{x}_1 \le 1 - \hat{z}_1\},\\
D_4 = \{(\hat{x}_1, \hat{z})\colon\ &0 \le \hat{z}_1 \le 1,\ \hat{z}_1 \le \hat{z}_2 \le 1,\\
&0 \le \hat{z}_3 \le \hat{z}_2 - \hat{z}_1,\ \hat{z}_2 - \hat{z}_1 \le \hat{x}_1 \le 1 - \hat{z}_1\},\\
D_5 = \{(\hat{x}_1, \hat{z})\colon\ &0 \le \hat{z}_1 \le 1,\ \hat{z}_1 \le \hat{z}_2 \le 1,\\
&\hat{z}_2 - \hat{z}_1 \le \hat{z}_3 \le 1 - \hat{z}_1,\ \hat{z}_3 \le \hat{x}_1 \le 1 - \hat{z}_1\}.
\end{aligned}
$$

Consider the mappings $T_k\colon [0,1] \times [0,1]^3 \to D_k$ $(k \in \{1, \dots, 5\})$,

$$
T_1 \begin{pmatrix} \xi \\ \eta \end{pmatrix} = \begin{pmatrix} \xi \\ -\xi\eta_1\eta_2 \\ \xi\eta_1(1-\eta_2) \\ \xi\eta_1\eta_3 \end{pmatrix}, \qquad
T_2 \begin{pmatrix} \xi \\ \eta \end{pmatrix} = \begin{pmatrix} \xi \\ -\xi\eta_1\eta_2\eta_3 \\ \xi\eta_1\eta_2(1-\eta_3) \\ \xi\eta_1 \end{pmatrix},
$$

$$
T_3 \begin{pmatrix} \xi \\ \eta \end{pmatrix} = \begin{pmatrix} \xi(1-\eta_1\eta_2) \\ \xi\eta_1\eta_2 \\ \xi\eta_1\eta_2\eta_3 \\ \xi\eta_1(1-\eta_2) \end{pmatrix}, \qquad
T_4 \begin{pmatrix} \xi \\ \eta \end{pmatrix} = \begin{pmatrix} \xi(1-\eta_1\eta_2\eta_3) \\ \xi\eta_1\eta_2\eta_3 \\ \xi\eta_1 \\ \xi\eta_1\eta_2(1-\eta_3) \end{pmatrix},
$$

$$
T_5 \begin{pmatrix} \xi \\ \eta \end{pmatrix} = \begin{pmatrix} \xi(1-\eta_1\eta_2\eta_3) \\ \xi\eta_1\eta_2\eta_3 \\ \xi\eta_1\eta_2 \\ \xi\eta_1(1-\eta_2\eta_3) \end{pmatrix},
$$

with Jacobian determinants given by

$$
|JT_1| = \xi^3\eta_1^2, \quad |JT_h| = \xi^3\eta_1^2\eta_2,\ h \in \{2, \dots, 5\}.
$$

Then, over D_h it holds that

$$
\int_{D_h} F_{ij} = \frac{1}{4-2s} \int_{[0,1]^3} \frac{\psi_i^{(h)}(\eta)\psi_j^{(h)}(\eta)}{|d^{(h)}(\eta)|^{2+2s}}\, J^{(h)}(\eta)\, d\eta,
$$

where

$$
\begin{aligned}
&\psi_1^{(1)}(\eta) = -\eta_1\eta_2, && \psi_2^{(1)}(\eta) = \eta_1(1-\eta_3),\\
&\psi_3^{(1)}(\eta) = \eta_1\eta_3, && \psi_4^{(1)}(\eta) = -\eta_1(1-\eta_2),\\
&\psi_1^{(2)}(\eta) = -\eta_1\eta_2\eta_3, && \psi_2^{(2)}(\eta) = -\eta_1(1-\eta_2),\\
&\psi_3^{(2)}(\eta) = \eta_1, && \psi_4^{(2)}(\eta) = -\eta_1\eta_2(1-\eta_3),\\
&\psi_1^{(3)}(\eta) = \eta_1\eta_2, && \psi_2^{(3)}(\eta) = -\eta_1(1-\eta_2\eta_3),
\end{aligned}
$$

$$
\begin{aligned}
\psi_3^{(3)}(\eta) &= \eta_1(1-\eta_2), & \psi_4^{(3)}(\eta) &= -\eta_1\eta_2\eta_3,\\
\psi_1^{(4)}(\eta) &= \eta_1\eta_2\eta_3, & \psi_2^{(4)}(\eta) &= \eta_1(1-\eta_2),\\
\psi_3^{(4)}(\eta) &= \eta_1\eta_2(1-\eta_3), & \psi_4^{(4)}(\eta) &= -\eta_1,\\
\psi_1^{(5)}(\eta) &= \eta_1\eta_2\eta_3, & \psi_2^{(5)}(\eta) &= -\eta_1(1-\eta_2),\\
\psi_3^{(5)}(\eta) &= \eta_1(1-\eta_2\eta_3), & \psi_4^{(5)}(\eta) &= -\eta_1\eta_2.
\end{aligned}
$$

Moreover, the functions $d^{(h)}$ are given by

$$
\begin{aligned}
d^{(1)}(\eta) &= B_\ell \begin{pmatrix} 1 \\ \eta_1\eta_3 \end{pmatrix} - B_m \begin{pmatrix} 1-\eta_1\eta_2 \\ \eta_1(1-\eta_2) \end{pmatrix},\\
d^{(2)}(\eta) &= B_\ell \begin{pmatrix} 1 \\ \eta_1 \end{pmatrix} - B_m \begin{pmatrix} 1-\eta_1\eta_2\eta_3 \\ \eta_1\eta_2(1-\eta_3) \end{pmatrix},\\
d^{(3)}(\eta) &= B_\ell \begin{pmatrix} 1-\eta_1\eta_2 \\ \eta_1(1-\eta_2) \end{pmatrix} - B_m \begin{pmatrix} 1 \\ \eta_1\eta_2\eta_3 \end{pmatrix},\\
d^{(4)}(\eta) &= B_\ell \begin{pmatrix} 1-\eta_1\eta_2\eta_3 \\ \eta_1\eta_2(1-\eta_3) \end{pmatrix} - B_m \begin{pmatrix} 1 \\ \eta_1 \end{pmatrix},\\
d^{(5)}(\eta) &= B_\ell \begin{pmatrix} 1-\eta_1\eta_2\eta_3 \\ \eta_1(1-\eta_2\eta_3) \end{pmatrix} - B_m \begin{pmatrix} 1 \\ \eta_1\eta_2 \end{pmatrix},
\end{aligned}
$$

and the Jacobians are

$$
J^{(1)}(\eta) = \eta_1^2, \quad J^{(h)}(\eta) = \eta_1^2\eta_2,\ h \in \{2,\dots,5\}.
$$

As in the case of vertex-touching elements, the problem is reduced to computing integrals on the unit cube. Let $p_1, ..., p_{27} \in [0,1]^3$ the quadrature points, and $w_1, ..., w_{27}$ their respective weights. For $h = 1, \dots, 5$ we have

$$
\int_{[0,1]^3} \frac{\psi_i^{(h)}(\eta)\psi_j^{(h)}(\eta)}{\left|d^{(h)}(\eta)\right|^{2+2s}} J^{(h)}(\eta)\, d\eta \approx \sum_k w_k \frac{\psi_i^{(h)}(p_k)\psi_j^{(h)}(p_k)}{\left|d^{(h)}(p_k)\right|^{2+2s}} J^{(h)}(p_k).
$$

Once more, the right hand side only depends on ℓ and m through $d^{(h)}$. So, with the purpose of computing $I_{\ell,m}$ efficiently, we define:

- A matrix $\Psi^h \in \mathbb{R}^{16\times 27}$, given by

$$
\Psi^h_{ij} = w_j\, \psi_{[i-1]_4+1}(p_j)\psi_{\lceil \frac{i}{4} \rceil}(p_j) J^{(h)}(p_j).
$$

- A vector $d^h \in \mathbb{R}^{27}$, such that

$$
d^h_k = \left|d^{(h)}(p_k)\right|^{-(2+2s)}.
$$

Therefore, considering $\hat{I}_{\ell,m} = \Psi^1 \cdot d^1 + \cdots + \Psi^5 \cdot d^5$, we reach the following relation:

$$I_{\ell,m}^{[i-1]_4+1,\lceil \frac{i}{4} \rceil} \approx \frac{4|T_\ell||T_m|}{4-2s} \hat{I}_{\ell,m}^i = \sum_h \sum_k w_k \frac{\psi^{(h)}_{[i-1]_4+1}(p_k)\psi^{(h)}_{\lceil \frac{i}{4} \rceil}(p_k)}{\left|d^{(h)}(p_k)\right|^{2+2s}},\ i \in \{1, ..., 16\}.$$

Using *MATLAB*® notation,

$$I_{\ell,m} \approx \frac{4|T_\ell||T_m|}{4-2s} \texttt{reshape}(\hat{I}_{\ell,m}, \texttt{ 4 , 4}).$$

As before, the matrices Ψ^1, ..., Ψ^5 do not depend on the elements under consideration, so they are precomputed and provided in `data.mat`, where they are stored as `epsi1`, ..., `epsi5`, respectively. Details about their calculation are given in Appendix A.3.4.

The function `edge_quad` performs the calculations we have explained in this section.

```
function ML = edge_quad(nodl,nodm,nod_diff,p,s,psi1,psi2,psi3,...
                        psi4,psi5,areal,aream,p_c)
xm = p(1, nodm);
ym = p(2, nodm);
xl = p(1, nodl);
yl = p(2, nodl);
x = p_c(:,1);
y = p_c(:,2);
z = p_c(:,3);
local_l = find(nodl~=nod_diff(1));
nsh_l = find(nodl==nod_diff(1));
nsh_m = find(nodm==nod_diff(2));
P1 = [xl(local_l(1)), yl(local_l(1))];
P2 = [xl(local_l(2)), yl(local_l(2))];
Bl = [P2(1)-P1(1) -P2(1)+xl(nsh_l);
      P2(2)-P1(2) -P2(2)+yl(nsh_l)];
Bm = [P2(1)-P1(1) -P2(1)+xm(nsh_m);
      P2(2)-P1(2) -P2(2)+ym(nsh_m)];
ML = ( 4*areal*aream/(4-2*s) ).*reshape(...
      psi1*( sum( ([ones(length(x),1)  x.*z]*(Bl')...
         - [1-x.*y  x.*(1-y)]*(Bm') ).^2, 2 ).^(-1-s) ) +...
      psi2*( sum( ([ones(length(x),1)  x]*(Bl')...
         - [1-x.*y.*z  x.*y.*(1-z)]*(Bm') ).^2, 2 ).^(-1-s) ) +...
      psi3*( sum( ([(1-x.*y)  x.*(1-y)]*(Bl')...
         - [ones(length(x),1) x.*y.*z]*(Bm') ).^2, 2 ).^(-1-s) ) +...
      psi4*( sum( ([1-x.*y.*z  x.*y.*(1-z)]*(Bl')...
         - [ones(length(x),1) x]*(Bm') ).^2, 2 ).^(-1-s) ) +...
```

```
      psi5*( sum( ([1-x.*y.*z  x.*(1-y.*z)]*(Bl')...
         - [ones(length(x),1) x.*y]*(Bm') ).^2, 2 ).^(-1-s) )...
      , 4 , 4);
end
```

Here, `nodl` and `nodm` are the indices of the vertices of T_ℓ and T_m respectively, `nod_diff` contains the not-shared-vertex index, `p` is an array that contains all the vertex coordinates, `areal` and `aream` are $|T_\ell|$ and $|T_m|$ respectively, `s` is s, `p_c` contains the coordinates of the quadrature points on $[0,1]^3$ (stored in `data.mat`, see Appendix A.3.1), `Bl` and `Bm` are B_ℓ and B_m, and `psi1`, ..., `psi5` are $\Psi^1, \dots, \Psi^5$ respectively.

The output of this function is a 4×4 matrix `ML` $\approx I_{\ell,m}$.

A.1.4 Identical elements

In the same spirit as before, let us consider $\hat{z} = \hat{y} - \hat{x}$, so that

$$I_{\ell,\ell} = 4|T_\ell|^2 \int_0^1 \int_0^{\hat{x}_1} \int_{-\hat{x}_1}^{1-\hat{x}_1} \int_{-\hat{x}_2}^{\hat{z}_1+\hat{x}_1-\hat{x}_2} F_{ij}(\hat{x}_1, \hat{x}_2, \hat{x}_1+\hat{z}_1, \hat{x}_2+\hat{z}_2)\, d\hat{z}_2\, d\hat{z}_1\, d\hat{x}_2\, d\hat{x}_1.$$

Let us decompose the integration region into

$$\begin{aligned}
D_1 = \{(\hat{x},\hat{z})\colon\ & -1 \le \hat{z}_1 \le 0,\ -1 \le \hat{z}_2 \le \hat{z}_1,\\
& -\hat{z}_2 \le \hat{x}_1 \le 1,\ -\hat{z}_2 \le \hat{x}_2 \le \hat{x}_1\},\\
D_2 = \{(\hat{x},\hat{z})\colon\ & 0 \le \hat{z}_1 \le 1,\ \hat{z}_1 \le \hat{z}_2 \le 1,\\
& \hat{z}_2 - \hat{z}_1 \le \hat{x}_1 \le 1 - \hat{z}_1,\ 0 \le \hat{x}_2 \le \hat{z}_1 - \hat{z}_2 + \hat{x}_1\},\\
D_3 = \{(\hat{x},\hat{z})\colon\ & -1 \le \hat{z}_1 \le 0,\ \hat{z}_1 \le \hat{z}_2 \le 0,\\
& -\hat{z}_1 \le \hat{x}_1 \le 1,\ -\hat{z}_2 \le \hat{x}_2 \le \hat{x}_1 + \hat{z}_1 - \hat{z}_2\},\\
D_4 = \{(\hat{x},\hat{z})\colon\ & 0 \le \hat{z}_1 \le 1,\ 0 \le \hat{z}_2 \le \hat{z}_1,\\
& 0 \le \hat{x}_1 \le 1 - \hat{z}_1,\ 0 \le \hat{x}_2 \le \hat{x}_1\},\\
D_5 = \{(\hat{x},\hat{z})\colon\ & -1 \le \hat{z}_1 \le 0,\ 0 \le \hat{z}_2 \le 1 + \hat{z}_1,\\
& \hat{z}_2 - \hat{z}_1 \le \hat{x}_1 \le 1,\ 0 \le \hat{x}_2 \le \hat{x}_1 + \hat{z}_1 - \hat{z}_2\},\\
D_6 = \{(\hat{x},\hat{z})\colon\ & 0 \le \hat{z}_1 \le 1,\ -1 + \hat{z}_1 \le \hat{z}_2 \le 0,\\
& -\hat{z}_2 \le \hat{x}_1 \le 1 - \hat{z}_1,\ -\hat{z}_2 \le \hat{x}_2 \le \hat{x}_1\}.
\end{aligned} \tag{A.1.6}$$

We begin by considering the first two sets. Making the change of variables $(\hat{x}', \hat{z}') = (\hat{x}, -\hat{z})$ on D_1 and $(\hat{x}', \hat{z}') = (\hat{x} + \hat{z}, \hat{z})$ on D_2, both regions are transformed into

$$D_1' = \{(\hat{x}', \hat{z}')\colon 0 \le \hat{z}_1' \le 1,\ \hat{z}_1' \le \hat{z}_2' \le 1,\ \hat{z}_2' \le \hat{x}_1' \le 1,\ \hat{z}_2' \le \hat{x}_2' \le \hat{x}_1'\},$$

so that

$$4|T_\ell|^2 \int_{D_1 \cup D_2} F_{ij}(\hat{x}, \hat{x}+\hat{z}) = 4|T_\ell|^2 \int_{D_1'} F_{ij}(\hat{x}', \hat{x}'-\hat{z}') + F_{ij}(\hat{x}'-\hat{z}', \hat{x}')\, d\hat{x}'\, d\hat{z}'$$

$$= 8|T_\ell|^2 \int_{D_1'} F_{ij}(\hat{x}', \hat{x}' - \hat{z}')\, d\hat{x}'\, d\hat{z}',$$

because

$$F_{ij}(\hat{x}', \hat{x}' - \hat{z}') = \frac{(\hat{\varphi}_i(\hat{x}') - \hat{\varphi}_i(\hat{x}' - \hat{z}'))(\hat{\varphi}_j(\hat{x}') - \hat{\varphi}_j(\hat{x}' - \hat{z}'))}{|B_\ell(\hat{z}')|^{2+2s}} = F_{ij}(\hat{x}' - \hat{z}', \hat{x}').$$

Next, consider the four-dimensional simplex

$$D = \{w \colon 0 \le w_1 \le 1,\ 0 \le w_2 \le w_1,\ 0 \le w_3 \le w_2,\ 0 \le w_4 \le w_3\},$$

the map $T_1 \colon D \to D_1'$,

$$\begin{pmatrix} \hat{x}' \\ \hat{z}' \end{pmatrix} = T_1 \begin{pmatrix} w_1 \\ w_2 \\ w_3 \\ w_4 \end{pmatrix} = \begin{pmatrix} w_1, \\ w_1 - w_2 + w_3, \\ w_4, \\ w_3 \end{pmatrix}, \quad |JT_1| = 1,$$

and the Duffy-type transform $T : [0,1]^4 \to D$,

$$w = T \begin{pmatrix} \xi \\ \eta \end{pmatrix} = \begin{pmatrix} \xi, \\ \xi\eta_1, \\ \xi\eta_1\eta_2, \\ \xi\eta_1\eta_2\eta_3 \end{pmatrix}, \quad |JT| = \xi^3\eta_1^2\eta_2. \tag{A.1.7}$$

The composition of these two changes of variables allows to write the variables in F_{ij} in terms of (ξ, η) in the following way:

$$\hat{x}' = \begin{pmatrix} \xi \\ \xi(1 - \eta_1 + \eta_1\eta_2) \end{pmatrix},\ \hat{z}' = \begin{pmatrix} \xi\eta_1\eta_2\eta_3 \\ \xi\eta_1\eta_2 \end{pmatrix},\ \hat{x} - \hat{z}' = \begin{pmatrix} \xi(1 - \eta_1\eta_2\eta_3) \\ \xi(1 - \eta_1) \end{pmatrix}.$$

Observe that

$$\Lambda_k^{(1)}(\xi, \eta) := \hat{\varphi}_k(\hat{x}') - \hat{\varphi}_k(\hat{x}' - \hat{z}') = \begin{cases} -\xi\eta_1\eta_2\eta_3 & \text{if } k = 1, \\ -\xi\eta_1\eta_2(1 - \eta_3) & \text{if } k = 2, \\ \xi\eta_1\eta_2 & \text{if } k = 3. \end{cases}$$

Thus,

$$4|T_\ell|^2 \int_{D_1 \cup D_2} F_{ij}(\hat{x}, \hat{x} + \hat{z}) = 8|T_\ell|^2 \int_D F_{ij}(w_1, w_1 - w_2 + w_3, w_4, w_3)\, dw =$$
$$= 8|T_\ell|^2 \int_{[0,1]^4} \frac{\Lambda_i^{(1)}(\xi, \eta)\, \Lambda_j^{(1)}(\xi, \eta)}{\left| B_\ell \begin{pmatrix} \xi\eta_1\eta_2\eta_3 \\ \xi\eta_1\eta_2 \end{pmatrix} \right|^{2+2s}} \xi^3\eta_1^2\eta_2\, d\xi\, d\eta.$$

Finally, as the functions $\Lambda_k^{(1)}$ may be rewritten as $\Lambda_k^{(1)}(\xi,\eta) = \xi\eta_1\eta_2\psi_k^{(1)}(\eta_3)$, where

$$\psi_1^{(1)}(\eta_3) = -\eta_3, \quad \psi_2^{(1)}(\eta_3) = -(1-\eta_3), \quad \psi_3^{(1)}(\eta_3) = 1,$$

we obtain

$$\begin{aligned} &4|T_\ell|^2 \int_{D_1\cup D_2} F_{ij}(\hat{x},\hat{x}+\hat{z}) = \\ &= 8|T_\ell|^2 \int_0^1 \xi^{3-2s} d\xi \int_0^1 \eta_1^{2-2s} d\eta_1 \int_0^1 \eta_2^{1-2s} d\eta_2 \int_0^1 \frac{\psi_i^{(1)}(\eta_3)\psi_j^{(1)}(\eta_3)}{\left| B_\ell \begin{pmatrix} \eta_3 \\ 1 \end{pmatrix} \right|^{2+2s}} d\eta_3. \end{aligned}$$

Obviously, the first three integrals above are straightforwardly calculated by hand, and the last one involves a regular integrand, so that it is easily estimated by means of a Gaussian quadrature rule.

It still remains to perform similar calculations on the rest of the sets in (A.1.6). Consider the new variables $(\hat{x}',\hat{z}') = (\hat{x},-\hat{z})$ on D_3, $(\hat{x}',\hat{z}') = (\hat{x}+\hat{z},\hat{z})$ on D_4, $(\hat{x}',\hat{z}') = (\hat{x}+\hat{z},\hat{z})$ on D_5 and $(\hat{x}',\hat{z}') = (\hat{x},-\hat{z})$ on D_6, so that

$$\begin{aligned} 4|T_\ell|^2 \int_{D_3\cup D_4} F_{ij}(\hat{x},\hat{x}+\hat{z}) &= 8|T_\ell|^2 \int_{D_2'} F_{ij}(\hat{x}',\hat{x}'-\hat{z}')\, d\hat{x}'\, d\hat{z}', \\ 4|T_\ell|^2 \int_{D_5\cup D_6} F_{ij}(\hat{x},\hat{x}+\hat{z}) &= 8|T_\ell|^2 \int_{D_3'} F_{ij}(\hat{x}',\hat{x}'-\hat{z}')\, d\hat{x}'\, d\hat{z}', \end{aligned}$$

where

$$\begin{aligned} D_2' &= \{(\hat{x}',\hat{z}')\colon 0 \le \hat{z}_1' \le 1,\ 0 \le \hat{z}_2' \le \hat{z}_1',\ \hat{z}_1' \le \hat{x}_1' \le 1,\ \hat{z}_2' \le \hat{x}_2' \le \hat{x}_1' - \hat{z}_1' + \hat{z}_2'\}, \\ D_3' &= \{(\hat{x}',\hat{z}')\colon -1 \le \hat{z}_1' \le 0,\ 0 \le \hat{z}_2' \le 1+\hat{z}_1',\ \hat{z}_2' \le \hat{x}_1' \le 1+\hat{z}_1',\ \hat{z}_2' \le \hat{x}_2' \le \hat{x}_1'\}. \end{aligned}$$

These domains are transformed into $[0,1]^4$ by the respective composition of the transformations $T_h\colon D \to D_h'$ $(h=1,2)$

$$T_2 \begin{pmatrix} w_1 \\ w_2 \\ w_3 \\ w_4 \end{pmatrix} = \begin{pmatrix} w_1 \\ w_2 - w_3 + w_4 \\ w_3 \\ w_4 \end{pmatrix}, \quad T_3 \begin{pmatrix} w_1 \\ w_2 \\ w_3 \\ w_4 \end{pmatrix} = \begin{pmatrix} w_1 - w_4 \\ w_2 - w_4 \\ -w_4 \\ w_3 - w_4 \end{pmatrix},$$

and the Duffy transformation (A.1.7). Simple calculations lead finally to

$$\begin{aligned} 4|T_\ell|^2 \int_{D_3\cup D_4} F_{ij}(\hat{x},\hat{x}+\hat{z}) &= \frac{8|T_\ell|^2}{(4-2s)(3-2s)(2-2s)} \int_0^1 \frac{\psi_i^{(2)}(\eta_3)\psi_j^{(2)}(\eta_3)}{\left| B_\ell \begin{pmatrix} 1 \\ \eta_3 \end{pmatrix} \right|^{2+2s}} d\eta_3, \\ 4|T_\ell|^2 \int_{D_5\cup D_6} F_{ij}(\hat{x},\hat{x}+\hat{z}) &= \frac{8|T_\ell|^2}{(4-2s)(3-2s)(2-2s)} \int_0^1 \frac{\psi_i^{(3)}(\eta_3)\psi_j^{(3)}(\eta_3)}{\left| B_\ell \begin{pmatrix} \eta_3 \\ 1-\eta_3 \end{pmatrix} \right|^{2+2s}} d\eta_3, \end{aligned}$$

where

$$\psi_1^{(2)}(\eta_3) = -1, \qquad \psi_2^{(2)}(\eta_3) = 1 - \eta_3, \qquad \psi_3^{(2)}(\eta_3) = \eta_3,$$
$$\psi_1^{(3)}(\eta_3) = \eta_3, \qquad \psi_2^{(3)}(\eta_3) = -1, \qquad \psi_3^{(3)}(\eta_3) = 1 - \eta_3.$$

For the sake of simplicity of notation, we write

$$d^{(1)}(x) := \left| B_\ell \begin{pmatrix} x \\ 1 \end{pmatrix} \right|^{2+2s}, \qquad d^{(2)}(x) := \left| B_\ell \begin{pmatrix} 1 \\ x \end{pmatrix} \right|^{2+2s},$$
$$d^{(3)}(x) := \left| B_\ell \begin{pmatrix} x \\ 1-x \end{pmatrix} \right|^{2+2s}.$$

In order to estimate the integrals in the unit interval, we use a 9 point Gaussian quadrature rule. Let $p_1, \ldots, p_9 \in [0,1]$ the quadrature points, and $w_1, ..., w_9$ their respective weights. Considering the integrals over the domains D'_h ($h \in \{1,2,3\}$), we may write

$$\int_0^1 \frac{\psi_i^{(h)}(\eta)\psi_j^{(h)}(\eta)}{d^{(h)}(\eta)} d\eta \approx \sum_{k=1}^{9} w_k \frac{\psi_i^{(h)}(p_k)\psi_j^{(h)}(p_k)}{d^{(h)}(p_k)}.$$

As before, we take advantage of the fact that the integrand only depends on ℓ through its denominator. We define:

- A 9×9 matrix Ψ^h, such that

$$\Psi^h_{ij} = w_j \, \psi_{[i-1]_3+1}(p_j)\psi_{\lceil \frac{i}{3} \rceil}(p_j) \, J^{(h)}(p_j).$$

- A vector $d^h \in \mathbb{R}^9$, given by

$$d^h_k = \frac{1}{d^{(h)}(p_k)}.$$

Setting $\hat{I}_{\ell,m} := \Psi^1 \cdot d^1 + \Psi^2 \cdot d^2 + \Psi^3 \cdot d^3$, we obtain, for $i \in \{1, ..., 9\}$,

$$\begin{aligned} I_{\ell,m}^{[i-1]_3+1,\lceil \frac{i}{3} \rceil} &\approx \frac{8|T_\ell|^2}{(4-2s)(3-2s)(2-2s)} \hat{I}^i_{\ell,m} \\ &= \frac{8|T_\ell|^2}{(4-2s)(3-2s)(2-2s)} \sum_{h=1}^{3} \sum_{k=1}^{9} w_k \frac{\psi^{(h)}_{[i-1]_3+1}(p_k)\psi^{(h)}_{\lceil \frac{i}{3} \rceil}(p_k)}{d^{(h)}(p_k)}, \end{aligned}$$

or in *MATLAB*® notation,

$$I_{\ell,m} \approx \frac{8|T_\ell|^2}{(4-2s)(3-2s)(2-2s)} \texttt{reshape}(\hat{I}_{\ell,m}\texttt{, 3 , 3}).$$

The matrices Ψ^1, Ψ^2 and Ψ^3 are supplied by `data.mat`, where they are respectively saved as `tpsi1`, `tpsi2` and `tpsi3`.

The code of the function `triangle_quad` is as follows.

```
function ML = triangle_quad(Bl,s,psi1,psi2,psi3,areal,p_I)
ML = ( 8*areal*areal/((4-2*s)*(3-2*s)*(2-2*s)) ).*reshape(...
  psi1*( (  sum( (Bl*[p_I'; ones(1,length(p_I))]).^2 ).^(-1-s) )' ) +...
  psi2*( (  sum( (Bl*[ones(1,length(p_I)) ; p_I']).^2 ).^(-1-s) )' ) + ...
  psi3*( (  sum( (Bl*[p_I' ; p_I' - ones(1,length(p_I))]).^2 ).^(-1-s) )' ) ...
  , 3 , 3);
end
```

The matrix `Bl` plays the role of B_ℓ, `s` is s, `areal` is $|T_\ell|$, and `p_I` contains the values of the quadrature points in $[0,1]$. The latter are stored in `data.mat` under the same name, see Appendix A.3.1. The matrices Ψ^1, Ψ^2 and Ψ^3 are respectively saved as `psi1`, `psi2` and `psi3`.

The output `ML` of this function is a 3×3 matrix, such that: `ML` $\approx I_{\ell,\ell}$.

A.1.5 Complement

Recall that we are assuming that the domain Ω is contained in a ball $B = B(0,R)$. Here we are considering the interaction of two basis functions φ_i, φ_j such that $\mathrm{supp}(\varphi_i) \cap \mathrm{supp}(\varphi_j) = T_\ell$, over the region $T_\ell \times B^c$. Namely, we aim to compute

$$\begin{aligned} J_\ell &= \int_{T_\ell} \int_{B^c} \frac{\varphi_i(x)\varphi_j(x)}{|x-y|^{2+2s}}\, dydx = \int_{T_\ell} \varphi_i(x)\varphi_j(x)\psi(x)\, dx \\ &= 2|T_\ell| \int_{\hat{T}} \hat{\varphi}_i(\hat{x})\hat{\varphi}_j(\hat{x})\psi(\chi_\ell(\hat{x}))\, d\hat{x}, \end{aligned}$$

where

$$\psi(x) = \int_{B^c} \frac{1}{|x-y|^{2+2s}}\, dy.$$

The integral above may be calculated by a Gauss quadrature rule in the reference element $\hat{T}$, provided that the values of ψ at the quadrature points are computed.

Observe that the function ψ is radial (see Figure A.2) and therefore it suffices to estimate it on points of the form $x = (x_1, 0)$, where $x_1 > 0$. For a fixed point x and given $\theta \in [0, 2\pi]$, let $\rho_0(\theta)$ be the distance between x and the intersection of the ray starting from x with angle θ with respect to the horizontal axis. Then, it is simple to verify that

$$\rho_0(\theta, x) = -x_1 \cos\theta + \sqrt{R^2 - x_1^2 \sin^2\theta},$$

and therefore, integrating in polar coordinates,

$$\psi(x) = \frac{1}{2s} \int_0^{2\pi} \frac{1}{\rho_0(\theta,x)^{2s}}\, d\theta.$$

In order to compute J_ℓ we perform two nested quadrature rules: one over $\hat{T}$ and, for each quadrature point p_k in $\hat{T}$, another one to estimate $\psi(p_k)$ over $[0, 2\pi]$. We apply a 12 point quadrature formula over $\hat{T}$ and a 9 point one on $[0, 2\pi]$. Let $p_1, \ldots, p_{12} \in \hat{T}$, $\theta_1, \ldots, \theta_9 \in [0, 2\pi]$

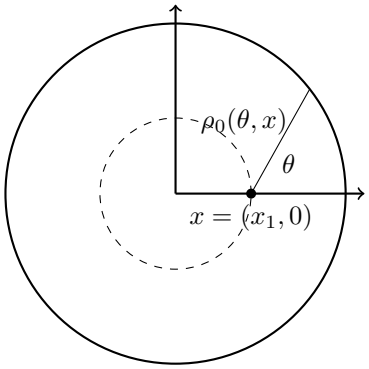

Figure A.2: Computing $\psi(x)$ in a point of $B = B(0, R)$. Due to the symmetry, the value of ψ is the same along the dashed circle, hence we may assume that $x = (x_1, 0)$ and $0 \leq x_1 < R$. For any $0 \leq \theta \leq \pi$, the function ρ_0 is given by $\rho_0(\theta, x) = -x_1 \cos\theta + \sqrt{R^2 - x_1^2 \sin^2\theta}$.

be these quadrature nodes, and $w_1, \ldots, w_{12}$, $W_1, \ldots, W_9$ their respective weights. Applying the rules we obtain

$$J_\ell \approx \frac{|T_\ell|}{s} \sum_{k=1}^{12} w_k \hat{\varphi}_i(p_k) \hat{\varphi}_j(p_k) \sum_{q=1}^{9} \frac{W_q}{\rho_0(\theta_q, \chi_\ell(p_k))^{2s}}.$$

In the same fashion as for the other computations, we write the previous expression as the product of a pre-computed matrix (that only depends on the choice of the quadrature rules) times a vector that depends on the elements under consideration. Indeed, we define:

- A matrix $\Phi \in \mathbb{R}^{9\times 12}$, such that

$$\Phi_{ij} = w_j \, \hat{\varphi}_{[i-1]_3+1}(p_j) \hat{\varphi}_{\lceil \frac{i}{3} \rceil}(p_j).$$

- A vector $\rho \in \mathbb{R}^{12}$, such that

$$\rho_k = \sum_q \frac{W_q}{\rho_0(\theta_q, \chi_\ell(p_k))^{2s}}.$$

Upon defining $\hat{J}_\ell := \Phi \cdot \rho$, we obtain

$$J_\ell^{[i-1]_3+1, \lceil \frac{i}{3} \rceil} \approx \frac{|T_\ell|}{s} \hat{J}_\ell^i, \; i \in \{1, ..., 9\}.$$

Using *MATLAB*® notation, the above identity may be written as

$$J_\ell \approx \frac{|T_\ell|}{s} \texttt{reshape}(\hat{J}_\ell, \texttt{ 3 , 3}).$$

The function `comp_quad` perform the previous computations.

```
function ML = comp_quad(Bl, x0, y0, s , phi , R, areal , p_I , w_I , p_T)
x = (Bl*p_T')' + [x0.*ones(length(p_T),1) , y0.*ones(length(p_T),1)];
aux = x(:,1)*cos(2*pi*p_I') + x(:,2)*sin(2*pi*p_I');
weight = ( ( -aux + sqrt( aux.^2 + R^2 - ( x(:,1).^2 +...
         x(:,2).^2 )*ones(1,length(p_I)) ) ).^(-2*s) )*w_I;
ML = (areal*2*pi/s).*reshape( phi*weight , 3 , 3);
end
```

Recall the parametrization $\chi_\ell(\hat{x}) = B_\ell \hat{x} + x_\ell^{(1)}$, so that `Bl`, `x0` and `y0` satisfy `Bl` $= B_\ell$ and $\begin{pmatrix} \texttt{x0} \\ \texttt{y0} \end{pmatrix} = x_\ell^{(1)}$. Moreover, `s` is s, `areal` is $|T_\ell|$, `p_I` contains the quadrature points in the interval $[0,1]$, so that 2π`p_I`$(q) = \theta_q$, `w_I`$(q) = W_q$, `p_T` contains 12 quadrature points over $\hat{T}$, stored in `data.mat` as `p_T_12` (see Appendix A.3.1) and `phi` is the matrix Φ, that is pre-computed and stored in `data.mat` as `cphi` (see Appendix A.3.6).

The output `ML` satisfies `ML` $\approx 2J_\ell$.

A.2 Two auxiliary functions

The main code uses two functions that have not been outlined yet. Here we show them in detail.

The function `setdiff_` takes as input two vectors `A` and `B`, such that `A` contains consecutive positive integers, ordered low to high, `B` contains positive integers and is such that `length(B)` $\leq$ `length(A)` and `max(B)` $\leq$ `max(A)`. The function computes the set difference `A` $\setminus$ `B`, taking advantage of the pre-condition.

```
function e = setdiff_( A , B )
e = A;
b = B - A(1) + 1;
b( b<1 )=[];
e(b) = [];
end
```

On the other hand, the function `fquad` calculates the entries of the right hand side vector in (3.2.2). Taking as input `areal` $:= |T_\ell|$, the vectors `xl` and `yl`, that contain the x and y coordinates of the vertices respectively, and a function f, `fquad` returns a vector in $\mathbb{R}^3$ array such that

$$\texttt{fquad}_k \approx \int_{T_\ell} f\, \varphi_{i_k}.$$

Here, for $k \in \{1,2,3\}$, i_k denotes the index of the k-th vertex of T_ℓ and φ_{i_k} the basis function corresponding to it.

```
function VL = fquad( areal, xl , yl , f )
VL = zeros(3,1);
```

```
xmid = [(xl(2)+xl(3))/2, (xl(1)+xl(3))/2, (xl(1)+xl(2))/2];
ymid = [(yl(2)+yl(3))/2, (yl(1)+yl(3))/2, (yl(1)+yl(2))/2];
for i=1:3
    for j=1:3
        if j~=i
            VL(i) = VL(i) + areal/6 * f(xmid(j), ymid(j));
        end
    end
end
end
```

A.3 Auxiliary data

In order to perform the necessary calculations efficiently, along the execution the code makes use of pre-computed data, stored in `data.mat`. Here we describe the variables provided by this file. It is convenient to clarify that all the *MATLAB*® code showed in this section does not belong to the program itself. It is included with an illustrative purpose.

A.3.1 Quadrature points and weights: `p_cube`, `p_T`, `p_T_comp`, `p_I` and `w_I`

We list the quadrature points used in all the quadrature rules and their respective weights.

The matrix `p_cube` is used as input on functions `vertex_quad` and `edge_quad`, and contains 27 quadrature points over $[0,1]^3$.

```
p_cube =

    0.1127    0.1127    0.1127
    0.1127    0.1127    0.5000
    0.1127    0.1127    0.8873
    0.1127    0.5000    0.1127
    0.1127    0.5000    0.5000
    0.1127    0.5000    0.8873
    0.1127    0.8873    0.1127
    0.1127    0.8873    0.5000
    0.1127    0.8873    0.8873
    0.5000    0.1127    0.1127
    0.5000    0.1127    0.5000
    0.5000    0.1127    0.8873
    0.5000    0.5000    0.1127
    0.5000    0.5000    0.5000
    0.5000    0.5000    0.8873
```

```
    0.5000    0.8873    0.1127
    0.5000    0.8873    0.5000
    0.5000    0.8873    0.8873
    0.8873    0.1127    0.1127
    0.8873    0.1127    0.5000
    0.8873    0.1127    0.8873
    0.8873    0.5000    0.1127
    0.8873    0.5000    0.5000
    0.8873    0.5000    0.8873
    0.8873    0.8873    0.1127
    0.8873    0.8873    0.5000
    0.8873    0.8873    0.8873
```

Over $\hat{T}$, we use two different quadrature rules, with 6 and 12 points. The set of nodes `p_T_6` is used to compute the non-touching element case and `p_T_12` as an input on `comp_quad`.

```
p_T_6 =

    0.5541    0.4459
    0.5541    0.1081
    0.8919    0.4459
    0.9084    0.0916
    0.9084    0.8168
    0.1832    0.0916

p_T_12 =

    0.7507    0.2493
    0.7507    0.5014
    0.4986    0.2493
    0.9369    0.0631
    0.9369    0.8738
    0.1262    0.0631
    0.6896    0.6365
    0.3635    0.0531
    0.9469    0.3104
    0.3635    0.3104
    0.6896    0.0531
    0.9469    0.6365
```

The 9×1 array `p_I` contains the quadrature points over $[0, 1]$, and `w_I` is a 9×1 array that contains their respective weights. These variables are used as input on `comp_quad`. The set of nodes `p_I` is also employed in `triangle_quad`.

```
p_I =                 w_I =
```

```
    0.5000              0.1651
    0.0820              0.0903
    0.9180              0.0903
    0.0159              0.0406
    0.9841              0.0406
    0.3379              0.1562
    0.6621              0.1562
    0.8067              0.1303
    0.1933              0.1303
```

A.3.2 Auxiliary variables to compute non-touching elements case: phiA, phiB and phiD

The variables `phiA`, `phiB` and `phiD` play the role of Φ^A , Φ^B and Φ^D (defined in Appendix A.1.1), respectively. We expose below the code used to set up these variables. We use the lists `p_T_6` and `w_T_6` of quadrature points and weights in $\hat{T}$ defined in Appendix A.3.1:

```
w_T_6 = zeros(6,1);
w_T_6(1) = 0.1117;
w_T_6(2) = w_T_6(1);
w_T_6(3) = w_T_6(1);
w_T_6(4) = 0.0550;
w_T_6(5) = w_T_6(4);
w_T_6(6) = w_T_6(4);

local = cell(1,6);
local{1} = @(x,y) 1-x;
local{2} = @(x,y) x-y;
local{3} = @(x,y) y;
local{4} = @(x,y) -(1-x);
local{5} = @(x,y) -(x-y);
local{6} = @(x,y) -y;

mat_loc = zeros(6);
for i = 1:6
    for j = 1:6
        mat_loc(i,j) = local{i}(p_T_6(j,1),p_T_6(j,2));
    end
end

W = w_T_6*(w_T_6');
M_aux = zeros(18);
N_aux = zeros(18);
```

```
L_aux = zeros(18);

phiB = zeros(9,36);
phiA = zeros(9,36);
phiD = zeros(9,36);

for i=1:3
    for j=1:3
        for k = 1:6
            for q=1:6
                M_aux( q + 6*(i-1) , k + 6*(j-1) ) =...
                W(q,k)*mat_loc(i,q)*mat_loc(j+3,k);
                N_aux( q + 6*(i-1) , k + 6*(j-1) ) =...
                W(q,k)*mat_loc(i,q)*mat_loc(j,q);
                L_aux( q + 6*(i-1) , k + 6*(j-1) ) =...
                W(q,k)*mat_loc(i+3,k)*mat_loc(j+3,k);
            end
        end
    end
end

for i=1:9
    [im jm] = ind2sub([3 3] , i);
    im = 6*(im - 1) + 1;
    jm = 6*(jm - 1) + 1;
    phiB(i,:) = reshape( M_aux( im:im+5 , jm:jm+5 ) , 1 , [] );
    phiA(i,:) = reshape( N_aux( im:im+5 , jm:jm+5 ) , 1 , [] );
    phiD(i,:) = reshape( L_aux( im:im+5 , jm:jm+5 ) , 1 , [] );
end
```

A.3.3 Auxiliary variables to compute vertex-touching elements case: `vpsi1` and `vpsi2`

The variables `vpsi1` and `vpsi2` are used as arguments of the function `vertex_quad` and play the role of the matrices Ψ^1 and Ψ^2 defined in Appendix A.1.2. Below we show the code used to initialize these variables.

First we define a variable `w_cube` that lists the weights associated with each quadrature point stored in `p_cube`:

```
w_cube =

    0.0214
    0.0343
```

```
    0.0214
    0.0343
    0.0549
    0.0343
    0.0214
    0.0343
    0.0214
    0.0343
    0.0549
    0.0343
    0.0549
    0.0878
    0.0549
    0.0343
    0.0549
    0.0343
    0.0214
    0.0343
    0.0214
    0.0343
    0.0549
    0.0343
    0.0214
    0.0343
    0.0214
```

The following lines generate `vpsi1` and `vpsi2`:

```
psi_D1 = cell(5,1);
psi_D1{1} = @(x,y,z) y-1;
psi_D1{2} = @(x,y,z) 1-x;
psi_D1{3} = @(x,y,z) x;
psi_D1{4} = @(x,y,z) -y.*(1-z);
psi_D1{5} = @(x,y,z) -y.*z;

psi_D2 = cell(5,1);
psi_D2{1} = @(x,y,z) -(y-1);
psi_D2{2} = @(x,y,z) y.*(1-z);
psi_D2{3} = @(x,y,z) y.*z;
psi_D2{4} = @(x,y,z) -(1-x);
psi_D2{5} = @(x,y,z) -x;

vpsi1 = zeros(25,27);
vpsi2 = zeros(25,27);
```

```
for i = 1:5
    for j = 1:5

        f1 = @(x,y,z) psi_D1{i}(x,y,z).*psi_D1{j}(x,y,z).*y;
        f2 = @(x,y,z) psi_D2{i}(x,y,z).*psi_D2{j}(x,y,z).*y;

        vpsi1( sub2ind([5 5], i , j) , : ) =...
        ( f1( p_cube(:,1) ,p_cube(:,2) , p_cube(:,3)) ).*w_cube;
        vpsi2( sub2ind([5 5], i , j) , : ) =...
        ( f2( p_cube(:,1) , p_cube(:,2) , p_cube(:,3)) ).*w_cube;

    end
end
```

A.3.4 Auxiliary variables to compute edge-touching elements case: `epsi1`, ..., `epsi5`

The variables `epsi1`, ..., `epsi5` are used as input on the function `edge_quad` and play the role of Ψ^1, ..., Ψ^5 defined in Appendix A.1.3, respectively. The code employed to set up these variables is exhibited below. We used the variable `w_cube` defined in the previous sub-section (containing weights associated to quadrature points stored in `p_cube`):

```
psi_D1 = cell(3,1);
psi_D1{1} = @(x,y,z) -x.*y;
psi_D1{2} = @(x,y,z) x.*(1-z);
psi_D1{3} = @(x,y,z) x.*z;
psi_D1{4} = @(x,y,z) -x.*(1-y);

psi_D2 = cell(3,1);
psi_D2{1} = @(x,y,z) -x.*y.*z;
psi_D2{2} = @(x,y,z) -x.*(1-y);
psi_D2{3} = @(x,y,z) x;
psi_D2{4} = @(x,y,z) -x.*y.*(1-z);

psi_D3 = cell(3,1);
psi_D3{1} = @(x,y,z) x.*y;
psi_D3{2} = @(x,y,z) -x.*(1-y.*z);
psi_D3{3} = @(x,y,z) x.*(1-y);
psi_D3{4} = @(x,y,z) -x.*y.*z;

psi_D4 = cell(3,1);
psi_D4{1} = @(x,y,z) x.*y.*z;
```

```
psi_D4{2} = @(x,y,z) x.*(1-y);
psi_D4{3} = @(x,y,z) x.*y.*(1-z);
psi_D4{4} = @(x,y,z) -x;

psi_D5 = cell(3,1);
psi_D5{1} = @(x,y,z) x.*y.*z;
psi_D5{2} = @(x,y,z) -x.*(1-y);
psi_D5{3} = @(x,y,z) x.*(1-y.*z);
psi_D5{4} = @(x,y,z) -x.*y;

epsi1 = zeros(16,27);
epsi2 = zeros(16,27);
epsi3 = zeros(16,27);
epsi4 = zeros(16,27);
epsi5 = zeros(16,27);

for i = 1:4
    for j = 1:4

        f1 = @(x,y,z) psi_D1{i}(x,y,z).*psi_D1{j}(x,y,z) .* (x.^2);
        f2 = @(x,y,z) psi_D2{i}(x,y,z).*psi_D2{j}(x,y,z) .* (x.^2).*y;
        f3 = @(x,y,z) psi_D3{i}(x,y,z).*psi_D3{j}(x,y,z) .* (x.^2).*y;
        f4 = @(x,y,z) psi_D4{i}(x,y,z).*psi_D4{j}(x,y,z) .* (x.^2).*y;
        f5 = @(x,y,z) psi_D5{i}(x,y,z).*psi_D5{j}(x,y,z) .* (x.^2).*y;

        epsi1( sub2ind([4 4], i , j) , : ) =...
        ( f1( p_cube(:,1) , p_cube(:,2) , p_cube(:,3)) ).*w_cube;
        epsi2( sub2ind([4 4], i , j) , : ) =...
        ( f2( p_cube(:,1) , p_cube(:,2) , p_cube(:,3)) ).*w_cube;
        epsi3( sub2ind([4 4], i , j) , : ) =...
        ( f3( p_cube(:,1) , p_cube(:,2) , p_cube(:,3)) ).*w_cube;
        epsi4( sub2ind([4 4], i , j) , : ) =...
        ( f4( p_cube(:,1) , p_cube(:,2) , p_cube(:,3)) ).*w_cube;
        epsi5( sub2ind([4 4], i , j) , : ) =...
        ( f5( p_cube(:,1) , p_cube(:,2) , p_cube(:,3)) ).*w_cube;

    end
end
```

A.3.5 Auxiliary variables to compute identical elements case: `tpsi1`, `tpsi2` and `tpsi3`

Here, the variables `tpsi1`, `tpsi2` and `tpsi3` are used as inputs on the function `triangle_quad` and play the role of the matrices Ψ^1, Ψ^2 and Ψ^3, defined in Appendix A.1.4, respectively. We describe the code used to set up these variables, where we use the quadrature data `p_I` and `w_I` introduced in Appendix A.3.1:

```
lambda_D1 = cell(3,1);
lambda_D1{1} = @(z) -z;
lambda_D1{2} = @(z) -(1-z);
lambda_D1{3} = @(z) 1;

lambda_D2 = cell(3,1);
lambda_D2{1} = @(z) -1;
lambda_D2{2} = @(z) (1-z);
lambda_D2{3} = @(z) z;

lambda_D3 = cell(3,1);
lambda_D3{1} = @(z) z;
lambda_D3{2} = @(z) -1;
lambda_D3{3} = @(z) 1-z;

tpsi1 = zeros(9,9);
tpsi2 = zeros(9,9);
tpsi3 = zeros(9,9);

for i = 1:3
    for j = 1:3

        f1 = @(z) lambda_D1{i}(z).*lambda_D1{j}(z);
        f2 = @(z) lambda_D2{i}(z).*lambda_D2{j}(z);
        f3 = @(z) lambda_D3{i}(z).*lambda_D3{j}(z);

        tpsi1( sub2ind([3 3], i , j) , : ) =  f1( p_I ).*w_I;
        tpsi2( sub2ind([3 3], i , j) , : ) =  f2( p_I ).*w_I;
        tpsi3( sub2ind([3 3], i , j) , : ) =  f3( p_I ).*w_I;

    end
end
```

A.3.6 Auxiliary variable to compute quadrature over complement: `cphi`

The matrix Φ, defined in Appendix A.1.5, is stored as the variable `cphi` and used as input on the function `comp_quad`. Before explaining the code we employed to build it, we define the 12 by 1 array `w_T_12` as the set of weights associated to the quadrature points stored in `p_T_12`:

```
w_T_12 =

    0.1168
    0.1168
    0.1168
    0.0508
    0.0508
    0.0508
    0.0829
    0.0829
    0.0829
    0.0829
    0.0829
    0.0829
```

Then, the following lines generate `cphi`:

```
local = cell(1,3);
local{1} = @(x,y) 1-x;
local{2} = @(x,y) x-y;
local{3} = @(x,y) y;

cphi = zeros(9,12);

for i = 1:3
    for j = 1:3

        f1 = @(z,y) local{i}(z,y).*local{j}(z,y);
        cphi( sub2ind([3 3], i , j) , : ) =...
        f1( p_T_12(:,1) , p_T_12(:,2) ).*w_T_12;

    end
end
```

A.4 Main Code

For the sake of the reader's convenience, we include here the main code described in sections 3.3 and 3.4.

```
clc
s = 0.5;
f = @(x,y) 1;
cns = s*2^(-1+2*s)*gamma(1+s)/(pi*gamma(1-s));
load('data.mat');
nn = size(p,2);
nt = size(t,1)
uh = zeros(nn,1);
K  = zeros(nn,nn);
b  = zeros(nn,1);
% Compute areas
area = zeros(nt,1);
for i=1:nt
    aux = p( : , t(i,:) );
    area(i) = 0.5.*abs( det(  [ aux(:,1) - aux(:,3)...
                                aux(:,2) - aux(:,3)]  ) );
end
% Build patches data structure
deg = zeros(nn,1);
for i=1:nt
    deg( t(i,:) ) = deg( t(i,:) ) + 1;
end
patches = cell(nn , 1);
for i=1:nn
    patches{i} = zeros( 1 , deg(i) );
end
for i=1:nt
    patches{ t(i,1) }(end - deg( t(i,1) ) + 1) = i;
    patches{ t(i,2) }(end - deg( t(i,2) ) + 1) = i;
    patches{ t(i,3) }(end - deg( t(i,3) ) + 1) = i;
    deg( t(i,:) ) = deg( t(i,:) ) - 1;
end
% Preallocate auxiliary memory
vl = zeros(6,2);
vm = zeros(6*nt,2);
norms = zeros(36,nt);
ML = zeros(6,6,nt);
empty = zeros(nt,1);
aux_ind = reshape( repmat( 1:3:3*nt , 6 , 1 ) , [] , 1 );
```

```
39 empty_vtx = zeros(2,3*nt);
40 BBm = zeros(2,2*nt);
41 for l=1:nt-nt_aux % Main Loop
42     edge =  [ patches{t(l,1)} patches{t(l,2)} patches{t(l,3)} ];
43     [nonempty M N] = unique( edge , 'first' );
44     edge(M) = [];
45     vertex = setdiff(  nonempty , edge  );
46     ll = nt - l + 1 - sum( nonempty>=l );
47     edge( edge<=l ) = [];
48     vertex( vertex<=l ) = [];
49     empty( 1:ll ) = setdiff_( l:nt , nonempty );
50     empty_vtx(: , 1:3*ll) = p( : , t( empty(1:ll) , : )' );
51     nodl = t(l,:);
52     xl = p(1 , nodl); yl = p(2 , nodl);
53     Bl = [xl(2)-xl(1) yl(2)-yl(1); xl(3)-xl(2) yl(3)-yl(2)]';
54     b(nodl) = b(nodl) + fquad(area(l),xl,yl,f);
55     K(nodl, nodl) = K(nodl, nodl)...
 + triangle_quad(Bl,s,tpsi1,tpsi2,tpsi3,area(l),p_I)...
 + comp_quad(Bl,xl(1),yl(1),s,cphi,R,area(l),p_I,w_I,p_T_12);
56     BBm(:,1:2*ll) = reshape( [ empty_vtx( : , 2:3:3*ll )...
 -  empty_vtx( : , 1:3:3*ll ) ,  empty_vtx( : , 3:3:3*ll )...
 - empty_vtx( : , 2:3:3*ll ) ] , [] , 2)' ;
57     vl = p_T_6*(Bl') + [ ones(6,1).*xl(1) ones(6,1).*yl(1) ];
58     vm(1:6*ll,:) = reshape(...
 permute(...
 reshape( p_T_6*BBm(:,1:2*ll) , [6 1 2 ll] ) , [1 4 3 2] ) , [ 6*ll 2 ] )...
 + empty_vtx(: , aux_ind(1:6*ll) )';
59     norms(:,1:ll) = reshape( pdist2(vl,vm(1:6*ll,:)), 36 , [] ).^(-2-2*s);
60     ML(1:3,1:3,1:ll) =  reshape( phiA*norms(:,1:ll) , 3 , 3 , [] );
61     ML(1:3,4:6,1:ll) =  reshape( phiB*norms(:,1:ll) , 3 , 3 , [] );
62     ML(4:6,4:6,1:ll) =  reshape( phiD*norms(:,1:ll) , 3 , 3 , [] );
63     ML(4:6,1:3,1:ll) =  permute( ML(1:3,4:6,1:ll) , [2 1 3] );
64     % Assembling stiffness matrix
65     for m=1:ll
66         order = [nodl t( empty(m) , : )];
67         K(order,order) = K(order,order)...
                + ( 8*area(empty(m))*area(l) ).*ML(1:6,1:6,m);
68     end
69     for m=vertex
70         nodm = t(m,:);
71         nod_com = intersect(nodl, nodm);
72         order = [nod_com nodl(nodl~=nod_com) nodm(nodm~=nod_com)];
73         K(order,order) = K(order,order)...
```

```
 + 2.*vertex_quad(nodl,nodm,nod_com,p,s,vpsi1,vpsi2,area(l),area(m),p_cube);
74      end
75      for m=edge
76          nodm = t(m,:);
77          nod_diff = [setdiff(nodl, nodm) setdiff(nodm, nodl)];
78          order = [ nodl( nodl~=nod_diff(1) ) nod_diff  ];
79          K(order,order) = K(order,order)...
 + 2.*edge_quad(...
nodl,nodm,nod_diff,p,s,epsi1,epsi2,epsi3,epsi4,epsi5,area(l),area(m),p_cube);
80      end
81 end
82 uh(nf) = ( K(nf,nf)\b(nf) )./cns;
83 trimesh(t(1:nt - nt_aux , :), p(1,:),p(2,:),uh);
```

Bibliography

[1] M. Abramowitz and I. Stegun. *Handbook of Mathematical Functions*. Dover Publications, 1965.

[2] P. J. Acklam. *MATLAB array manipulation tips and tricks*. Notes, 2003.

[3] G. Acosta and J. P. Borthagaray. A fractional Laplace equation: Regularity of solutions and finite element approximations. *SIAM J. Numer. Anal.*, 55(2):472–495, 2017.

[4] Gabriel Acosta and Francisco M Bersetche. Numerical approximations for a fully fractional allen-cahn equation. *arXiv preprint arXiv:1903.08964*, 2019.

[5] Gabriel Acosta, Francisco M Bersetche, and Juan Pablo Borthagaray. Finite element approximations for fractional evolution problems. *arXiv preprint arXiv:1705.09815*, 2017.

[6] Gabriel Acosta, Francisco M Bersetche, and Juan Pablo Borthagaray. A short fe implementation for a 2d homogeneous dirichlet problem of a fractional Laplacian. *Computers & Mathematics with Applications*, 74(4):784–816, 2017.

[7] Gabriel Acosta, Juan Pablo Borthagaray, Oscar Bruno, and Martín Maas. Regularity theory and high order numerical methods for the (1d)-fractional Laplacian. *Mathematics of Computation*, 87(312):1821–1857, 2018.

[8] Mark Ainsworth and Christian Glusa. Aspects of an adaptive finite element method for the fractional laplacian: a priori and a posteriori error estimates, efficient implementation and multigrid solver. *Computer Methods in Applied Mechanics and Engineering*, 327:4–35, 2017.

[9] Mark Ainsworth and Zhiping Mao. Analysis and approximation of a fractional Cahn–Hilliard equation. *SIAM Journal on Numerical Analysis*, 55(4):1689–1718, 2017.

[10] Mark Ainsworth and Zhiping Mao. Well-posedness of the Cahn–Hilliard equation with fractional free energy and its fourier galerkin approximation. *Chaos, Solitons & Fractals*, 102:264–273, 2017.

[11] Goro Akagi, Giulio Schimperna, and Antonio Segatti. Fractional Cahn–Hilliard, Allen–Cahn and porous medium equations. *Journal of Differential Equations*, 261(6):2935–2985, 2016.

[12] J. Alberty, C. Carstensen, and S. A. Funken. Remarks around 50 lines of Matlab: short finite element implementation. *Numer. Algorithms*, 20(2-3):117–137, 1999.

[13] Samuel M Allen and John W Cahn. A microscopic theory for antiphase boundary motion and its application to antiphase domain coarsening. *Acta Metallurgica*, 27(6):1085–1095, 1979.

[14] E. Bazhlekova, B. Jin, R. Lazarov, and Z. Zhou. An analysis of the Rayleigh–Stokes problem for a generalized second-grade fluid. *Numer. Math.*, 131(1):1–31, 2015.

[15] D. A. Benson, S. W. Wheatcraft, and M. M. Meerschaert. Application of a fractional advection-dispersion equation. *Water Resources Research*, 36(6):1403–1412, 2000.

[16] B. Berkowitz, A. Cortis, M. Dentz, and H. Scher. Modeling non-Fickian transport in geological formations as a continuous time random walk. *Reviews of Geophysics*, 44(2):n/a–n/a, 2006. RG2003.

[17] J. Bertoin. *Lévy processes*, volume 121 of *Cambridge Tracts in Math.* Cambridge University Press, Cambridge, 1996.

[18] Andrea Bonito, Wenyu Lei, and Joseph E Pasciak. Numerical approximation of space-time fractional parabolic equations. *Computational Methods in Applied Mathematics*, 17(4):679–705, 2017.

[19] Juan Pablo Borthagaray. *Laplaciano fraccionario: regularidad de soluciones y aproximaciones por elementos finitos.* PhD thesis, Uninversidad de Buenos Aires, 2017.

[20] Juan Pablo Borthagaray, Leandro M Del Pezzo, and Sandra Martínez. Finite element approximation for the fractional eigenvalue problem. *Journal of Scientific Computing*, 77(1):308–329, 2018.

[21] Andrea Braides. *Gamma-convergence for Beginners*, volume 22. Clarendon Press, 2002.

[22] Haim Brezis. *Functional analysis, Sobolev spaces and partial differential equations.* Universitext. Springer, New York, 2011.

[23] D. Brockmann, L. Hufnagel, and T. Geisel. The scaling laws of human travel. *Nature*, 439(7075):462–465, 2006.

[24] John W Cahn and John E Hilliard. Free energy of a nonuniform system. i. interfacial free energy. *The Journal of chemical physics*, 28(2):258–267, 1958.

[25] S. Chaturapruek, J. Breslau, D. Yazdi, T. Kolokolnikov, and S. G. McCalla. Crime modeling with Lévy flights. *SIAM J. Appl. Math.*, 73(4):1703–1720, 2013.

[26] Paulo Mendes de Carvalho Neto. *Fractional differential equations: a novel study of local and global solutions in Banach spaces.* PhD thesis, ICMC-USP, 2013.

[27] D. del Castillo-Negrete, B. A. Carreras, and V. E. Lynch. Fractional diffusion in plasma turbulence. *Phys. Plasmas*, 11(8):3854–3864, 2004.

[28] D. del Castillo-Negrete, B. A. Carreras, and V. E. Lynch. Nondiffusive transport in plasma turbulence: A fractional diffusion approach. *Phys. Rev. Lett.*, 94:065003, 2005.

[29] M. D'Elia and M. Gunzburger. The fractional Laplacian operator on bounded domains as a special case of the nonlocal diffusion operator. *Comp. Math. Appl.*, 66(7):1245 – 1260, 2013.

[30] Eleonora Di Nezza, Giampiero Palatucci, and Enrico Valdinoci. Hitchhiker's guide to the fractional Sobolev spaces. *Bull. Sci. Math.*, 136(5):521–573, 2012.

[31] K. Diethelm. *The analysis of fractional differential equations*, volume 2004 of *Lecture Notes in Mathematics*. Springer-Verlag, Berlin, 2010. An application-oriented exposition using differential operators of Caputo type.

[32] B. Dyda, A. Kuznetsov, and M. Kwaśnicki. Fractional Laplace operator and Meijer G-function. *Constr. Approx.*, 45(3):427–448, 2017.

[33] Xavier Fernández-Real and Xavier Ros-Oton. Boundary regularity for the fractional heat equation. *Revista de la Real Academia de Ciencias Exactas, Fisicas y Naturales. Serie A. Matematicas*, 110(1):49–64, 2016.

[34] A. Freed, K. Diethelm, and Y. Luchko. Fractional-order viscoelasticity (FOV): Constitutive development using the fractional calculus: First annual report. Technical report, NASA's Glenn Research Center, 2002.

[35] Ciprian Gal and Mahamadi Warma. Fractional in time semilinear parabolic equations and applications. *HAL Id: hal-01578788*, 2017.

[36] Roberto Garrappa. Numerical evaluation of two and three parameter mittag-leffler functions. *SIAM Journal on Numerical Analysis*, 53(3):1350–1369, 2015.

[37] Rudolf Gorenflo, Yuri Luchko, and Masahiro Yamamoto. Time-fractional diffusion equation in the fractional sobolev spaces. *Fractional Calculus and Applied Analysis*, 18(3):799–820, 2015.

[38] G. Grubb. Fractional Laplacians on domains, a development of Hörmander's theory of μ-transmission pseudodifferential operators. *Adv. Math.*, 268:478 – 528, 2015.

[39] G. Grubb. Spectral results for mixed problems and fractional elliptic operators. *J. Math. Anal. Appl.*, 421(2):1616–1634, 2015.

[40] E. Hanert. On the numerical solution of space–time fractional diffusion models. *Comput. & Fluids*, 46(1):33 – 39, 2011. 10th {ICFD} Conference Series on Numerical Methods for Fluid Dynamics (ICFD 2010).

[41] Dongdong He, Kejia Pan, and Hongling Hu. A fourth-order maximum principle preserving operator splitting scheme for three-dimensional fractional Allen-Cahn equations. *arXiv preprint arXiv:1804.07246*, 2018.

[42] Tianliang Hou, Tao Tang, and Jiang Yang. Numerical analysis of fully discretized crank–nicolson scheme for fractional-in-space Allen–Cahn equations. *Journal of Scientific Computing*, 72(3):1214–1231, 2017.

[43] Y. Huang and A. M. Oberman. Numerical methods for the fractional Laplacian: A finite difference-quadrature approach. *SIAM J. Numer. Anal.*, 52(6):3056–3084, 2014.

[44] B. Jin, R. Lazarov, and Z. Zhou. Error estimates for a semidiscrete finite element method for fractional order parabolic equations. *SIAM J. Numer. Anal.*, 51(1):445–466, 2013.

[45] B. Jin, R. Lazarov, and Z. Zhou. Two fully discrete schemes for fractional diffusion and diffusion-wave equations with nonsmooth data. *SIAM J. Sci. Comput.*, 38(1):A146–A170, 2016.

[46] Bangti Jin, Raytcho Lazarov, Joseph Pasciak, and Zhi Zhou. Galerkin fem for fractional order parabolic equations with initial data in H^s, $0 \leq s \leq 1$. In *International Conference on Numerical Analysis and Its Applications*, pages 24–37. Springer, 2012.

[47] Bangti Jin, Raytcho Lazarov, Joseph Pasciak, and Zhi Zhou. Error analysis of semidiscrete finite element methods for inhomogeneous time-fractional diffusion. *IMA Journal of Numerical Analysis*, 35(2):561–582, 2014.

[48] Bangti Jin, Raytcho Lazarov, and Zhi Zhou. Error estimates for a semidiscrete finite element method for fractional order parabolic equations. *SIAM Journal on Numerical Analysis*, 51(1):445–466, 2013.

[49] M Karkulik. Variational formulation of time-fractional parabolic equations. *Computers & Mathematics with Applications*, 75(11):3929–3938, 2018.

[50] M. Karkulik and J.M. Melenk. H -matrix approximability of inverses of discretizations of the fractional Laplacian. *arXiv preprint arXiv:1808.04274*, 2018.

[51] A Anatolii Aleksandrovich Kilbas, Hari Mohan Srivastava, and Juan J Trujillo. *Theory and applications of fractional differential equations*, volume 204. Elsevier Science Limited, 2006.

[52] T. A. M. Langlands, B. I. Henry, and S. L. Wearne. Fractional cable equation models for anomalous electrodiffusion in nerve cells: finite domain solutions. *SIAM J. Appl. Math.*, 71(4):1168–1203, 2011.

[53] Stig Larsson. Semilinear parabolic partial differential equations: theory, approximation, and application. *New trends in the mathematical and computer sciences*, 3:153–194, 2006.

[54] Zheng Li, Hong Wang, and Danping Yang. A space–time fractional phase-field model with tunable sharpness and decay behavior and its efficient numerical simulation. *Journal of Computational Physics*, 347:20–38, 2017.

[55] Huan Liu, Aijie Cheng, Hong Wang, and Jia Zhao. Time-fractional Allen–Cahn and Cahn–Hilliard phase-field models and their numerical investigation. *Computers & Mathematics with Applications*, 76(8):1876–1892, 2018.

[56] C. Lubich. Convolution quadrature and discretized operational calculus. I. *Numer. Math.*, 52(2):129–145, 1988.

[57] C. Lubich. Convolution quadrature revisited. *BIT*, 44(3):503–514, 2004.

[58] Yuri Luchko. Fractional wave equation and damped waves. *J. Math. Phys.*, 54(3):031505, 16, 2013.

[59] Alessandra Lunardi. *Interpolation theory*, volume 16. Springer, 2018.

[60] F. Mainardi, Y. Luchko, G. Pagnini, and Dedicated To Rudolf Gorenflo. The fundamental solution of the space-time fractional diffusion equation. *Fract. Calc. Appl. Anal*, 4(2):153–192, 2001.

[61] F. Mainardi and P. Paradisi. Fractional diffusive waves. *J. Comput. Acoust.*, 09(04):1417–1436, 2001.

[62] F. Mainardi, M. Raberto, R. Gorenflo, and E. Scalas. Fractional calculus and continuous-time finance II: the waiting-time distribution. *Phys. A*, 287(3–4):468 – 481, 2000.

[63] Arakaparampil M Mathai and Hans J Haubold. *Special functions for applied scientists*, volume 4. Springer, 2008.

[64] W. McLean. Regularity of solutions to a time-fractional diffusion equation. *ANZIAM J.*, 52(2):123–138, 2010.

[65] W. McLean and V. Thomée. Numerical solution via Laplace transforms of a fractional order evolution equation. *J. Integral Equations Appl.*, 22(1):57–94, 2010.

[66] Kalle Mikkola. *Infinite-Dimensional Linear Systems, Optimal Control and Algebraic Riccati Equations*. PhD thesis, Helsinki University of Technology Institute of Mathematics, 2002.

[67] E. W. Montroll and G. H. Weiss. Random walks on lattices. II. *J. Mathematical Phys.*, 6:167–181, 1965.

[68] K. Mustapha and W. McLean. Superconvergence of a discontinuous Galerkin method for fractional diffusion and wave equations. *SIAM J. Numer. Anal.*, 51(1):491–515, 2013.

[69] R. H. Nochetto, E. Otárola, and A. J. Salgado. A PDE approach to space-time fractional parabolic problems. *SIAM J. Numer. Anal.*, 54(2):848–873, 2016.

[70] Y. Pachepsky, D. Timlin, and W. Rawls. Generalized Richards' equation to simulate water transport in unsaturated soils. *Journal of Hydrology*, 272(1–4):3 – 13, 2003. Soil Hydrological Properties and Processes and their Variability in Space and Time.

[71] I. Podlubny. *Fractional differential equations*, volume 198 of *Mathematics in Science and Engineering*. Academic Press, Inc., San Diego, CA, 1999. An introduction to fractional derivatives, fractional differential equations, to methods of their solution and some of their applications.

[72] X. Ros-Oton and J. Serra. Local integration by parts and Pohozaev identities for higher order fractional Laplacians. *Discrete Contin. Dyn. Syst.*, 35(5):2131–2150, 2015.

[73] L. Rosasco, M. Belkin, and E. De Vito. On learning with integral operators. *J. Mach. Learn. Res.*, 11:905–934, 2010.

[74] K. Sakamoto and M. Yamamoto. Initial value/boundary value problems for fractional diffusion-wave equations and applications to some inverse problems. *J. Math. Anal. Appl.*, 382(1):426 – 447, 2011.

[75] S. A. Sauter and C. Schwab. *Boundary element methods*, volume 39 of *Springer Ser. Comput. Math.* Springer-Verlag, Berlin, 2011. Translated and expanded from the 2004 German original.

[76] Ovidiu Savin and Enrico Valdinoci. γ-convergence for nonlocal phase transitions. In *Annales de l'Institut Henri Poincare (C) Non Linear Analysis*, volume 29, pages 479–500. Elsevier Masson, 2012.

[77] D. Sims, E. Southall, N. Humphries, G. Hays, C. Bradshaw, J. Pitchford, A. James, M. Ahmed, A. Brierley, M. Hindell, D. Morritt, M. Musyl, D. Righton, E. Shepard, V. Wearmouth, R. Wilson, M. Witt, and J. Metcalfe. Scaling laws of marine predator search behaviour. *Nature*, 451(7182):1098–1102, 2008.

[78] Fangying Song, Chuanju Xu, and George Em Karniadakis. A fractional phase-field model for two-phase flows with tunable sharpness: Algorithms and simulations. *Computer Methods in Applied Mechanics and Engineering*, 305:376–404, 2016.

[79] Q. Yang, I. Turner, F. Liu, and M. Ilić. Novel numerical methods for solving the time-space fractional diffusion equation in two dimensions. *SIAM J. Sci. Comput.*, 33(3):1159–1180, 2011.